(1)

CONTRACT NO: DAMD17-93-C-3098

TITLE: USE OF COMBINATION THERMAL THERAPY AND RADIATION IN BREAST CONSERVING TREATMENT OF EXTENSIVE INTRODUCTAL BREAST CANCER

PRINCIPAL INVESTIGATOR: Goran K. Svensson, Ph.D.

CONTRACTING ORGANIZATION: New England Deaconess Hospital
185 Pilgrim Road
Boston, Massachusetts 02215-5399

REPORT DATE: April 28, 1994

TYPE OF REPORT: Annual Report

PREPARED FOR: U.S. Army Medical Research, Development, Acquisition and Logistics Command (Provisional), Fort Detrick, Frederick, Maryland 21702-5012

DISTRIBUTION STATEMENT: Approved for public release; distribution unlimited

The views, opinions and/or findings contained in this report are those of the author(s) and should not be construed as an official Department of the Army position, policy or decision unless so designated by other documentation.

REPORT DOCUMENTATION PAGE

Form Approved
OMB No. 0704-0188

1. AGENCY USE ONLY (Leave blank)	2. REPORT DATE 4/28/94 Revised 7/11/94	3. REPORT TYPE AND DATES COVERED Annual Report (3/29/93-3/28/94)

4. TITLE AND SUBTITLE
"Use of Combination Thermal Therapy and Radiation in Breast Conserving Treatment of Extensive Intraductal Breast Cancer

5. FUNDING NUMBERS
Contract No.
DAMD17-93-C-3098

6. AUTHOR(S)
Goran K. Svensson, Ph.D.
Everette C. Burdette, Ph.D.

7. PERFORMING ORGANIZATION NAME(S) AND ADDRESS(ES)
New England Deaconess Hospital
185 Pilgrim Road
Boston, Massachusetts 02215-5399

8. PERFORMING ORGANIZATION REPORT NUMBER

9. SPONSORING/MONITORING AGENCY NAME(S) AND ADDRESS(ES)
U.S. Army Medical Research, Development, Acquisition and Logistics Command (Provisional),
Fort Detrick
Frederick, Maryland 21702-5012

10. SPONSORING/MONITORING AGENCY REPORT NUMBER

11. SUPPLEMENTARY NOTES
Prepared with contributions from: B.A. Bornstein, M.D., J.R. Harris, M.D., Xing-Qi Lu, Ph.D. Subcontract work: Dornier Medical Systems, Inc. 510 Devonshire Drive, Champaign, Illinois 61820

12a. DISTRIBUTION/AVAILABILITY STATEMENT
Approved for public release; distribution unlimited

12b. DISTRIBUTION CODE

13. ABSTRACT *(Maximum 200 words)*

Year 01 of this contract supports the development of a technique for treatment of breast cancer, with an Extensive Intraductal Component (EIC) or pure Ductal Carcinoma in Situ (DCIS) using thermal therapy generated from ultrasound transducers. We have studied the technial approach for these treatments using complex computer simulations. The thermal treatment of the breast will be done with the patient in prone position with the breast submerged into a water filled applicator. A cylindrical array of individually controlled ultrasound transducers surround the breast. The cylindrical applicator consists of a stack of 10 rings, each being approximately 1.5 cm high. The ring located at the base of the breast contains 48 transducers. The number of transducers in each ring decrease toward the apex of the breast. Altogether there are 320 transducer elements requiring sophisticated computer control of power and frequency. The system is being built and subsystems are undergoing tests. Two clinical treatment protocols are currently being written; one for evaluation of the equipment treating approximately six patients and one for a larger Phase I/II study. An IDE will be submitted to FDA in July 94. A work schedule for future year 02 and 03 is presented

14. SUBJECT TERMS	15. NUMBER OF PAGES
Thermal Therapy, Breast Cancer, Extensive Intraductal Component, Ductal Carcinoma in Situ, Ultrasound Transducers, Thermometry	70
	16. PRICE CODE

17. SECURITY CLASSIFICATION OF REPORT	18. SECURITY CLASSIFICATION OF THIS PAGE	19. SECURITY CLASSIFICATION OF ABSTRACT	20. LIMITATION OF ABSTRACT
Unclassified	Unclassified	Unclassified	Unlimited

FOREWORD

Opinions, interpretations, conclusions and recommendations are those of the author and are not necessarily endorsed by the US Army.

____ Where copyrighted material is quoted, permission has been obtained to use such material.

____ Where material from documents designated for limited distribution is quoted, permission has been obtained to use the material.

____ Citations of commercial organizations and trade names in this report do not constitute an official Department of Army endorsement or approval of the products or services of these organizations.

____ In conducting research using animals, the investigator(s) adhered to the "Guide for the Care and Use of Laboratory Animals," prepared by the Committee on Care and Use of Laboratory Animals of the Institute of Laboratory Resources, National Research Council (NIH Publication No. 86-23, Revised 1985).

____ For the protection of human subjects, the investigator(s) adhered to policies of applicable Federal Law 45 CFR 46.

____ In conducting research utilizing recombinant DNA technology, the investigator(s) adhered to current guidelines promulgated by the National Institutes of Health.

____ In the conduct of research utilizing recombinant DNA, the investigator(s) adhered to the NIH Guidelines for Research Involving Recombinant DNA Molecules.

____ In the conduct of research involving hazardous organisms, the investigator(s) adhered to the CDC-NIH Guide for Biosafety in Microbiological and Biomedical Laboratories.

Accession For	
NTIS GRA&I	☑
DTIC TAB	☐
Unannounced	☐
Justification	
By	
Distribution/	
Availability Codes	
Dist	Avail and/or Special
A-1	

Grant Ferguson 4/25/94
PI - Signature Date

III. Table of Contents:

Page number.		
1	I.	SF 298 Report Documentation Page
2	II.	Forewor
3	III.	Table of Contents.
4	IV.	Introduction
4		1. Purpose and Rationale
5		2. Research Objectives
6-49	V.	Body of Annual Progress Report
6		1. Research Methodology
6		A. Program Organization
6		B. Summary of First Year Progress
12		2. Ultrasound Breast Applicator Design
12		A. Breast Applicator Design Criteria
13		B. Review of Designs Evaluated
18		C. Theoretical Simulation of Applicator
29		3. System Design and Development
29		A. General System Description
31		B. Applicator Subsystem
33		C. Patient Table Subsystem
35		D. System Control and Computer
37		E. RF Power Subsystem
37		F. Thermometry Subsystem
39		G. Non-Invasive Monitoring
42		H. Software development
43		4. Experimental Studies and Testing
43		A. RF Generator, Amplifier test.
45		B. MTR switch test.
45		C. 16 channel T/R board test.
47		D. Single ring test.
48		5. Breast Treatment Protocol
49	VI.	Conclusions and Statement of Work
52	VII.	References
54	VIII.	Appendices
		1. Paper submitted to IEEE meeting.
		2. Review paper

IV. Introduction

1. Purpose and Rationale:

Contract DAMD17-93-C-3098 supports the development of a technique for adjuvant treatment of breast cancer using thermal therapy (hyperthermia). The contract will also support a clinical study of the safety and efficacy of using thermal therapy in combination with radiation for treatment of breast cancer patients with an extensive intraductal component of their infiltrating tumor or patients with pure intraductal carcinoma. Breast cancer patients with these histologies have a higher risk of local recurrence than patients without these histologies.

Intraductal carcinoma is characterized by cancer cells spreading within the lactiferous ducts. It is suggested that intraductal carcinoma is associated with tumor necrosis within the ducts and that the necrotic tumor cells are related to the absence of blood supply with resulting hypoxia. It is well known that thermal therapy, in contrast to radiation, is more effective in killing hypoxic cells as compared to well oxygenated cells.

The clinical rationale and hypothesis for this work remain unchanged, namely that patients with infiltrating breast cancer containing an extensive intraductal component or patients with pure intraductal carcinoma will have a reduced risk for local recurrence from a combined and non-disfiguring treatment approach using thermal therapy and irradiation. This will extend the indications for breast conserving therapy and eliminate the need for mastectomy for many patients.

We also postulate that the thermal therapy is most effectively and controllably delivered to the breast tissue using a breast site specific ultrasound applicator. Most of the work during year 01, has been focused on the specifications, design, and fabrication of the breast applicator.

The technical rationale and criteria for the design of the ultrasound applicator are derived from the tissue characteristics and features of the breast:

a. The breast is an external, convex shaped organ. When submerged into a temperature controlled water bath, the temperature boundaries are well defined and the skin temperature can be well controlled.

b. Ultrasound heating is suitable for the breast, because there is no intervening gas or bone in the breast tissue. With the patient in prone position and the breast submerged into a water bath, we can surround the breast tissue with an array of ultrasound transducers and achieve tangential incidence of the

ultrasound beam relative to the chest wall. Tangential incidence is desired to avoid interaction between the ribcage and the ultrasound pressure wave.

c. There are no major blood vessels that carry away heat from the breast tissue, reducing the ability to deliver therapeutic heat.

d. The hyperthermia target volume can be the whole breast, a quadrant of the breast, or even a smaller specific tumor mass. Energy deposition, which may heat sensitive regions, such as a lumpectomy scar must be avoided or minimized. It is therefore essential that the energy deposition be controlled and focused on specific sites within the breast tissue. Ultrasound permits this level of control.

e. Although our initial pilot study will aim for a target temperature of $T_{90} \geq 40.5^0C$ and $T_{max} < 45^0C$, the device must be able to heat the breast tissue within an even more narrow temperature range (42^0C - 44^0C) over a reasonable range of tissue perfusion, i.e. 30 to 200 ml, kg^{-1}, min^{-1}.

2. Research Objectives.

One research objective is to build a cylindrical, multi-transducer, dual frequency, intensity controlled ultrasound applicator for treatment of breast cancer. The device must be capable of delivering controllable energy for the purpose of heating the whole breast or a small volume of breast tissue as defined by the clinical situation and the criteria in section IV-1. The intensity control of the applicator must permit heating within a narrow temperature range, i.e. $42^0C \leq T_{tissue} \leq 44^0C$.

A second objective is to develop an effective pre-treatment planning and real-time treatment control system. One aspect of this effort is to perform the thermal therapy using dense thermometry. It is essential for the assessment of outcome that temperatures are measured during thermal therapy in a large number of points throughout the breast tissue volume. The objective is to accomplish this through new technologies using minimally invasive or non-invasive thermometry. The minimally invasive temperature measurements will be achieved by using special micro-electronics technology currently under development at the Massachusetts Institute for Technology (MIT) under the direction of Dr. F. Bowman, who is a consultant to our contract. To augment the dense thermometry mapping, the use of non-invasive thermometry will be investigated during years two and three of this contract.

A third objective is to develop ultrasound thermal therapy protocols for a phase I/II study to begin during year 02 and for a phase III study to begin by the end of year 03.

V. Body of Report

1. Research Methodology.

A. Program Organization.

The contract is sponsored by the New England Deaconess Hospital (NEDH); a Harvard Medical School (HMS) affiliated hospital in Boston, Massachusetts. The program director, Goran K. Svensson, Ph.D. is an Associate Professor at HMS and he is responsible for the progress of the scientific, technical and clinical developments.

Most of the theoretical work requiring large computational resources and all clinical work take place at the NEDH. The electronic design and the fabrication of the ultrasound treatment system is subcontracted to Dornier Medical Systems Inc. (DMSI) with headquarters in Atlanta, Georgia. The actual subcontract work is performed at the DMSI laboratory in Champaign, Illinois under the direction of Everette C. Burdette, Ph.D. The work has progressed in a satisfactory and efficient manner and the collaboration between the group at the NEDH and the DMSI has been of the highest quality.

B. Summary of first year progress.

On page 49 in the original application, a Statement of Work (SoW) was outlined for the overall program. Many of the technical details requiring attention were not specifically included in the original SoW but they are now included in Table 1 on page 11, showing work completed during year 01.

The main emphasis during year 01 (See table 1) has been on the design and building of the various subsystems that comprises the total thermal therapy system. The computer tasks include the design and computer simulations of the transducer assembly. This has been successfully completed. Eighteen rings (enough for two systems) and transducers for one complete system were built during the first year. One ring including the electronics was assembled and electronically tested by the end of year 01. A rigorous testing of this ring using a breast phantom will be initiated during the first month of year 02. Two tissue mimicking breast phantoms were built during year 01, one of which will be used during the single ring test. The electronic controls and much of the control software have been completed and is being tested.

The invasive thermometry system exists as a stand-alone system and will be integrated into the final product. It consists of 14-sensor linear arrays of thermistors mounted in a 19 gauge needle. The patient support table is finished and will be mounted on the support structure that also holds the electronics and the computer control system. All aspects of the design and fabrication

have been done in accordance with practices that will lead to future compliance with FDA manufacturing guidelines.

Therefore, by and large, the technical work presented in the original application has been followed.

However, there are changes in the completion schedule resulting from the advice received from the external scientific review committee. These changes, discussed below, are clearly shown in Table 1, and in the SoW, Table 5 on page 49.

A project of this complexity has many scientific uncertainties that will require continuous re-assessment of both technical and clinical approaches and solutions to accomplish our clinical goal. To achieve the scientific review and assessment, we have established a peer review mechanism involving two internationally known experts on the technical and clinical use of thermal therapy for breast cancer, chestwall, recurrent breast cancer and other sites. They are Daniel Kapp, M.D., Ph.D., Professor of Radiation Oncology at Stanford University Medical Center and Mark Dewhirst, DVM, Ph.D., Professor of Radiation Oncology at Duke University Medical Center. The first sitevisit by these experts took place in July 1993, just a few months after the beginning of this contract. We spent 1.5 days analyzing our thermal therapy program and our team received valuable suggestions on how to develop our clinical protocols and how to improve our design concepts for the site specific device. In addition to these sitevisits, the Harvard team has had design discussions with Michael Slayton, Ph.D. Research Director at Acoustic Imaging, Phoenix, AZ and Everette C. Burdette, Ph.D. Co-Investigator and Subcontractor for this research and Research Director at Dornier Medical Systems Inc. Champaign, Illinois and Atlanta, GA.

Several important clinical considerations were identified during the July 93 sitevisit.

The adjuvant thermal therapy must be non-disfiguring. The main concern when adding heat to the radiation is that the incidence of fibrosis may increase thus creating undesirable toxicity. It was recommended that we carefully perform a temperature escalation study, where the maximum temperature should not exceed 44°C and the minimum temperature should start at 40.5°C to be escalated to 42°C with careful analysis of short term toxicity. To achieve a narrow temperature range of 42°C to 44°C in heterogeneous breast tissue requires highly interactive power deposition control with knowledge of the effect of perfusion on the heat transfer.
Another clinical consideration pertains to women that have undergone lumpectomy/biopsy. The lumpectomy procedure leaves behind a scar cavity within the breast. The scar tissue has in general lower perfusion than surrounding normal tissue. The clinical experience of our site visitors is that the scar tissue easily over-heats during thermal therapy leaving burns and

blisters as undesired toxicity. The treatment system must have enough power control and power deposition resolution to reduce the temperature in and around the scar tissue.

The discussions with our site visitors as well as within the design team prompted the following changes in the system design and the clinical trials procedure:

1. The original design consisted of transducer elements arranged on a cylindrical surface that extends a solid angle enclosing the breast. The insonation portal is then chosen by geometrically rotating the device before or during therapy to deposit energy in the desired volume. This is described on page 13, the last paragraph, in the original proposal. To achieve the level of control recommended by Dr. Kapp and Dr. Dewhirst, we decided that geometric rotation was not ideal and a simpler solution is to completely surround the breast tissue with a cylindrical array that can be electronically scanned. An additional compelling reason for completely surrounding the breast is to utilize opposing transducers for measurement of transmission/attenuation of energy through the breast. This is discussed in section V-2-B and in section V-3. This design change has not resulted in any delays of the project.

2. Our original design specified the use of 1 to 2 MHz transducers (original proposal, page 13, last line). However, with this choice of frequency, we could not achieve the desired very narrow temperature range (42°C to 44°C) over a wide range of breast sizes. Thus, we had to perform additional computer simulations to determine the exact frequencies and characteristics of the applicator. Our extensive computer simulations have demonstrated that with multiple broad band frequencies (2.0 MHz, 2.5 MHz and 4.5 MHz) the temperature distribution can be controlled over a wide range of tissue perfusion characteristics. The optimal size of each transducer element was determined to be 1.5 cm square. This will give good enough geometric resolution to allow power deposition control in the lumpectomy scar cavity. This is described in section V-2-C. The modeling efforts and the need to determine optimal frequencies did result in a delay of specifying and building the transducer elements.

3. The need for monitoring the power deposition in three dimensions throughout the breast tissue was emphasized. In the final contract document, in the budget justification (under Non-Invasive Monitoring Equipment), we disclosed two alternative monitoring methods. The discussion stated that either non-invasive microwave radiometry or non-invasive ultrasound monitoring of acoustic parameters will be examined and evaluated. During year 01, we have selected to use ultrasound monitoring because:

a. Radiometry has limitations as to its ability to measure temperature beyond 3 cm depths and with good spatial resolution.

b. The modified applicator design surrounds the breast tissue completely with ultrasound transducers. We can operate opposing transducer elements in Transmit/Receive mode (T/R). By using T/R switching, we can monitor the attenuated and reflected energy in the tissue and calculate three-dimensional energy distribution patterns in breast tissue as well as determining the breast contour in real time.

c. The ultrasound monitoring capability was integrated into the overall system design as Task 8 (as opposed to be added after the completion of the therapy system) because of the requirement to multiplex numerous signals, add T/R capability to each transducer, and link to pulse control of the therapy power modules. Thus the actual design and building of a non-invasive monitoring system has moved from year 02 into year 01/02 (Task 16 in Table 1 and Table 5). The use of ultrasound for non-invasive monitoring of breast contour and attenuation will accelerate the fabrication and use of the breast treatment device as compared to the retrofitting of a radiometry system. The non-invasive monitoring subsystem is descibed in section V-3-G.

4. One main clinical task during year 01 was the development of a clinical phase I/II protocol. This work begun as planned but there was a change in the Phase I/II study originally proposed. Following recommendations from Dr. Kapp and Dr. Dewhirst during their first review visit (July 1993), we decided to start the clinical investigations with an equipment performance evaluation (Task 20) treating about six patients before embarking on a phase I/II study. The development of a protocol for this equipment evaluation phase is near completion and will be submitted early in year 02. After IRB approval it will be submitted to the USAMRDC for Human Subjects approval.

5. An early application for an IDE is recommended by Dr. Kapp. Dr. Burdette and Dr. Svensson are preparing the application, which is planned for submission during July 1994.(Task 15)

All theoretical simulations to aid the design have been completed during year 01 and the design and fabrication of subsystems have proceeded well. One important endpoint for judging progress in year 01 is the testing of the subsystems. The software testing started as scheduled in November 1993 and the test of one ultrasound applicator ring is currently underway (March-April, 1994). We expect to have the total treatment system constructed and tested during the second to the third quarter of year 02 (see task 16, 17 in Table 1 and 5), coinciding with the beginning of the patient/equipment evaluation phase.

On March 10 - 11, 1994, the same sitevisit team came back for a review of scientific progress during year 01. In general they were impressed by the advances during the first year and they felt that our response to suggestions from the previous sitevisit had been "innovative and thorough". During the March 10-11 sitevisit,

there were additional suggestions from our visitors that must be seriously considered in the interest of providing the best possible treatment to our patients. These are discussed in section VI. The new task/time schedule presented for year 01 (Table 1) reflects the program enhancements recommended through our peer review process. The suggestions have resulted in changes relative to the original proposal. Some of these changes are delays, and some represent improvements in the system delivery schedule, i.e. Task 8. Most of the task changes affect the schedule during the fourth quarter of year 01 and the first and second quarter of year 02. However, the main goal of the program, which is to offer a sophisticated thermal therapy option to women with breast cancer remains unchanged and is anticipated to be within the originally established three year time frame.

Table 1. Work year 01

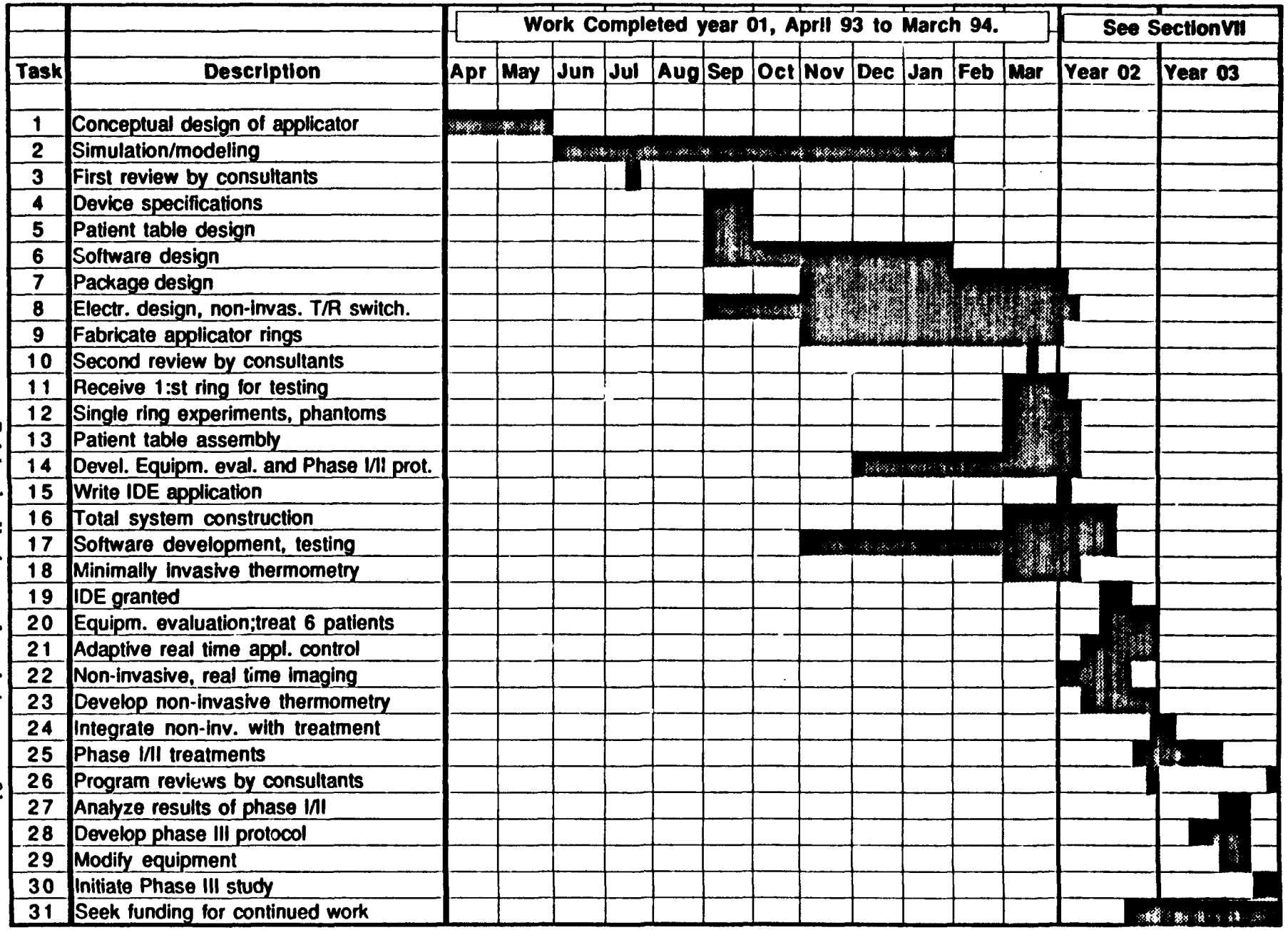

2. Ultrasound breast applicator design.

A. Breast applicator design criteria.

Design criteria for the breast therapy applicator include the ability to treat a wide range of breast sizes while providing control of power deposition in a manner which permits therapy of the entire breast or of a pre-defined sub-region, such as a quadrant of the breast. The applicator must be able to accommodate sizes of the breast ranging from a few cm diameter up to a maximum of about 15 cm at the base (See Table 2) and still provide control of treatment within a narrow temperature range (42^0C - 44^0C) over a reasonably wide range of tissue perfusion, i.e. 30 to 200 ml, kg^{-1}, min^{-1}. The therapy system includes the ability to monitor temperature and other vital tissue characteristics by using minimally invasive techniques, later to be extended to non-invasive monitoring techniques.

Based on these requirements, design criteria were developed for the breast therapy applicator. Included in the criteria is the patient positioning specification, which is essential in defining the applicator geometry.

Design Criteria:

- Prone patient position with breast extended downward.
- Cylindrical applicator geometry surrounding breast target.
- Ability to accommodate breast diameters of 15 cm or less, measured at the chestwall.
- Ability to accommodate treatment of breast length between 3 cm and 15 cm.
- Spatial resolution control of therapy field to within 1.5 cm vertically and to within one quadrant of the breast.
- Optimize temperature distribution and minimize any potential toxicity to the breast by:
  a. providing temperature control of the breast surface using the surrounding temperature controlled water bath.
  b. provide means for monitoring of the operation of the applicator using opposing pairs of transducers to measure the energy transmitted through the breast.
  c. provide means for accommodating probes for invasive measurements of temperature during therapy.
  d. provide means for using reflected ultrasound energy to define the contour of the breast within the applicator.

B. Review of designs evaluated.

During the preparation of the proposal and during the course of the first year of the contract, a number of different approaches for therapy delivery and monitoring of therapy were examined. Among the approaches and designs considered, were multiple planar ultrasound transducer arrays and curvilinear arrays for therapeutic application. For both approaches we planned the use of microwave radiometry for non-invasive monitoring of the temperature during therapy. The radiometry evaluated consisted of two separate planar arrays of microwave stripline antennas on opposing sides of the breast. Each of the arrays would sense the tissues directly beneath the individual elements and by sensing from opposing sides, adequate penetration depth for most typical breast sizes would potentially be achievable. A diagram of the applicator and radiometer design set-up is shown in Figure 1.

Padded Patient Table

TOP VIEW

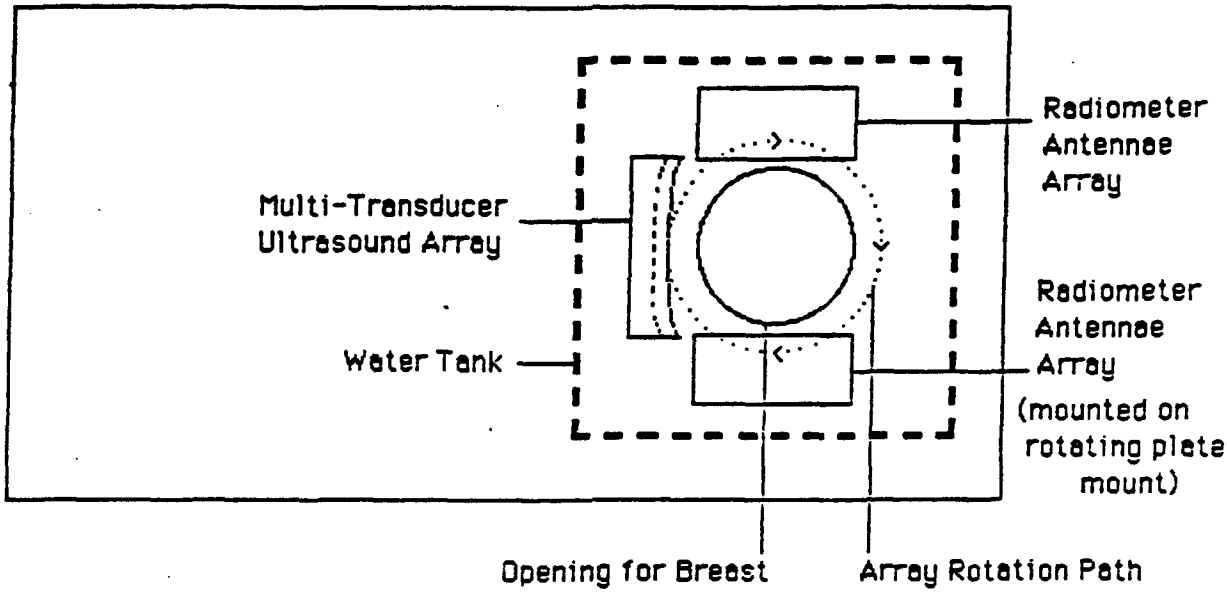

SIDE VIEW

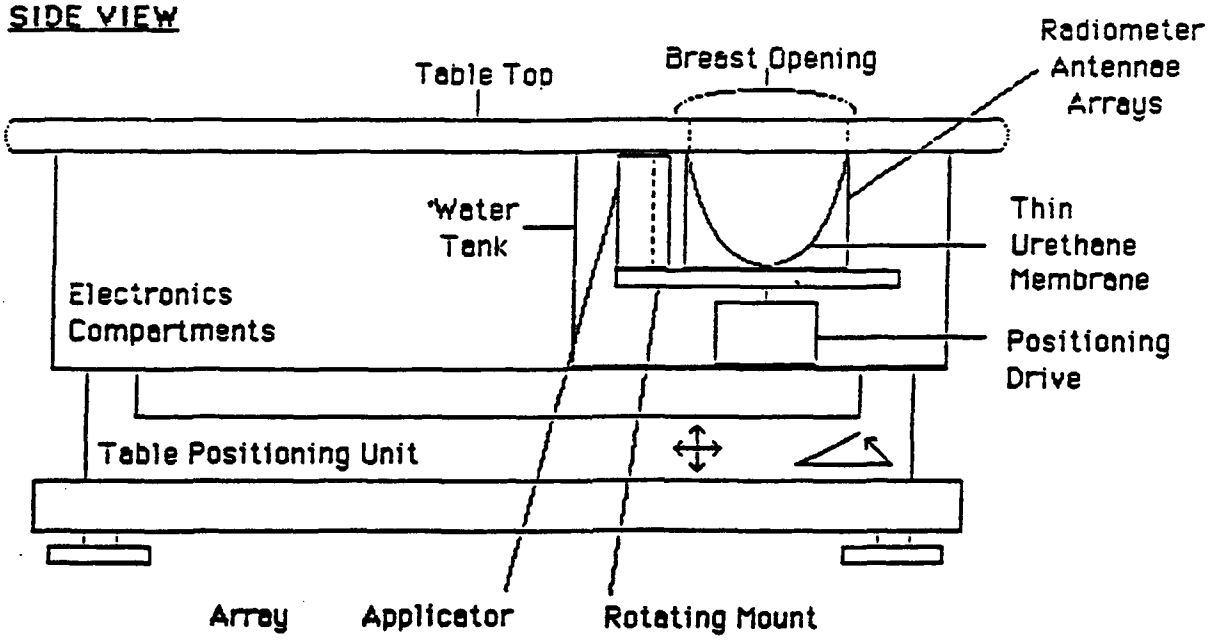

Figure 1. Diagram of an early design of the breast treatment system with two microwave antennae arrays located on opposing sides of the breast and orthogonal to the ultrasound therapy array.

As a result of analyses performed, we learned that planar or curvilinear arrays do not take advantage of the cylindrical breast geometry and consequently, the geometric gain factor is relatively small, thus limiting the size of the breast which could be treated. Furthermore, with the planar geometry, control of the power deposition to achieve adequate therapy to edges of the treated breast would be quite difficult to attain. Our external review committee emphasized the need for sophisticated power deposition control to avoid heating the lumpectomy scar and to achieve a controlled, narrow therapeutic temperature range over a realistic range of tissue perfusion. Thus, the planar geometry was abandoned and a cylindrical geometry for the breast applicator design was chosen. With the cylindrical transducer array completely surrounding the breast an increased aperture gain (geometric gain factor) is obtained, resulting in increased penetration into the breast tissue. Large size breasts can be more uniformly heated with this geometry. The diameter of the cylindrical applicator is 25 cm. Based on our experience of treating approximately 500 breast cancer patients per year, we "bracketed" a range of breast sizes, by selecting and measuring a few very large, medium and small breasts (altogether 10 patients). The chosen applicator diameter is large enough to treat the largest of the breasts identified in this manner.

Various applicator designs using a cylindrical geometry were evaluated. Each of these were modeled using the simulation program described in section V:2:C. The modeling included examination of various ultrasound excitation frequencies, applicator diameters, transducer aperture dimensions, excitation wave forms and transducer configurations. The conclusion of this effort is the applicator parameter configuration as depicted in Figure 2a and Figure 2b. These applicator design parameters (transducers, frequencies, size, etc.) were utilized in the theoretical simulations. The applicator rings are loaded with multi-frequency transducers operating at 2.0 MHz, 2.5 MHz and 4.5 MHz.

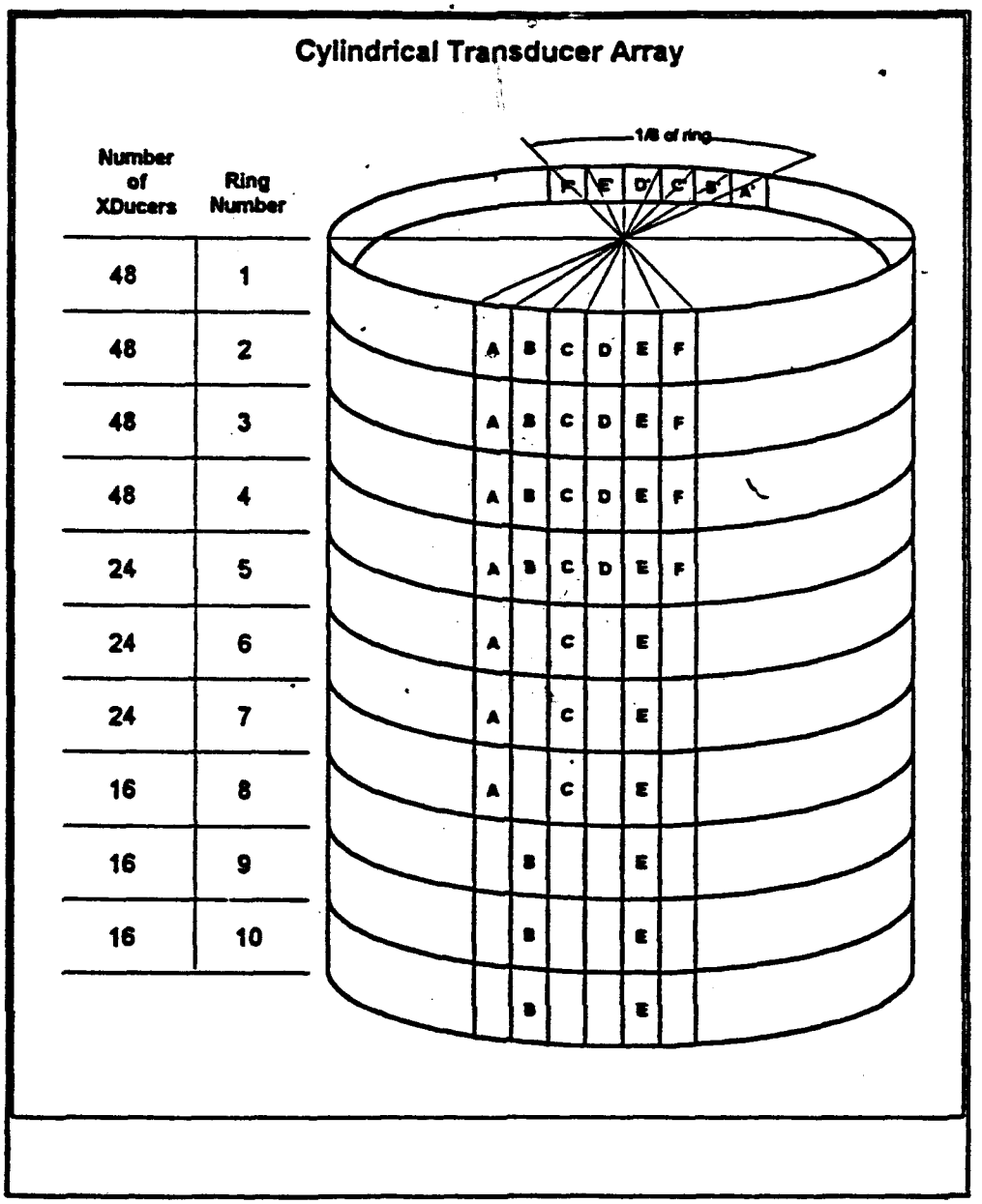

Figure 2 a. Applicator showing ten stacked rings forming a cylinder. The table on the left shows the number of transducers loaded in each ring.

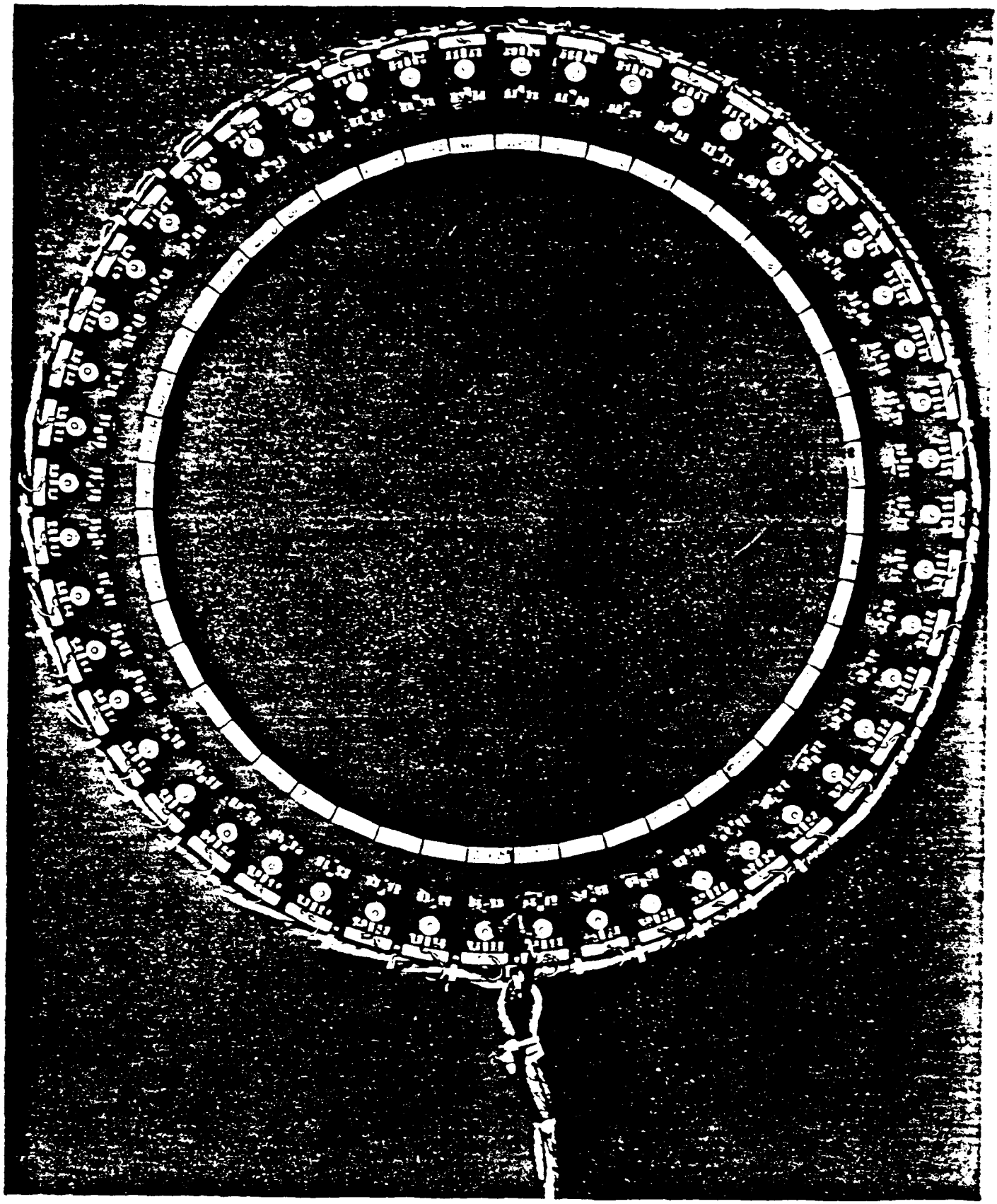

Figure 2b. Photograph of a single ring transducer assembly

C. Theoretical simulation of the breast ultrasound applicator.

Some of the results from the theoretical simulations will be presented at the North American Hyperthermia Society Meeting in Nashville TN, April 1994 and at the IEEE Meeting on Electromagnetic Compatibility, Sendai, Japan, May 1994 (See Appendix 1).

(1) Methodology:

The thermal treatment of the breast will be done with the patient in prone position. The breast is submerged through a hole in the treatment table into a water filled applicator housing (Figure 10, 11). A cylindrical array of individually controlled ultrasound transducers surround the breast (Figure 2a). The ultrasound wave enters the breast tissue tangential to the chest wall to minimize the interaction with the ribs. To accommodate a large sized breast, the diameter of the cylindrical array is 25 cm. This is enough of a margin to accommodate asymmetry in the breast contour and alignment of the breast in the cylinder. The cylindrical applicator consists of a stack of 9 rings (10 rings are shown in figure 2 a), each being approximately 1.5 cm high. The ring located at the base of the breast contains 48 transducers. The number of transducers in each ring decreases toward the apex of the breast. The ring closest to the nipple contains 16 transducers (Table 3 and 4 in Section V-3). Each ring deposits power in a plane parallel to the chest wall and the heating effect of each ring is relatively independent of adjacent rings. This property facilitates control of heating.

The clinical specifications and capabilities of the breast applicator are listed in Section IV-1. The technical specifications and operating parameters for the cylindrical array were determined by computer simulations using several common treatment conditions. The Hewlett-Packard 9000/735 workstation purchased from this contract made these complex and lengthy calculations practical. A three-dimensional acoustic and thermal computer model was used. The simulation consists of three parts.

The first part is the geometric model, which is shown in Figure 3. The breast surface is assumed to be a parabola with a height of H cm and a diameter of D cm at the base. The clinically relevant breast sizes, with the patient prone and the breast submerged into the water filled cylindrical applicator, were determined by measuring ten volunteer patients in our clinic. The intent was not to make a random statistical study of breast sizes. Instead, we use our experience of treating 500 breast cancer patients per year and select and measure a few very large, medium and small breasts. The data show that the average breast in prone position was 11 cm long with a maximum diameter at the chest wall of 12 cm. The maximum breast dimensions in this group of ten patients was 15 cm long and 15 cm diameter. The temperature

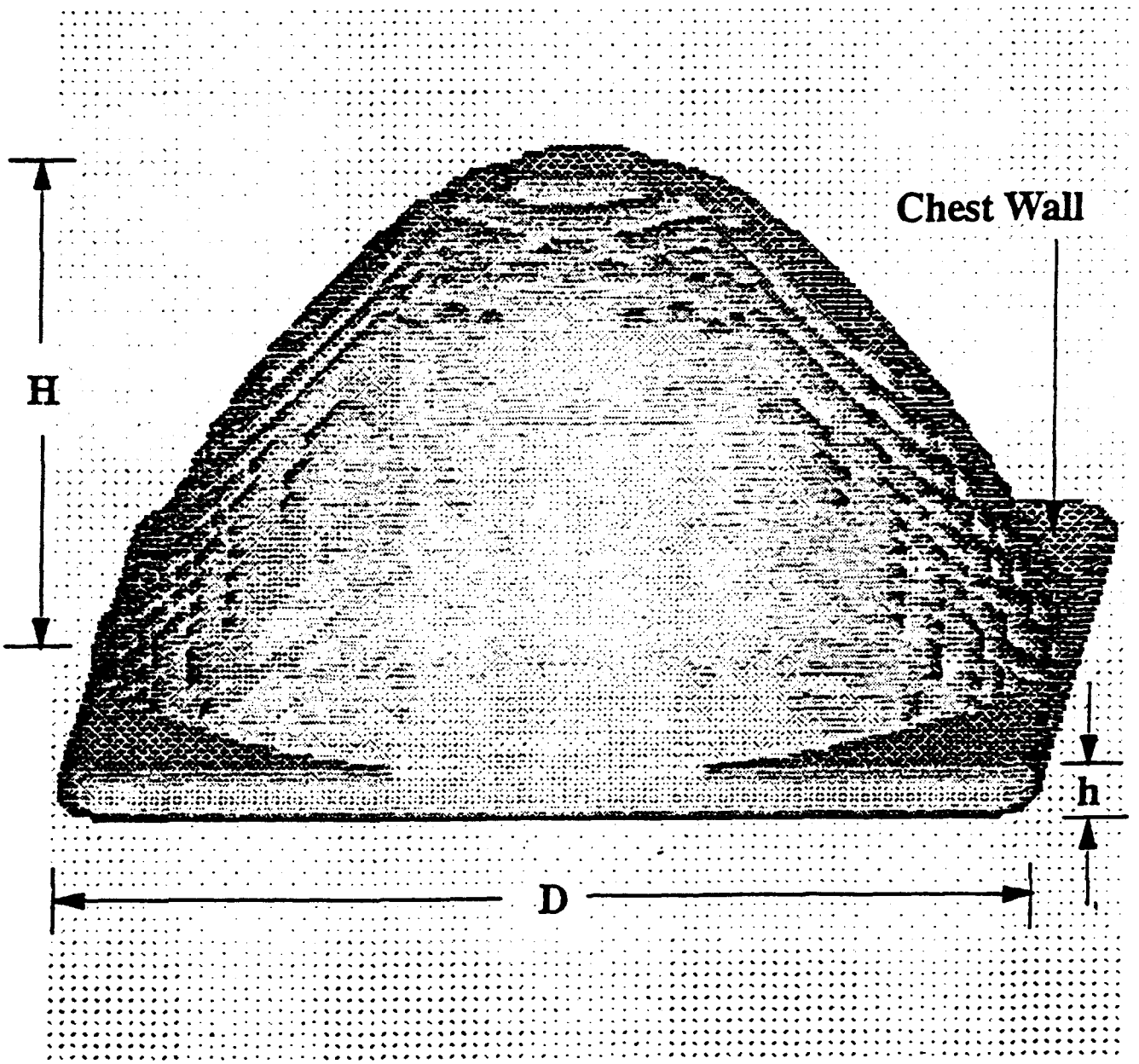

Figure 3. Theoretical breast model. *D* is the diameter at the base of the breast. *H* is the height of the breast. At a depth *h* into the chestwall we assume the temperature boundary to be 37°C.

border conditions at the external breast surface can be controlled by adjusting the temperature of the water inside the cylindrical applicator. The temperature border condition at the chestwall is assumed to be 37°C at a depth of h cm below the chestwall. The parameters H, D and h are listed in Table 2 together with several other important ultrasound interaction parameters.

Table 2. Parameters used in the model.

Parameter [Ref.]	Default value	Range studied
Attenuation breast, [11]	0.086 ($f^{1.5}$ Np,cm^{-1})	0.052-0.12
Attenuation water, [13]	0.0002 (f^2 Np,cm^{-1})	0.0002
Conductivity [3]	0.5 (W,m^{-1},K^{-1})	0.4 - 0.8
Perfusion, [20]	30 at 37°C 100 at 44°C (ml,Kg^{-1},min^{-1})	30 -100 30 - 200
T_{water}, °C	37°C	30°C - 40°C
D, cm	15	10 - 15
H, cm	8	5 - 11
h, cm	0.9	0 - 1.2

The second part of the model calculates the energy deposition in the breast tissue resulting from absorption of ultrasound energy. The ultrasound is assumed to originate from a continuous wave (CW) rectangular plane source [15]. In this method, the plane source is divided into rectangular elements, surrounded by a rigid baffle. The method sums contributions from these small elements to a given field point. The model is limited by only allowing one medium for the calculations. However, we have modified the Ocheltree model to allow two media, namely the water in the applicator housing and the breast tissue submerged into the water. This modification is possible under the assumption that the physical density and the speed of sound for water and breast tissue are very close so that their acoustic impedance is about the same. With about the same acoustic impedance between breast tissue and water, the energy loss due to ultrasound reflection from the breast surface can be ignored. Reflection from breast

tissue has been measured to be about - 40 dB [19], which suggests that our assumption is reasonable. It also means that the acoustic impedance match between water and breast tissue is excellent and that very little energy is reflected away from the breast surface.

Under the condition of good acoustic impedance match we can follow the same arguments as used in the deduction of the Ocheltree formula for one medium. [15], except a change of the exponential decay factor from $e^{-\alpha r - jkr}$ to $e^{-\alpha_w r_w - \alpha_b r_b - jkr_w - jkr_b}$.

α is the attenuation coefficient and r is the distance between the field point to the elemental area of the planar source and k is he wave number. α_w and α_b are the attenuation coefficients in ater and breast. $r_w + r_b$ is the distance from the field point to the planar source and r_w and r_b is the distance in water and breast tissue respectively. For a uniformly excited rectangular planar source, the sound pressure amplitude P_0 at a point inside the breast is given by a summation of complex terms, representing the pressure due to a rectangular elemental source.

$$P_0 = \frac{j\rho\Delta A}{\lambda} \cdot \sum_{n=1}^{N} \frac{u}{R} \cdot e^{-(\alpha_w r_w + \alpha_b r_b + jkr_w + jkr_b)} \cdot \sin c\left(\frac{kx_n' \Delta w}{2(r_w + r_b)}\right) \cdot \sin c\left(\frac{ky_n' \Delta w}{2(r_w + r_b)}\right)$$

ρ is the density, c is the phase velocity of the sound waves, u is the complex surface velocity for all the elements, λ is the wavelength, $\Delta A = \Delta h \times \Delta w$ is the elements size, x_n^1 and y_n^1 are the coordinates of the field point with respect to the center of the element n.

The SAR (specific absorption rate) deposited by the transducer inside the breast can be calculated from the sound pressure amplitude P_0 at the point:

$$SAR = \frac{\alpha_b \cdot P_0^2}{\rho \cdot c}$$

The breast volume is divided into voxels and the SAR is calculated to the center of each voxel. These voxels are also used in the thermal calculation, which will be discussed in the following paragraph. The SAR in each voxel is normalized to the total energy deposited inside the breast from all the transducers. Since this calculation is very CPU consuming, it is done once for each configuration and then stored in the data base. The total SAR in the field point is the arithmetic sum of that contributed by each transducer.

The third part of the model provides a solution to the standard bio-heat transfer equation. Such solutions result in temperature distributions as a function of time in the breast tissue.

It is convenient to write the bio-heat transfer equation

$$\frac{\partial T}{\partial t} = (K/c_v)\nabla^2 T - (T - T_0)/\tau + q_v/c_v$$

T is the temperature and T_0 is the body temperature, i.e. 37°C. K is the thermal conductivity coefficient (W, m^{-1}, K^{-1}), c_v is the heat capacity per unit volume (J, g^{-1}, K^{-1}), q_v is the heat production rate per unit volume (W, kg^{-1}), i.e. SAR. τ is the perfusion constant (s), which most commonly is expressed as perfusion rate (ml, Kg^{-1}, min^{-1}),
where $\tau = \rho \times c_v \times (w \times c_{vb})^{-1}$.

The usefulness and limitations of this model has been discussed by many authors (7, 9, 3, 18]. A major limitation of this model is the incorporation of perfusion resulting from the blood flow. However, for breast tissue, we assume that, although variable, local perfusion changes are not the dominating factor, due to absence of large blood vessels. Therefore, we believe that the bio-heat transfer model shown above is reasonable.

The finite difference method is used in the 3-D numerical calculation [16]. This method gives a great deal of flexibility to deal with different geometries and boundary conditions. Starting from a given initial condition the temperature evolution for a whole treatment session can be simulated. A voxel size of 2x2x2 mm^3 or 3x3x3 mm^3 is used for the two breast sizes listed in Table 2. This matrix size is a compromise between an acceptable accuracy and reasonable CPU time required. The calculation of T is performed at every three second interval. This time step is sufficiently small to satisfy the temperature stability criteria.

The tissue parameters listed in Table 2 are based on the published data [11, 13, 3, 20]. Relevant perfusion rate data for breast is not available. Instead, we used data for resting muscle tissue [20]. In this model the perfusion rate is increasing linearly by a factor of three when the temperature is elevated from 37 ^{o}C to 44 ^{o}C.

The initial temperature inside the breast is assumed to be 37^{o}C uniformly. Near the surface the temperature could be lower than this, but it makes little difference after a few minutes of heating. The temperature in the water can be adjusted and maintained at any value between 30^{o}C and 40^{o}C. Again, at depth h cm below the chest wall, the temperature is assumed being always maintained at 37 ^{o}C.

(2) Results:

The computer model calculates the SAR and temperature distribution at three minutes interval during the complete treatment simulation. Initially the default values in Table 2 are used for the treatment simulation.

The range of values shown in the third column of Table 2 is then used to determine the optimal operating characteristics and design specifications of the breast applicator. The range of values account for uncertainties and normal variations in these parameters.

As seen in Figure 2a, the transducer rings are stacked to form a cylinder into which the breast is submerged. The power deposition to a certain point in the breast is delivered primarily from the ring that defines the plane in which the point is located. The control of the temperature at that point is thus, to a first approximation, reduced to control of the power deposition within each ring. This is seen in the top panel of Figure 4, where the SAR distribution show five distinct cross-sectional planes, each plane defined by the individual rings. As shown in the lower panel of Figure 4, at steady state temperature, most of the breast tissue is surrounded by the 42^{o}C iso-temperature line and the maximum temperature is 43.7^{o}C.

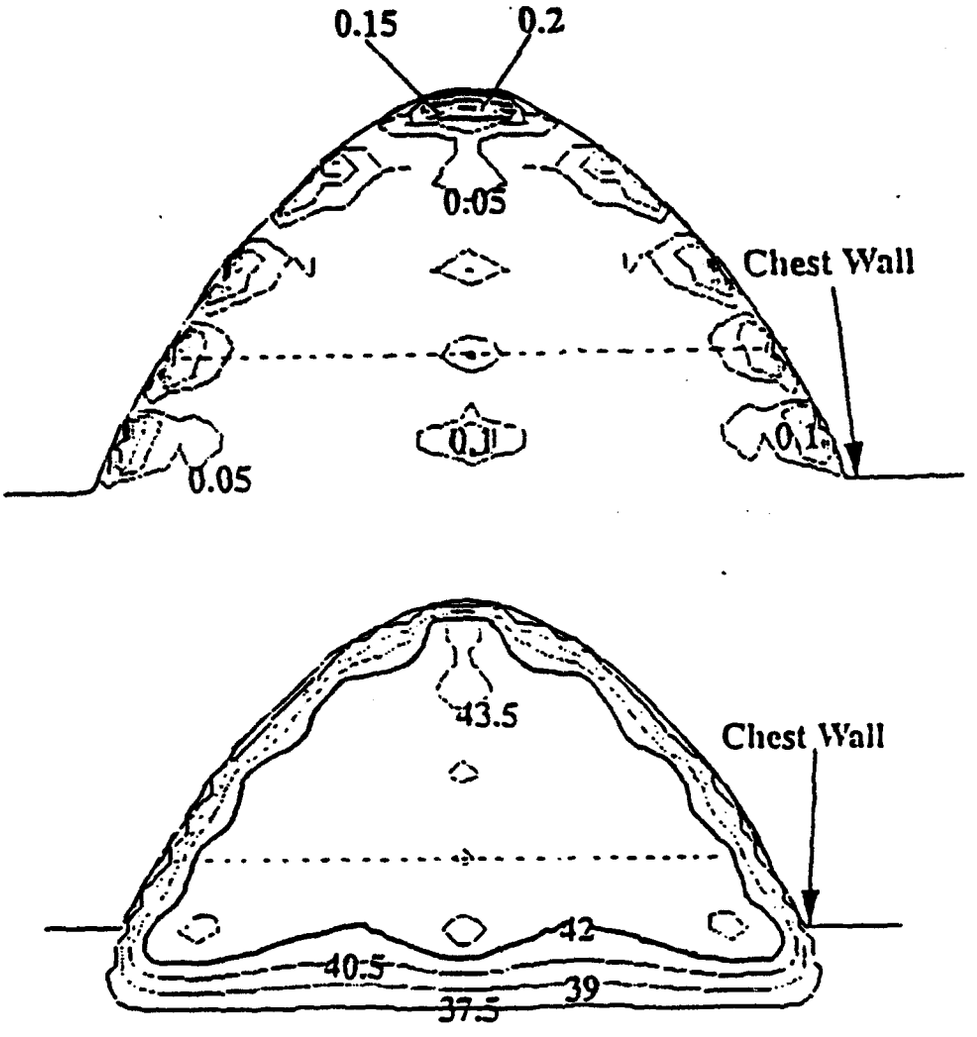

Figure 4. Top panel: SAR distribution (W/cm^3) required to maintain steady state temperature $42^oC \leq T \leq 44^oC$. The calculation is for a large breast with D = 15 cm, H = 8 cm and h = 0.9 cm.
Bottom panel: The steady state temperature distribution. The calculation is optimized for perfusion rate of 30 ml,kg^{-1},min^{-1} at 37^oC increasing linearly with temperature to 100 ml,kg^{-1},min^{-1} at 44^oC. The maximum temperature is 43.7^oC. Dotted line is the level of the cross-sectional view shown in Figure 5.

Figure 5 shows the SAR and the equilibrium temperature distributions of Figure 4 in the cross-sectional plane.

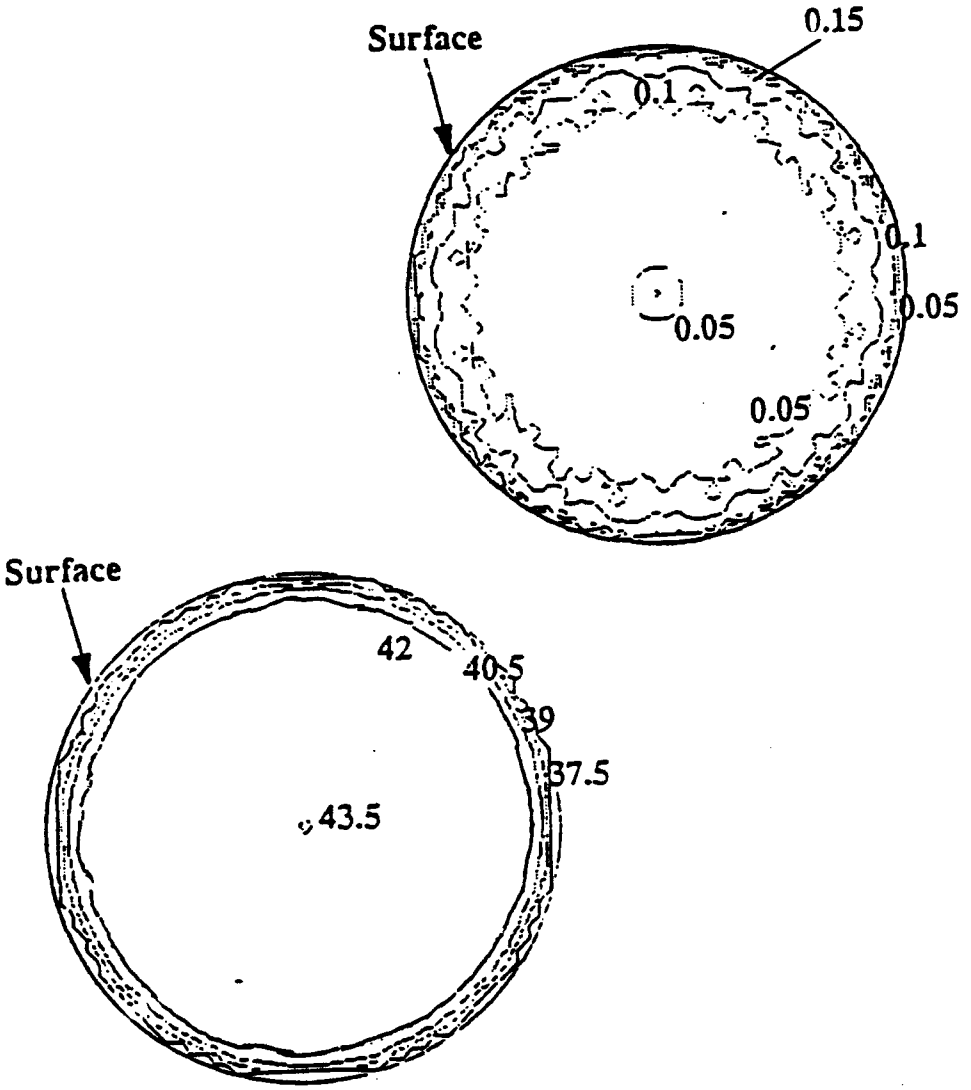

Figure 5. Top panel: SAR distribution (W/cm^3) required to maintain steady state temperature equilibrium $42^oC \leq T \leq 44^oC$. The displayed cross-section is shown as a dotted line in Figure 4. The diameter is 12 cm.
Bottom panel: The steady state temperature distribution. Perfusion rate 30 ml,kg^{-1},min^{-1} at 37^oC and 100 ml,kg^{-1},min^{-1} at 44^oC. The maximum temperature is 43.7^oC.

Breast tissue perfusion rate and its dependence on the temperature and other physiological factors determine the choice of ultrasound frequency and power. We have assumed that the perfusion rate in breast is similar or less than that of resting muscle, because we were unable to find that specific value in the literature [8]. This is a reasonable assumption because breast tissue has a high content of adipose tissue, which would tend to reduce the perfusion rate relative to muscle. However, it is desirable to test the effect of increased perfusion rate on the ability to control the equilibrium temperature distribution.
If we increase the perfusion rate to 100 ml,kg^{-1},min^{-1} at 37°C and 200 ml,kg^{-1},min^{-1} at 44°C, and if we maintain the same SAR distribution as shown in Figure 5 (top panel), than the corresponding equilibrium temperature distribution is shown in Figure 6. The temperature distribution show heterogeneity and does not reach the required $42°C \leq T \leq 44°C$.

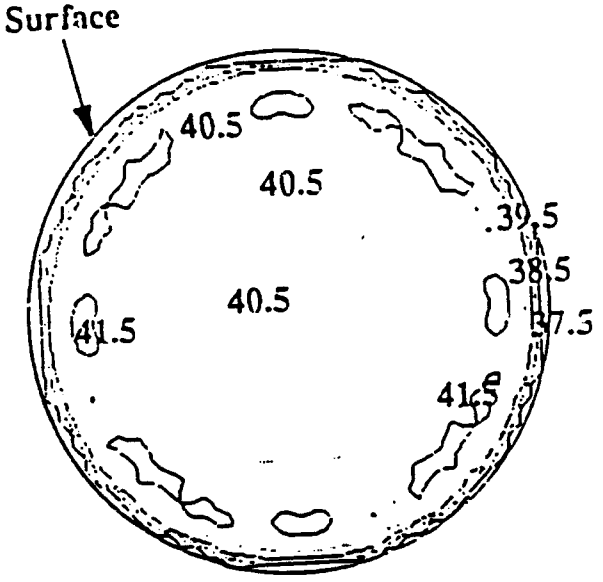

Figure 6. The steady state temperature distribution. Perfusion rate increased to 100 ml,kg^{-1},min^{-1} at 37°C and 200 ml,kg^{-1},min^{-1} at 44°C. SAR distribution as in top panel Figure 5.

To achieve an acceptable equilibrium temperature distribution, under this high perfusion rate, we need to increase the SAR distribution. Figure 7 (top panel) shows the SAR distribution, which results in an acceptable equilibrium temperature distribution, $42^{o}C \leq T \leq 44^{o}C$ (bottom panel in Figure 7).

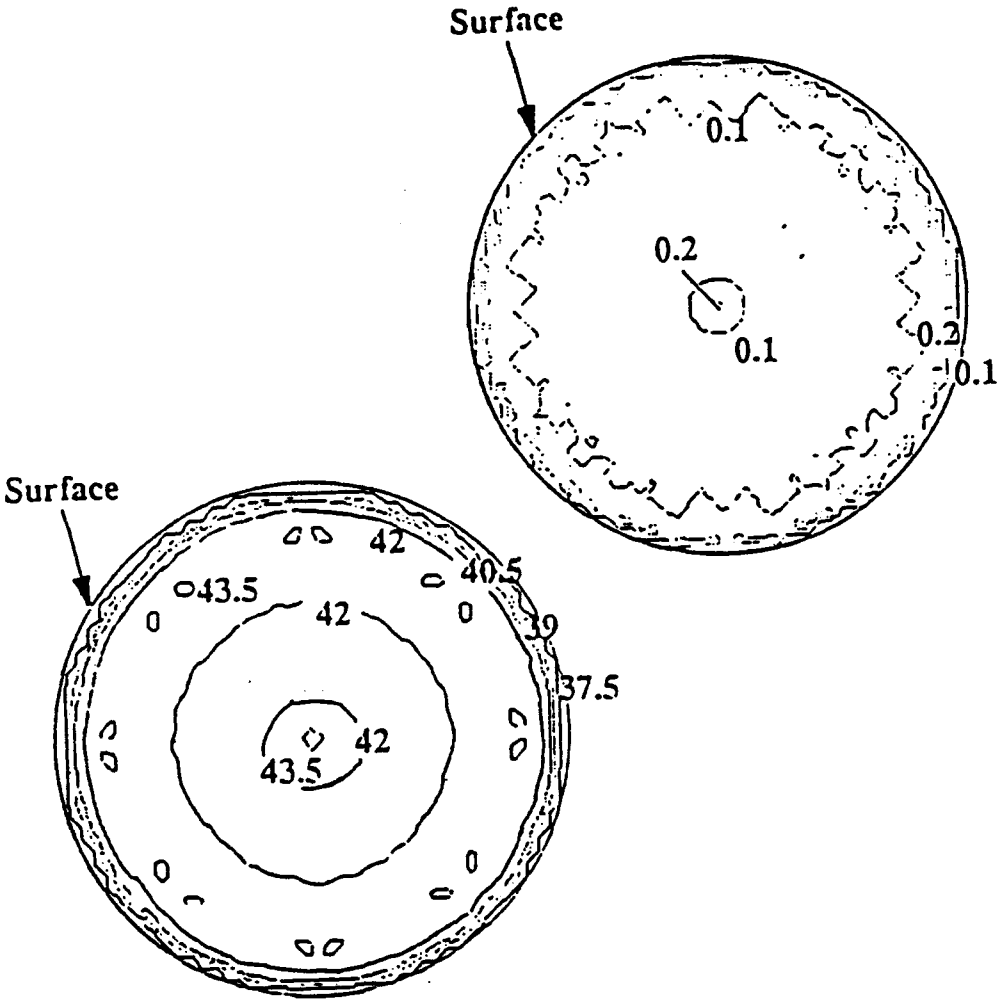

Figure 7. Top panel: SAR distribution (W/cm^3) to maintain steady state temperature equilibrium $42^{o}C \leq T \leq 44^{o}C$. Perfusion rate increased to 100 ml,kg^{-1},min^{-1} at $37^{o}C$ and 200 ml,kg^{-1},min^{-1} at $44^{o}C$.
Bottom panel: The resulting steady state temperature distribution.

Figure 8 illustrates the ability to heat a quadrant of the breast. It is achieved by depositing energy in the periphery of the target volume using a proper mix of high and low frequency ultrasound.

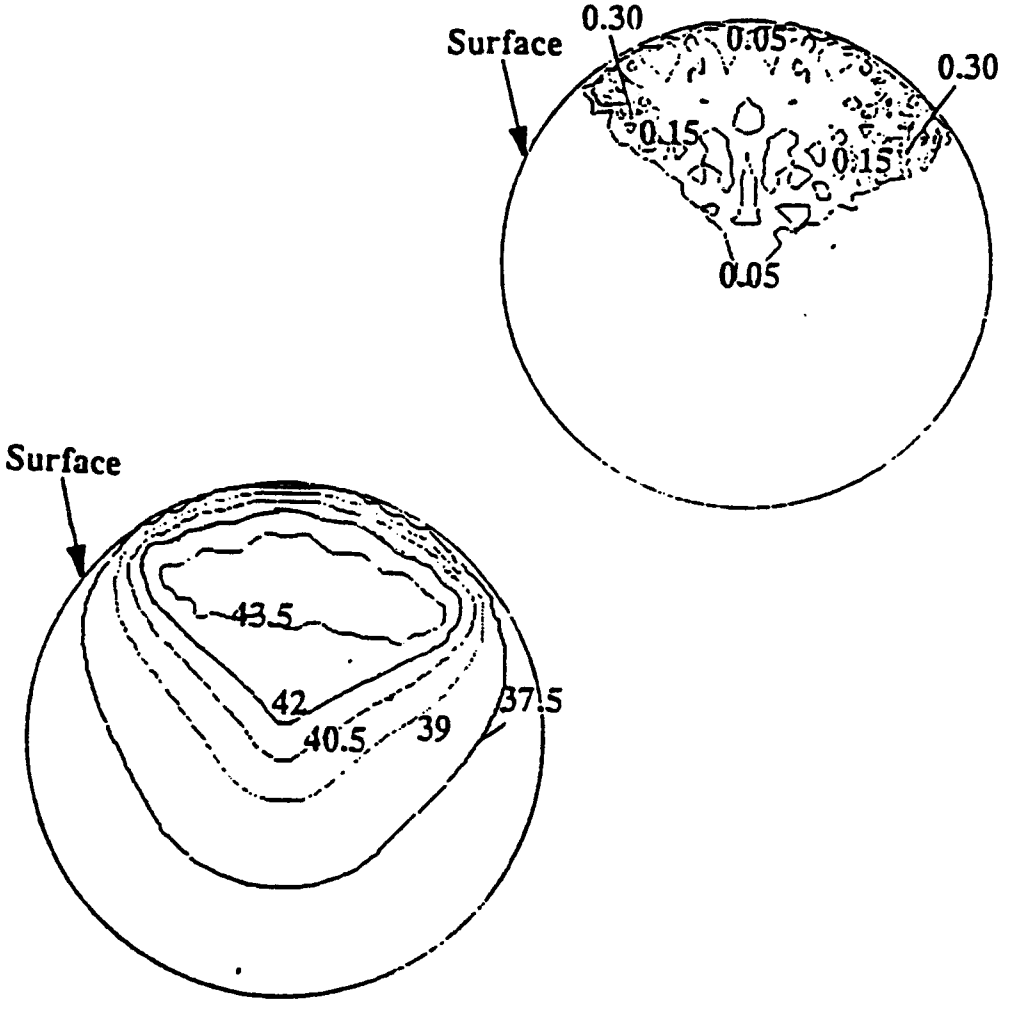

Figure 8. Top panel: SAR distribution (W/cm^3) required to maintain steady state temperature equilibrium $42^oC \leq T \leq 44^oC$ for treatment of a quadrant of the breast.
Bottom panel: The resulting steady state temperature distribution. The maximum temperature is 43.7^oC.

(3) Conclusions:

There is a significant normal variation in the numerical values of ultrasound interaction parameters and heat transfer parameters in tissue. There is also a great deal of uncertainty in these values. We have determined a range of operating characteristics of the breast applicator accounting for these variations and uncertainties by using computer simulations. We have concluded that there exists a need to build a multiple frequency transducer array. A low ultrasound frequency, in the range of 1.5 - 2.5 MHz, is needed to compensate for the heat removed by the blood flow and permits an initial quick temperature elevation at depth in the breast tissue. Due to considerable uncertainty in the breast tissue attenuation, a broad frequency band for the low frequency transducers is desired. A high frequency transducer, in the range of 4-4.5 MHz, is needed to maintain a steep temperature gradient near the surface of the target volume. In these models, the high and low frequency transducers are mounted alternatively in each ring. Each ring offer power and frequency control sufficient to heat the whole breast or a quadrant of the breast to a minimum of 42°C but not exceeding 44°C.

3. System Design and Development

A. General System Description and Intended Use

The breast ultrasound therapy system is intended for use in thermal therapy of breast cancer. The synergism of thermal therapy with radiation is well known, and the rationale and potential roles for thermal therapy with this device for treatment of breast cancer have been discussed in Section IV of this report. Thermal therapy is attained by means of a breast site-specific ultrasound applicator coupled with minimally-invasive and non-invasive thermometry.

The device consists of the hardware components illustrated in Figure 9. A breast site-specific cylindrical array applicator of ultrasound transducers is used for thermal therapy induction and for multiple monitoring functions. The "heart" of the hardware consists of the cylindrical array of transducers which both deposits power into the breast tissue for therapy and monitors the dynamic course of the treatment. The ultrasound array applicator subsystem is described in more detail in subsection V:3:B.

The ultrasound transducers are geometrically arranged and operated to provide several monitoring functions. One important monitoring function is to determine the breast contour and the location of the breast within the treatment cylinder. This is done by operating the transducers in diagnostic pulse echo mode.

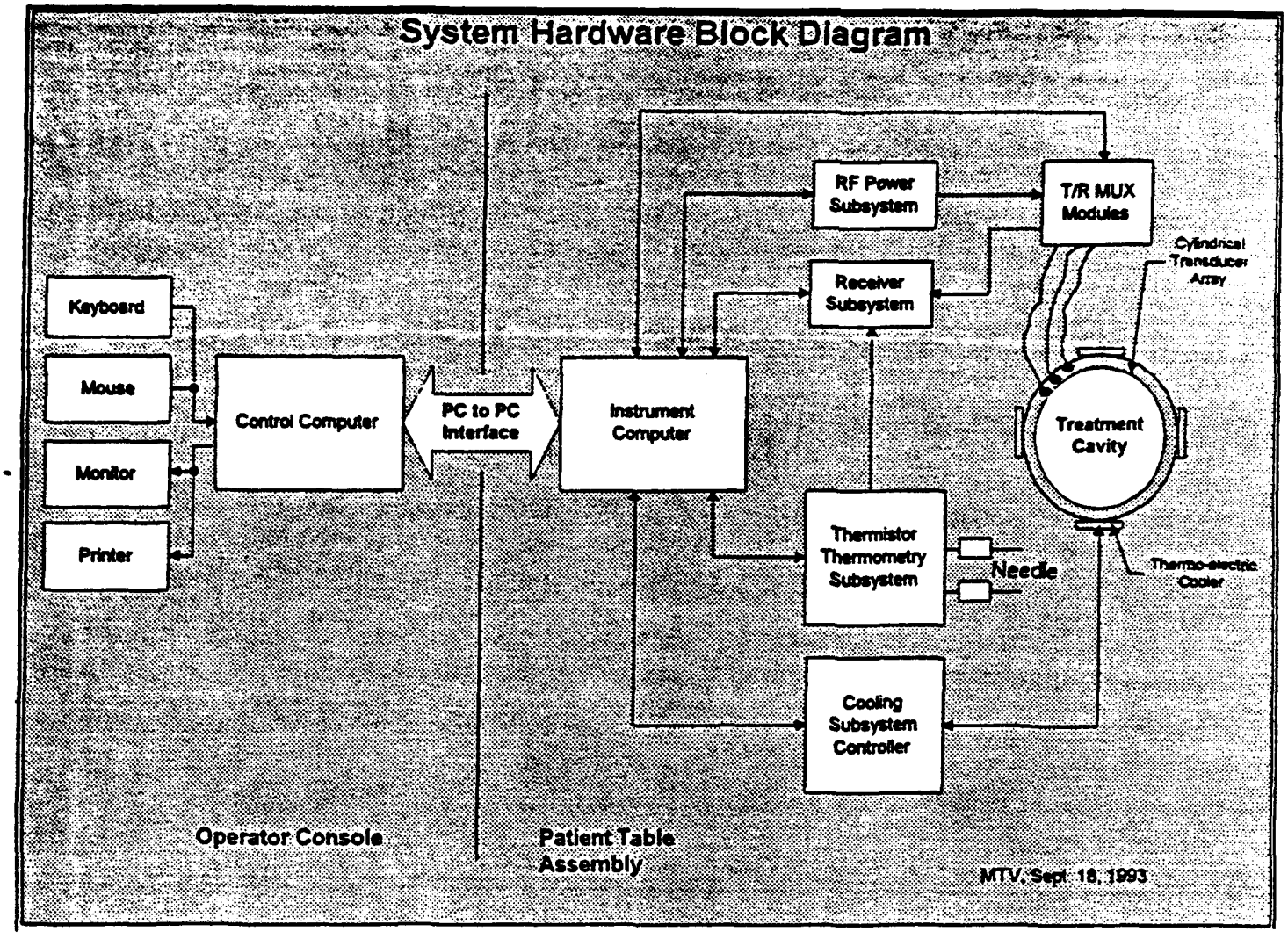

Figure 9. System hardware block diagram.

The use of through-transmission of power during therapy for determination of absorbed power distribution (SAR) in the breast tissue is being examined for monitoring. Also, measurements of ultrasound "time-of-flight" throughout regions of the target breast tissue during therapy will be performed. Such data referenced to a limited number of invasive temperature measurements and SAR measurements may provide for non-invasive mapping of temperatures throughout the treatment volume. It will also be indicative of tissue changes that may be important in correlating tissue toxicity with the breast treatment.

The system consists of an Instrument Computer (Figure 9) which provides all direct control and data interaction with the RF Power Subsystem, Receiver Subsystem, Transmit/Receive/Multiplexing Modules, Thermistor Thermometry Subsystem, and Cooling Subsystem. The system electronics, Instrument Computer, and Cylindrical Transducer Array/Treatment Cavity are integrated into a Patient Table Assembly/Subsystem, which provides a comfortable treatment support for the patient, accurate positioning of the breast within the treatment cavity, and a convenient means for consolidating system components and functions. All system design was completed during year 01 of the contract. A comprehensive system design document is available upon request.

The table system is discussed further in section V-3-C below. The RF Power Subsystem generates the drive power for the transducers during therapy and is used for pulse-echo imaging of the breast contour and for velocity measurements during a brief period every 4 seconds when the therapy is gated "off". The T/R MUX Modules select which transducers are active for receiving or transmitting at any given moment during therapy.

The Thermometry Subsystem is used to provide high density (14 sensors per needle) invasive thermistor thermometry information within the breast regions of interest. This is a stand-alone module, which will be integrated into the overall system in year 02.

The Cooling Subsystem consists of thermoelectric coolers attached to the cylindrical array shell and a temperature controller interfaced to the Instrument Computer. The Control computer, including all operator interfaces, display and treatment recording functions, is located separately in the Operator Console.

B. Transducer Array Applicator Subsystem

The Transducer Array Subsystem is illustrated graphically in Figure 2a. The array will consist of nine (9) individual rings (10 rings are shown in figure 2a), which are "stacked" with water-tight seals between rings. Each ring accommodates up to 48 transducers. The exact configuration and operating characteristics of the cylindrical transducer array has been extensively studied

using theoretical simulations described in Section V-2-C. Based on the analyses performed, it is not necessary to "fill" all available ring locations with transducers. Table 3 states the planned transducer configuration and number of transducers for each ring. Each transducer is square having dimensions of 1.5 cm x 1.5 cm on a side. Spacing between transducers along vertical dimension of the cylinder is 2.4 mm. Therefore, 9 rings accommodate breast "lengths" of 15 cm or less. The top five rings (1-5) in the cylinder (closest to patient table top and patient chest wall) will each have 48 transducers. The next two (6-7) will each have 24 equally-spaced transducers. The lowest two rings (8-9) will each have 16 equally-spaced transducers. Table 4 shows the number of rings, transducers per ring, and dimensions of a "large" and "small" breast within the treatment cylinder.

Ring No.	FQ 1 (MHz)/No. XDCRS	FQ 2 (MHz)/No. XDCRS	Total XDCRS
1	4.5 / 24	2.0 / 24	48
2	4.5 / 24	2.0 / 24	48
3	4.5 / 24	2.5 / 24	48
4	4.5 / 24	2.5 / 24	48
5	4.5 / 24	2.5 / 24	48
6	4.5 / 12	2.5 / 12	24
7	4.5 / 12	2.5 / 12	24
8	4.5 / 12	2.5 / 4	16
9	4.5 / 16		16
10	4.5/16	Total	320

Note: All transducers have 30% frequency bandwidth

Boards	RF Amplifiers
20 Amp/Mux/RCUR Boards	80 Channels
x 4 Channels/board	x 4 XDCRS/channel (Mux)
80 Channels	320 XDCRS

Table 3. Specifications of the ten rings in the cylindrical array.

CYLINDRICAL ARRAY APPLICATOR DESIGN				
Total Cylinder I.D. = 25 cm Transducers: 15 mm x 15 mm Rings of Transducers: 10 (numbered from top down) Each 1/8 ring vertical section driven by RF Amplifiers whose outputs are multiplexed to "step around" ring				
Ring No.	No. Transducers	Breast Size (cm) Large	Small	No. Transducers in 1/8 of ring
1	48	16	8	6
2	48	14	7	6
3	48	12	6	6
4	48	10	5	6
5	48	8	4	6
6	24	7	3	3
7	24	6	2	3
8	16	4	0	2
9	16	3	0	2

Table 4. The table illustrates how many rings and transducer elements in a ring that will be activated when treating a large breast and a small breast respectively.

C. Patient Table Subsystem

The patient table subsystem in shown in the two perspective illustrations in Figures 10 and 11. The patient table is designed to maximize utilization of symmetry of the breast by positioning the patient in a prone position with the breast suspended through an opening in the table top. The table top consists of sheet steel with a tubular steel outer frame fabricated to provide for insertion of a 1.5" foam padding insert. The foam is sealed and the entire table top covered with a naugahyde covering which is stretched tight and snapped into place, and easily removed for

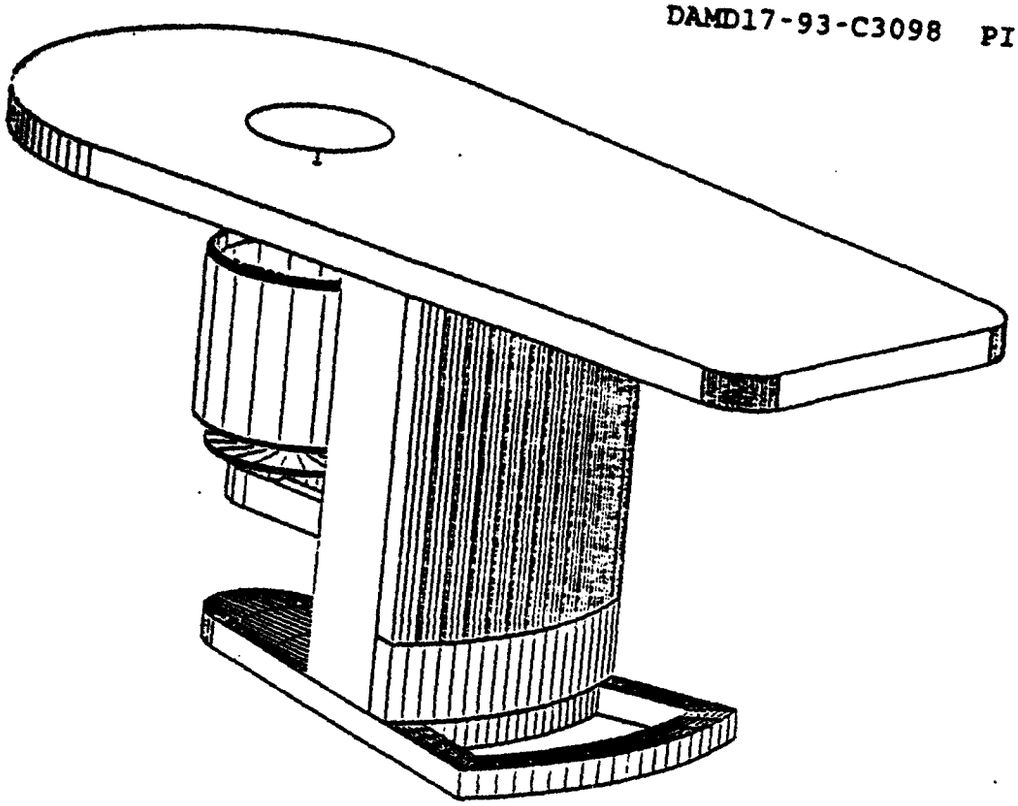

Figure 10. The patient treatment table.

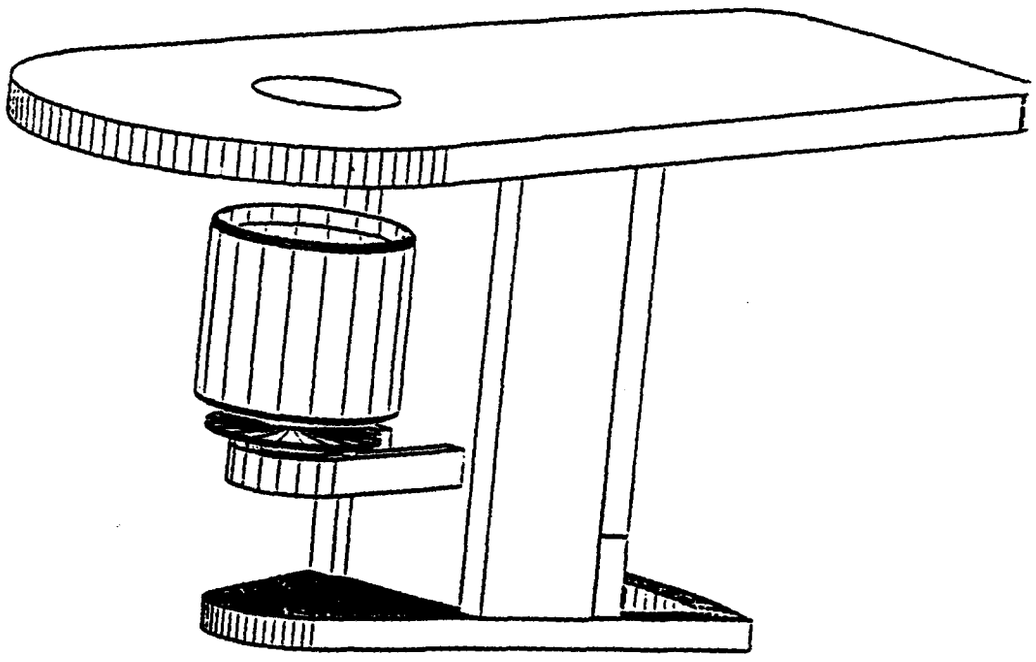

Figure 11. The patient treatment table.

cleaning. The foam insert (and naugahyde) taper near the hole through which the breast is suspended in order to ensure that the entire breast can be extended beneath the table top for treatment if indicated. The patient table top was completed in year 01 and delivered to NEDH for evaluation.

D. System Control and Computer Subsystem

(1) System Control Design

When power is turned on to the system, the treatment software will execute automatically so that no interaction is required by the user to start the software. All available options will be displayed to the user in a graphical format. Options that will be available at the startup screen include access to the treatment planning software, file handling utilities, diagnostic mode selections, treatment record printing, and treatment initiation. The user makes requests of the system via the computer keyboard, computer mouse, or a mechanical pause switch during all phases of the treatment. A hardware Pause switch will be provided that guarantees no output power can be achieved in case of emergency.

Prior to beginning a treatment, the user will be required to complete a treatment plan. The treatment planning software will be in graphical form to simplify data entry, such as target volume locations, the number and location of temperature sensors, target temperatures for each sensor, scar tissue locations, and patient information.

The computer system will perform the treatment in both automated and manual modes. When performing a treatment in the automated mode, very little user interaction will be required during the treatment; however, the user will still be capable of interrupting the computer and/or provide advice to the computer concerning the treatment. When in manual mode, the user will be allowed to select different target tissue regions on the computer screen and set a new target temperature value for each region. The computer system will then determine which ultrasound transducers output power should be adjusted to accommodate the users request.

Treatment progress and status information will be available to the user via a graphical user interface that provides treatment information such as temperature distribution, power absorption distribution, thermal dose distribution, target contour information, and treatment time information. The user will not be required to determine power levels for the individual transducers since temperature distribution information is continually available on a graphics screen. The user will have the capability to make suggestions about the target temperatures for locations where implanted sensors are placed as well as other locations in the target volume.

Once a treatment has been completed, the user will be returned to the startup screen so that printing of the treatment

information may be performed, and duplication of the treatment files may be accomplished.

(2) Computer Subsystems

The computational functions of the system will be divided between two computers, the Control Computer and the Instrument Computer. The control computer's primary responsibility is to control the overall treatment functions and provide an intuitive user interface via a graphics monitor, keyboard, and mouse. The Instrument Computer is primarily responsible for communicating with other hardware devices such as the Cylindrical Array Applicator, the Video system, Cooling System, Thermometry system, and the Pause switch. The system software diagram is shown in Figure 12.

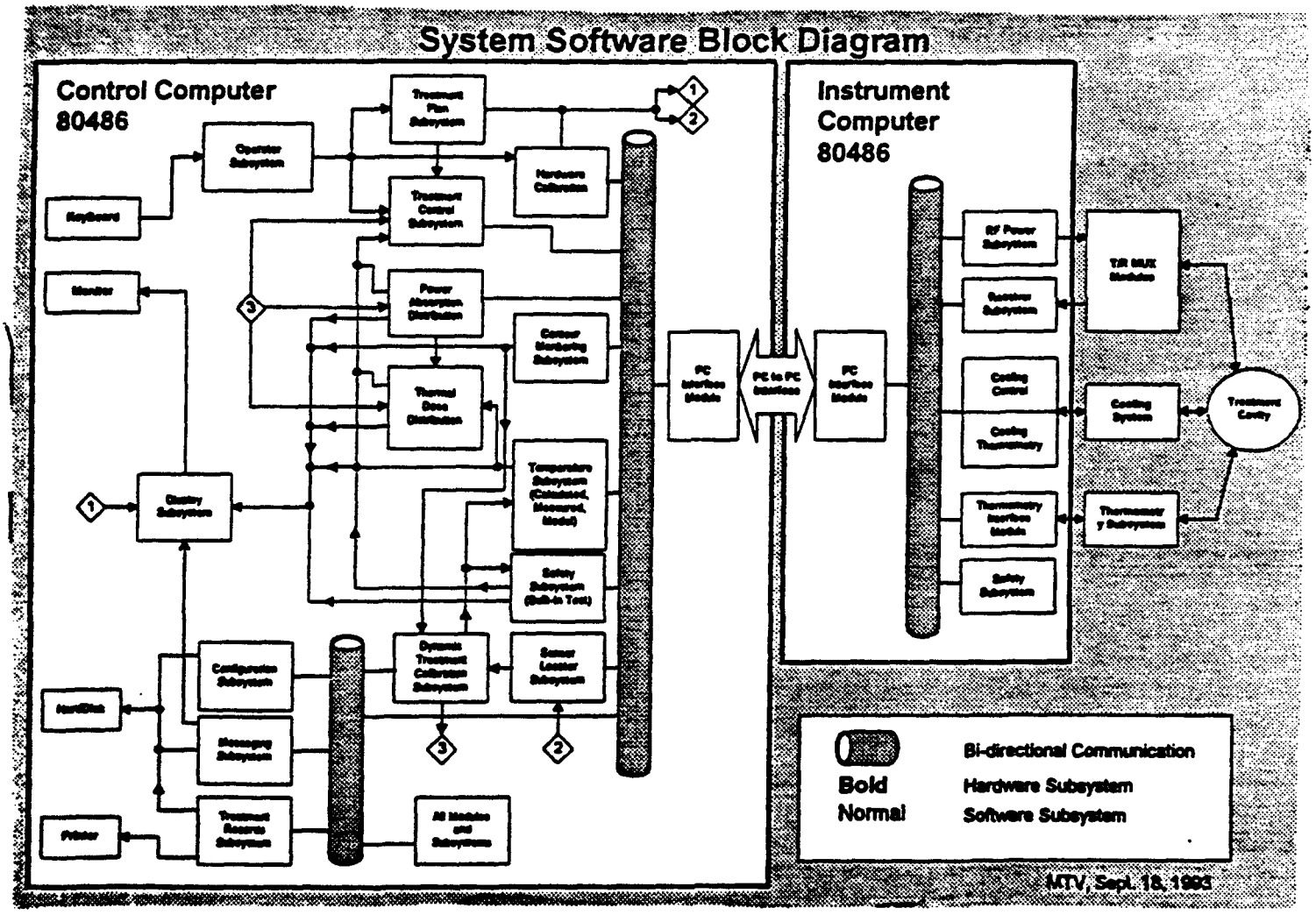

Figure 12. System Software block diagram

The Control Computer will be a standard architecture machine with no custom hardware interfacing requirements that connects to the Instrument Computer via a communications link and is also connected to a printer to allow hard copy of the treatment information. For treatment results analysis, demonstrations, and software development purposes the Control Computer can be operated without the Instrument Computer connected.

The Instrument Computer will implement the user control and measurement interfaces to other hardware portions of the treatment instrument, will be located near the control and measurement points, and will communicate with the Control Computer via a bi-directional communications link. For software design consistency and to avoid unnecessary costs, the Instrument Computer will be implemented as PC-AT compatible computer filled with interface cards.

E. RF Power Subsystem

The RF Power Subsystem consists of 80 independent RF amplifiers driven by 20 separate oscillator sources. Each oscillator consists of a computer-controlled voltage controlled oscillator (VCO) operating over the frequency range of 1 - 5 MHz and is used to drive 4 RF amplifiers. The individual VCOs may be frequency-swept by as much as 250 kHz $\pm$ the VCO center frequency. Each of the 80 independent RF amplifiers incorporates its own voltage control/regulator circuit which provides independent computer control of amplitude (output power level) for each amplifier channel. A block diagram of the RF Amplifier Subsystem is shown in Figure 13. Each RF amplifier output is connected to a T/R MUX input circuit.

F. Thermometry Subsystem

The thermometry to be utilized for invasive measurements in the breast is a multi-channel thermistor-based profilometer system [6] (stand-alone module incorporated into therapy system) which provides a large number of sensor points within a single needle probe. The probes used to measure temperature are thermistors mounted on needles, molded into catheters, or other designs as desired. Stainless steel needles are planned for use with this system. These are 19 ga. needles, from 6" to 12" long, and contain 14 or more thermistor sensors. This range of probe configurations permits selection of a probe appropriate for the particular site being monitored. The multi-channel temperature instrument drives up to 8 multi-channel temperature probes. Since each needle can measure temperature at up to 14 sites (thermistors), resulting in a total of 8*14=112 measurement sites. Dr. Bowman, who is a consultant on this contract will provide the temperature probes.

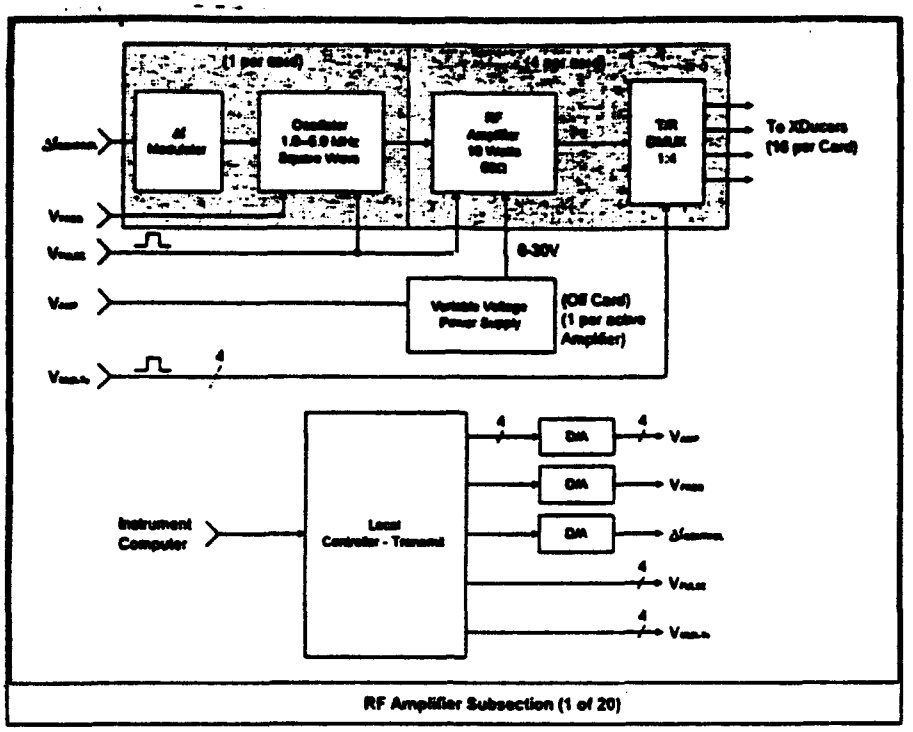

Figure 13. RF amplifier subsystem

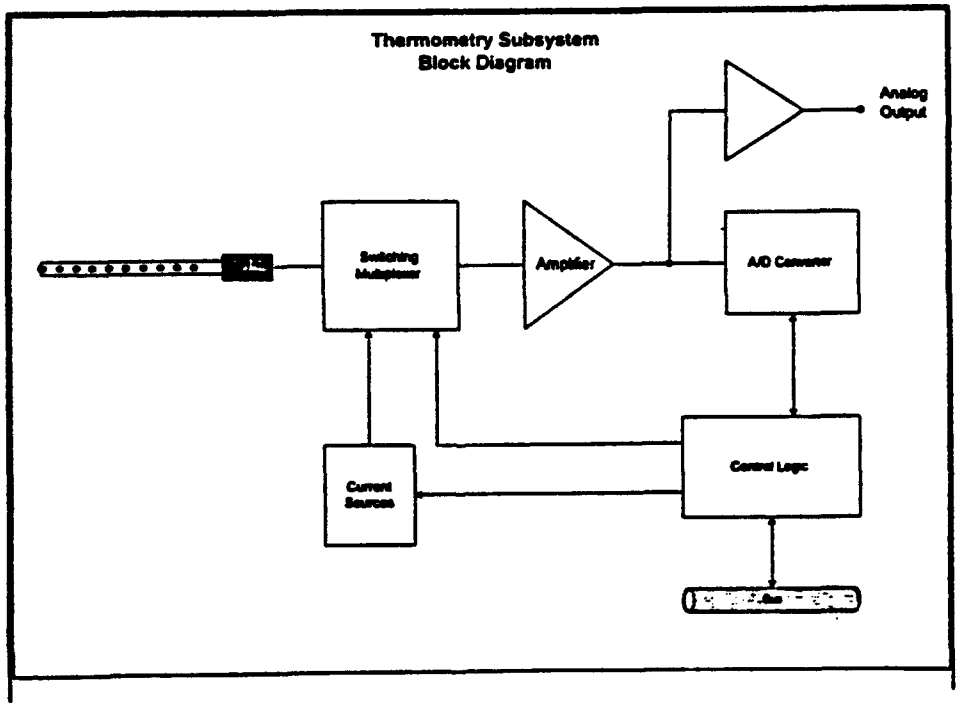

Figure 14. Thermometry subsystem.

The present instrumentation has a resolution down to 5-10 millidegrees Celsius, and the temperature can be sampled at variable rates dependent on the data acquisition system being used and the amount of data averaging and signal processing.

Experiments using signal averaging at each of 112 sites, at a composite sampling rate 2 Hz, have been conducted.

The instrument consists of a medically isolated driver card for each channel, a controller card, and an interface card, which are illustrated in Figure 14. Each channel card contains excitation and signal conditioning circuitry for the sensors. The controller card coordinates the different channel cards. The interface card handles communication to and from a host PC. Analog-digital conversion is presently handled by a commercially available system in the PC, and all instrument control, data display, and data storage is handled by the PC.

G. Non-Invasive Monitoring Subsystem

As previously discussed, we have chosen to perform real-time measurements of ultrasound attenuation, velocity and backscatter in the breast tissue. This offers real-time assessment of the breast position within the cylinder and of the three-dimensional power deposition, which can be correlated with temperature.

(1) Contour Monitoring

Pulse-echo reflection data is collected using the cylindrical transducer array. The reflection data is collected by the Instrument Computer's Receiver subsystem and sent to the Contour Monitoring subsystem. The Contour Monitoring subsystem will convert this information into 3D image data that outlines the contour of the breast and prepare it for display. It will also map 3D image data into a 2D image space for the generation of 2D displays. This subsystem will also provide information to the Dynamic Treatment Calibration Subsystem to locate the breast within the treatment cylinder for detection of breast movement within extreme boundaries set in the Configuration file, and for updating the treatment cells in which the contour (surface of the breast) resides. Figure 15 is a simplified depiction of the pulse-echo monitoring method.

Contour Monitoring is performed by selecting a single ultrasound transducer to transmit an ultrasound pulse into the treatment cavity and then receiving the same pulse while measuring the time it takes for the pulse to return. This measurement is called a "Pulse-Echo" measurement since it measures the time it takes for a pulse to return to the transducer. The sooner a pulse returns the closer the object is to the face of the transducer. The spatial resolution of this technique is about 2 mm. By pulsing all of the transducers one at a time a 3 dimensional contour map of the target tissue located in the applicator can be generated.

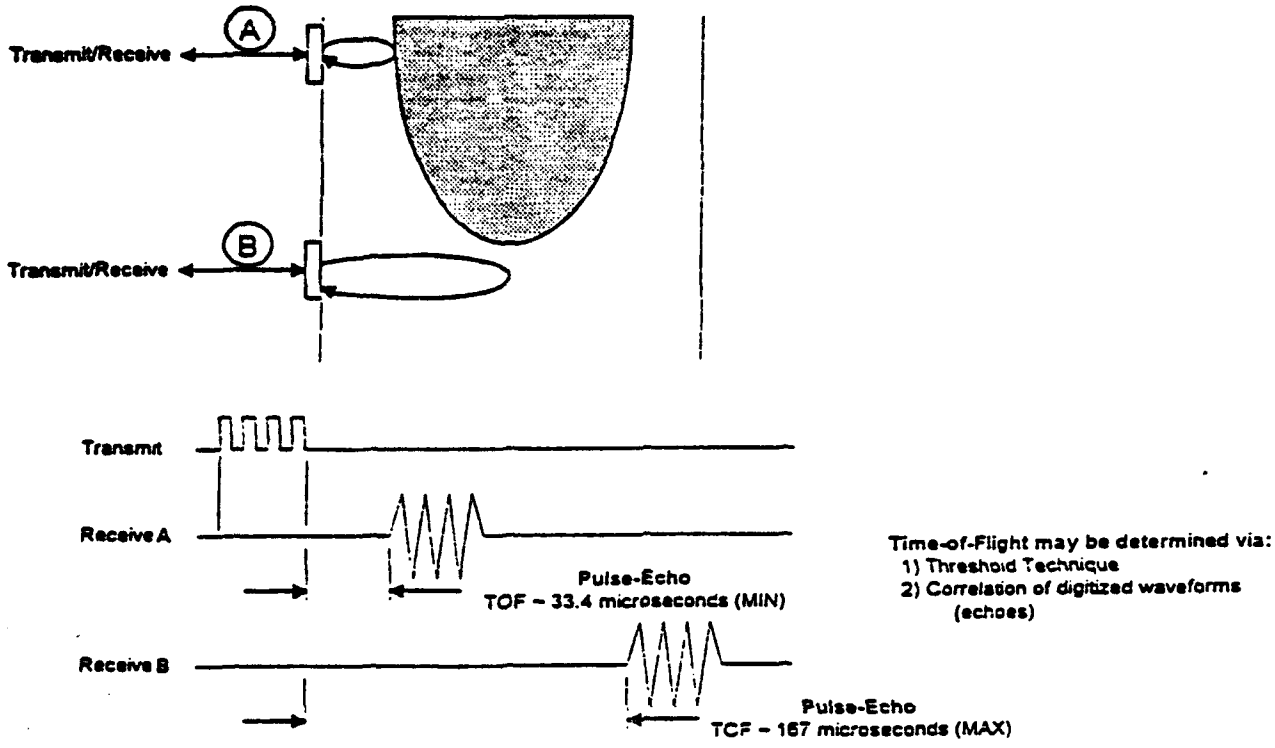

Figure 15. Schematic illustration of contour monitoring.

(2) Power Absorption/Attenuation Monitoring

The Power Absorption Distribution Subsystem calculates the power deposition within the tissue based on current temperature and power information and absorption models. Figure 16 is a simplified depiction of the "Through Transmission" power measurement.

During treatment, the power absorption throughout the target volume for each transducer pair is measured by the Instrument Computer, and sent to this subsystem. The Power Absorption Distribution subsystem converts this information into an array representing the computed absorption or SAR in (W/cm^3) for each treatment cell (minimum unit treatment volume). This computed absorption array is then sent to the Thermal Dose Distribution subsystem for its next simulation model cycle.

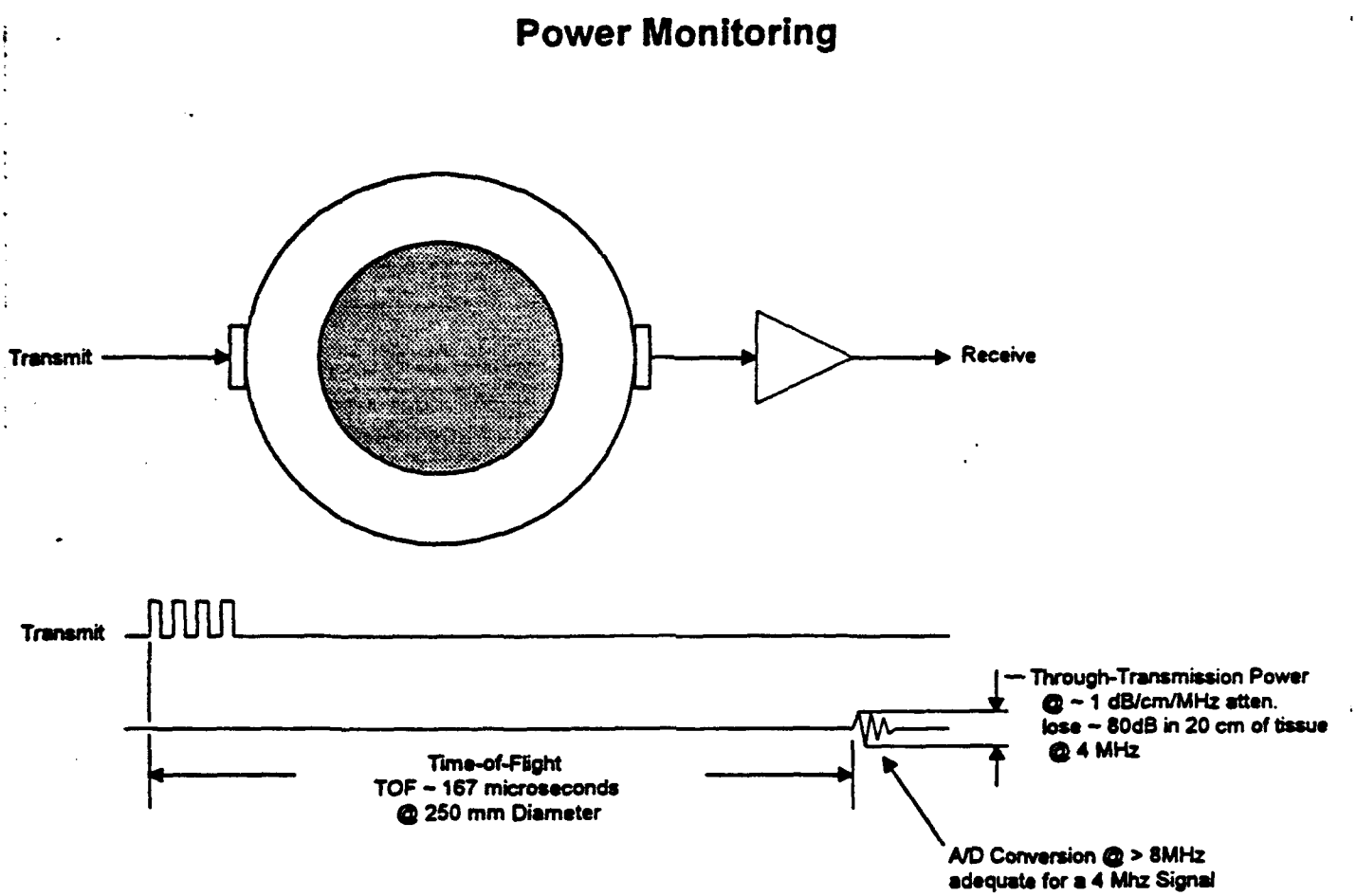

Figure 16. Schematic illustration of power monitoring.

The "Through-Transmission" power is calculated by selecting a single transducer to produce an ultrasound pulse while at the same time having the transducers that are located on the other side of the cylinder (through the tissue) receive the pulse and measure the change in magnitude of the pulse (Pulse Amplitude Degradation) once it has been received. A correlation between the transmitted magnitude and the received magnitude can then be used to determine the amount of power that was absorbed in the tissue.

H. Software Development

The System Software Block Diagram (refer to Figure 12) shows the system control implementation approach. System control is divided between two computers, the Control Computer and the Instrument Computer. The Control Computer provides an operator control interface, measurement interpretation, feedback control, and data recording. The Instrument Computer provides direct hardware interfacing for collecting temperature measurements, collecting measured data from receivers, setting control output levels, and controlling the timing for multiplexing the transducer array.

(1) Operator Interface

The Control Computer performs several interrelated functions. The operator input and display subsystem provides control over the treatment and feedback to the user as the treatment progresses. User control over the treatment is at a high interaction level; actual control over the timing, power levels, and frequencies applied to the large numbers of individual transducer elements is complex and must be controlled rapidly. Therefore, an operator is not capable of controlling the individual transducer parameters directly.

The operator interface is one of the most important parts of the treatment system since it represents "the system" to the users. Therefore, the engineering design approach must be secondary to the user-oriented approach in this instance. Not only must the data interfaces be considered, but also the tools (keyboard, mouse, etc.) and the display organization and options. The operator interface will define the treatment control and reference data and display a variety of types of treatment progress and general display information.

The displays to be provided during treatment include:

1) A breast contour.
2) Periodic imaging of the temperature probes(s).
3) 2D cross sections and 3D breast images, each with selected overlays of calculated isotherms, T_{50} and T_{90}.
4) Hot spot alerting.
5) An optional display of 2D cross sections by location.
6) Continuous time and temperature monitoring displayed as a graph for each cross section.

(2) Treatment Planning

The Treatment Plan Subsystem is responsible for obtaining information from the user necessary for proper treatment operation. Information required by this subsystem includes the number of treatment sensor probes, number of sensors per probe, spacing of the sensors on the probe, target temperature and

temperature limits for individual sensors and/or subregion locations in the treatment volume, patient name and/or number identifier, and possibly suggestions about the method of heating. The treatment plan subsystem maintains this information and provides it to other subsystems.

The Treatment Plan Subsystem will also provide a method for the user to select regions as small as an octant and select a temperature setpoint for the entire octant at once.

(3) Treatment Control

The Treatment Control Subsystem makes transducer output power and frequency decisions based on information received from the Power Absorption Distribution Subsystem, Thermal Dose Distribution Subsystem, Treatment Plan Subsystem, Dynamic Treatment Calibration Subsystem, and Temperature Subsystem. Once output power and frequency settings have been determined the Treatment Control Subsystem sends those data to the RF Power Subsystem via the PC Interface Module so that actual power changes can be made for the Transducer Array.

The Treatment Control Subsystem operates on pre-defined Treatment Cell Volumes. The actual volume of each treatment cell is determined by the configuration file. The Treatment Cell center points, volume corners, and transducers that affect a treatment cell are stored in a Treatment Cell Information File. If the volume defined in the configuration file for a treatment cell does not match the volume used to calculate the current treatment cell information file, the Treatment Control Subsystem will generate a new treatment cell information file.

The Treatment Control Subsystem will operate in automatic mode, yet it will be capable of allowing the user to make manual adjustments of the temperature set-points for each treatment cell volume during the treatment. The default control method will be to heat the entire breast to 43^0C in all treatment volume cells.

4. Experimental Studies and Testing

A. RF Generator and Amplifier Tests

A block diagram of the RF Generator-Amplifier board is shown in Figure 17. The design consists of an onboard VCO connected through an on/off channel gate to a driver stage which is in turn

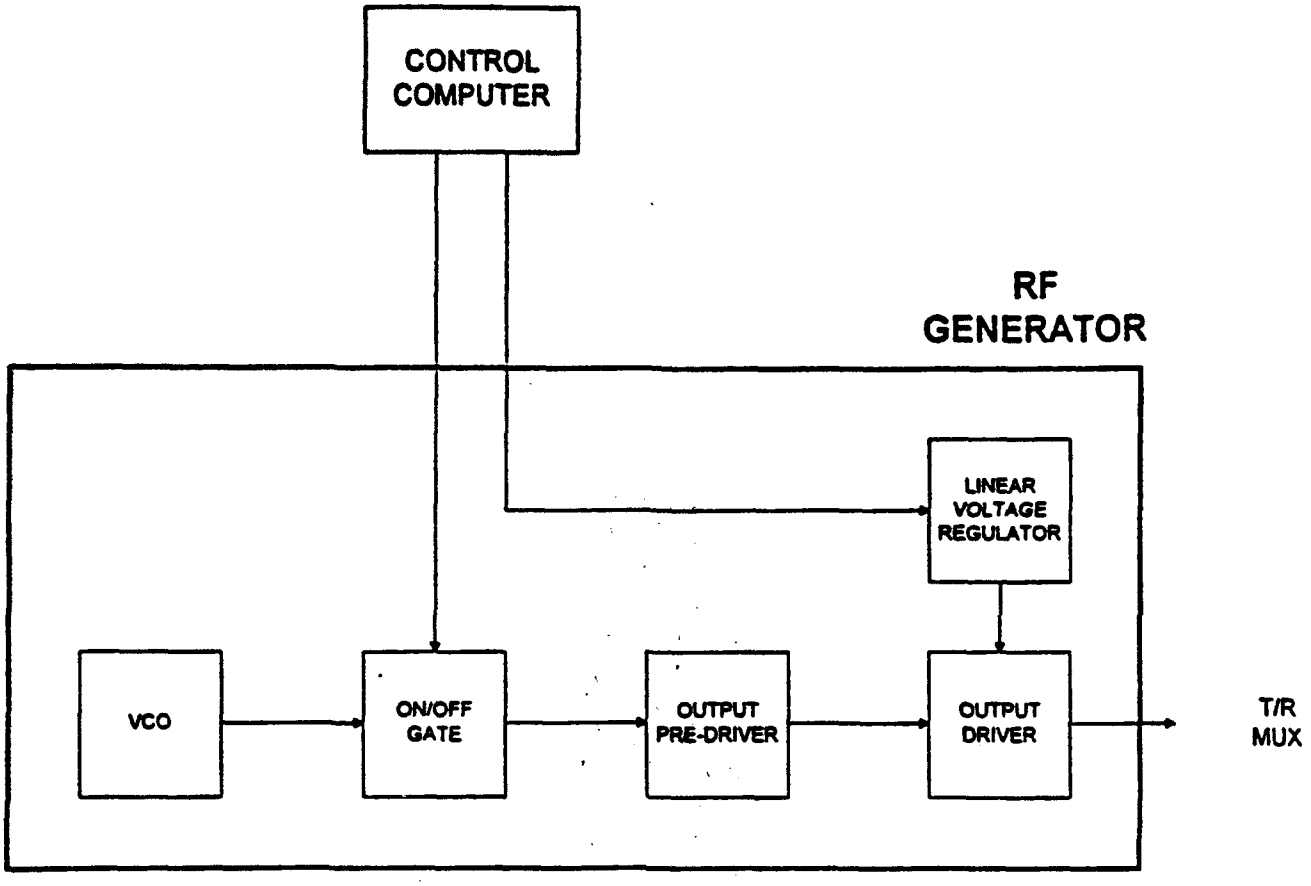

Figure 17. RF Generator block diagram.

connected to the output driver (amplifier) stage. The design operates in Class D-E using a bipolar and dual switched FET's in the output stage. The output power is also variable from 0 watts to approximately 10 watts and is controlled by a linear voltage regulator circuit. The linear voltage regulator and on/off gate are controlled via a D/A line from the Instrument Computer. Each RF Generator-Amplifier in the breast therapy system is individually computer controlled.

The RF Generator-Amplifier design was developed during the first year of the contract, with numerous design variations and board configurations being tested. The final configuration incorporates 4 channels per circuit card. A total of 20 cards provide 80 channels which are multiplexed to drive the individual array transducers. This was described in Section V .3.D.

Operating specifications and test results for the RF Generator-Amplifier are consistent with the design criteria. These are summarized as follows:

SPECIFICATIONS

- Square Wave Generator
- Frequency Range: 1-5 MHz
- Oscillator consists of a computer controlled VCO
- On/Off Gating
- 10 W Continuous Power Output
- Computer controlled with a DC/DC Linear Voltage Regulator
- Short Circuit Current Limiting

TEST RESULTS

Frequency Range
- 0.8 MHz to 6.2 MHz with a little signal degradation

Power Output
- 10 W to 15 W over frequency range
- 12 W Continuous at 2.0 MHz
- 10 W Continuous at 4.5 MHz

Gating and Current Limiting Function as designed

B. Multiplexer/Transmit-Receive Switch Tests

The multiplexer design was also completed and tested during the first year of the program. The multiplexer switches the RF Generator-Amplifier outputs among different transducers and also selects transducers in the "receive" mode through the multiplexer's transmit-receive select function. Each multiplexer/transmit-receive switch connects to four transducers. Test results for the transmit-receive switch functions are shown in Figure 18.

C. 16 Channel Transmit-Receive Board

Boards, which integrate control of 16 transducers into a single circuit card were constructed and tested. On these cards are 4 RF Generator-Amplifier channels, 4 separate 4-channel multiplexer/transmit-receive switches, and a receiver section. These are illustrated in the block diagram of Figure 19.

These will be used in the single ring tests which are described in the subsequent subsection of this report.

The receivers used for monitoring tissue attenuation and for measuring reflected signals for determination of the breast contours have been designed and will be completed and tested as a part of the second year effort. The transmit-receive board is used to acquire acoustic information regarding the breast tissue

during therapy. We plan to use this information as a real-time monitor of the treatment.

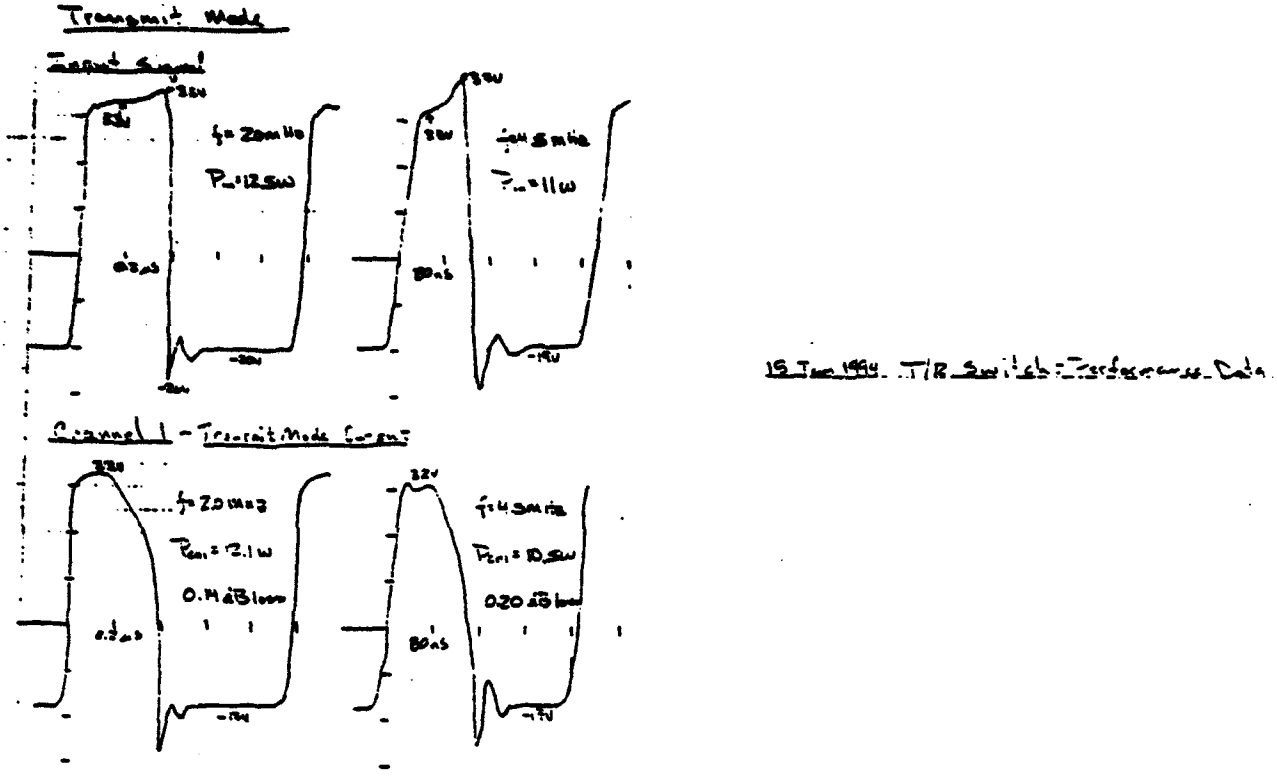

Figure 18. Preliminary results from testing of the T/R switch functions. Signal strenght versus time.

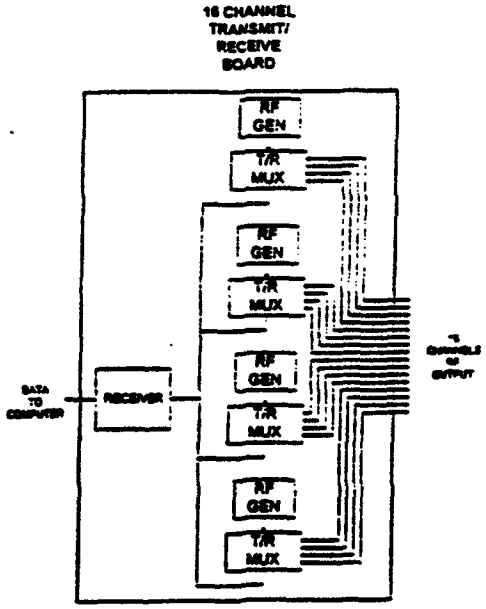

Figure 19. Schematic drawing of board controlling 16 transducers.

D. Single Ring Tests

A single ring system has been built and electronically tested. One of the first tasks to be performed during the second year of the contract will be the testing of the single 48-transducer ring array to evaluate the performance of the cylindrical array (in a single circular plane) by heating tissue-equivalent phantoms. Two tissue mimicking breast phantoms have been built for this purpose. To receive an Investigative Device Exemption (IDE) we may have to perform testing on a limited number of animals. An animal test protocol has been written and approved by the hospital Animal Use Committee. If such tests are needed we will make separate requests and forms for animal studies to be submitted to USAMRDC for the purpose of conducting these tests.

The single ring test will also permit critical examination of the hardware and software design including temporal multiplexing of the therapy transducers. A block diagram depicting the single ring tests is shown in Figure 20.

The single ring electronics control and testing was not explicitly spelled out in the original SoW. However, we added this task in order to properly test the final design prior to fabrication of the entire system.

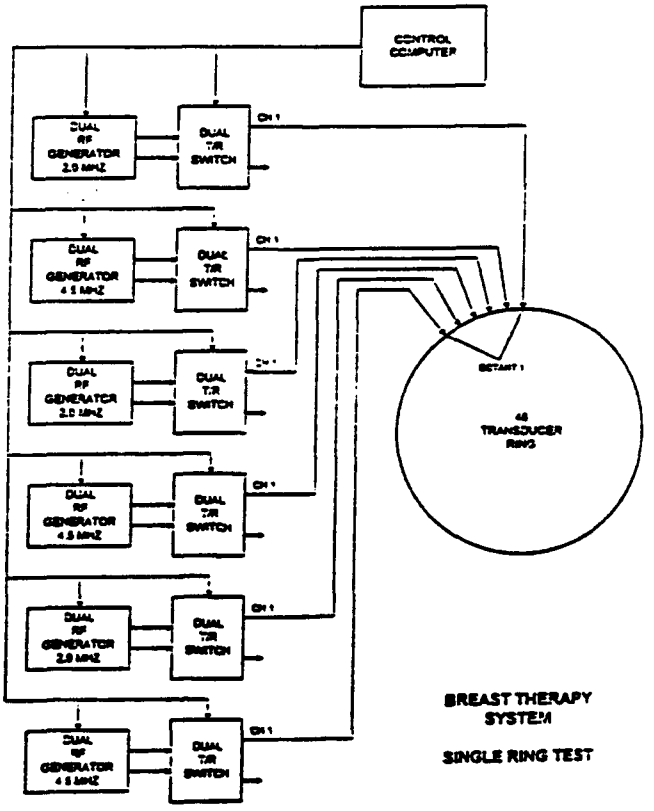

Figure 20. Schematic illustration of the single ring systems test.

Equipment utilized in the testing will include several 48-transducer multiple-frequency rings, RF generating and multiplexing circuitry, T/R switching circuitry, and Instrument Computer system. The hardware will be connected to the transducers in the ring such that 2.0 and 4.5 MHz transducers will alternate around the ring. The same channel of each dual T/R mux will connect to the same octant of the ring, the position in the octant corresponding to which T/R multiplexer is used. The circuitry is connected such that one octant of the ring (six transducers) can be turned on simultaneously and then each next group of six others progressively excited until the entire ring excitation has been completed. The initial octant is then ready for excitation to restart the circumferential octant excitation cycle again. Single transducer operation may also be accomplished with this configuration and this will be tested to examine characteristics of individual pulse-excitation.

The system's Instrument Computer will be used to control hardware to "sweep around" the ring at least once in an eight second interval.

Heating of phantoms will be studied with extensive invasive thermometry used to characterize performance. Conditions as close as possible to modeled parameters from the simulation studies will be created and comparisons made between the simulation study and measured results in phantoms.

5. Breast Treatment Protocol

Our aim is to improve the local control of patients with tumors with extensive intraductal carcinoma, who choose to be treated with breast conserving therapy.

Over the past year, with the help of our outside consultants, Dr. Mark Dewhirst and Dr. Daniel Kapp, we have refined the specifics of the clinical study. Initially we intended to study equipment performance, toxicity and efficacy in a Phase I/II study. We were advised not to do the equipment evaluation as a part of the Phase I/II study, but rather design a separate clinical pilot study for equipment evaluation to preceed the phase I/II study. In this pilot study (See SoW in section VI) we will treat approximately six patients. The objective of the pilot study is to determine if we can heat the breast tissue to a specific thermal dose (i.e. T_{90} = 40.5 ^{0}C), operate and control the therapy machine quickly and to accomplish this with minimal toxicity and discomfort to the patients during the therapy session. We also need to evaluate our ability to model individual patients using our treatment planning system. For instance, to determine if predicted critical tissue regions, such as biopsy cavities and scars can be prevented from being too hot during treatment.

Eligible patients for the pilot study would be those with infiltrating ductal carcinoma of the breast with an extensive intraductal component and a re-excision of the biopsy cavity with greater than 4 high power fields showing positive margins. These

patients would be considered at high risk for local failure using conservative therapy with radiation therapy alone [17]. The treatment plan specifies standard radiation therapy. Our protocol will then add two thermal therapy treatments. Limiting the pilot study to two treatments per patient, is felt to reduce the potential risk of patient morbidity. The thermal therapy target volume is the quadrant of the breast originally containing the lesion or half of the breast if the lesion extends over two adjacent quadrants. The treatment time for ultrasound heating is 45 minutes to 60 minutes. The final time will be fixed, but depends on the anticipated set-up time required prior to treatment. If the set-up time is considered long, then the time for treatment will be 45 minutes to help relieve patient fatique and improve patients tolerance and comfort. The treatment will be considered to start when any target temperature reaches 40 ^{o}C. For the pilot study, the target temperature range will be fixed at T_{90} = 40.5 ^{o}C and T_{max} = 44 ^{o}C.

Temperature monitoring will be done with two orthogonal invasive probes, placed under ultrasound guidance. At least one of the probes must be placed through the biopsy cavity as we expect higher temperatures requiring ultrasound intensity adjustments to reduce the energy deposition in this region. The nipple, biopsy scar and any other location where a hot spot is predicted will also be monitored.

Endpoints of the pilot study include a measure of our ability to control the machine, produce the desired temperatures and predict hot and cold spots using our theoretical models (See section V:2:C). We also need to determine that our treatment table and treatment procedure does not cause patient discomfort and morbidity. The number of patients for the pilot study is approximately six. Our biostatistics group will review all treatment protocols before final patient numbers are determined.

Following the pilot study and confidence in our ability to safely control the machine, we will embark on a dose escalation study (Phase I/II) to evaluate both thermal therapy treatment toxicity and efficacy.

The equipment evaluation and Phase I/II protocol are near completion and will be submitted for hospital IRB review in July 1994 and subsequently submitted to the Human Use Review Specialist at the USAMRDALC.

VI. Conclusions and Statement of Work.

This annual progress report covers year 01 of DAMD17-93-C-3098 from 3/29/93 to 3/28/94. The contract supports the development of a technique to use thermal therapy for adjuvant treatment of breast cancer. The technique will be applied to an equipment evaluation study and a clinical phase I/II study. A

phase III randomized study is planned to start at the end of year 03, depending on the findings of the phase II studies. In these studies we will investigate if patients with an extensive intraductal component of their infiltrating tumor, or patients with pure intraductal carcinoma will benefit from adjuvant thermal therapy by having improved local control.

The technical aspects of the work consists of the design of a site specific ultrasound transducer array for thermal therapy of the breast. The transducer array will be the core component of a treatment system that allows controlled heating of the whole breast, or a smaller volume of the breast as well as monitoring of energy deposition (SAR), temperature distribution and tissue characteristics that are important for the control and prediction of outcome of the thermal therapy.

Much of the system design objectives, computational simulations and all of the clinical work is performed at the New England Deaconess Hospital (NEDH), Boston, MA. The device specification design, drawings and fabrication of the thermal therapy system is sub-contracted to Dornier Medical Systems Inc. (DMSI) and that work is being done at their laboratory in Champaign, Illinois. The interaction between NEDH and DMSI has been excellent and the two review visits by our consultants have enhanced the clinical and scientific value of the breast treatment program.

The main emphasis during year 01 (See table 1) has been on the design and building of the various subsystems that comprises the total thermal therapy system. This is discussed in section V-1-B.

The Statement of Work (SoW) for year 02 and 03 is shown in Table 5. At the suggestion of our external site visitors, we have added a task (Task 15 and 19) related to an institutional IDE for using the breast applicator in patient therapy. This IDE application will be written and submitted by NEDH to FDA in July 1994. A recent conversation with the FDA official dealing with hyperthermia devices indicate that FDA must review and return an institutional IDE application within 30 days. On the average, approval is granted after 2-3 cycles. Therefore we expect to need a little more than three months to receive approval for clinical use of this applicator. The initial SoW indicated the first patient to be treated by the end of the first quarter (i.e. June 1994) of year 02. If approval is granted in October 1994 (end of second quarter of year 02) we will immediately start the first patient. This is not a significant set-back because, at the advice of our consultants, the first 6 patient treatments will focus on equipment evaluation. Such a focused effort is likely to bring about important equipment modifications faster than otherwise could be anticipated. The clinical protocol for the equipment evaluation phase is near completion and will be submitted for approval to the IRB of the NEDH and to the Human Subjects Committee of the USAMRDC.

Table 5. SoW year 02, 03

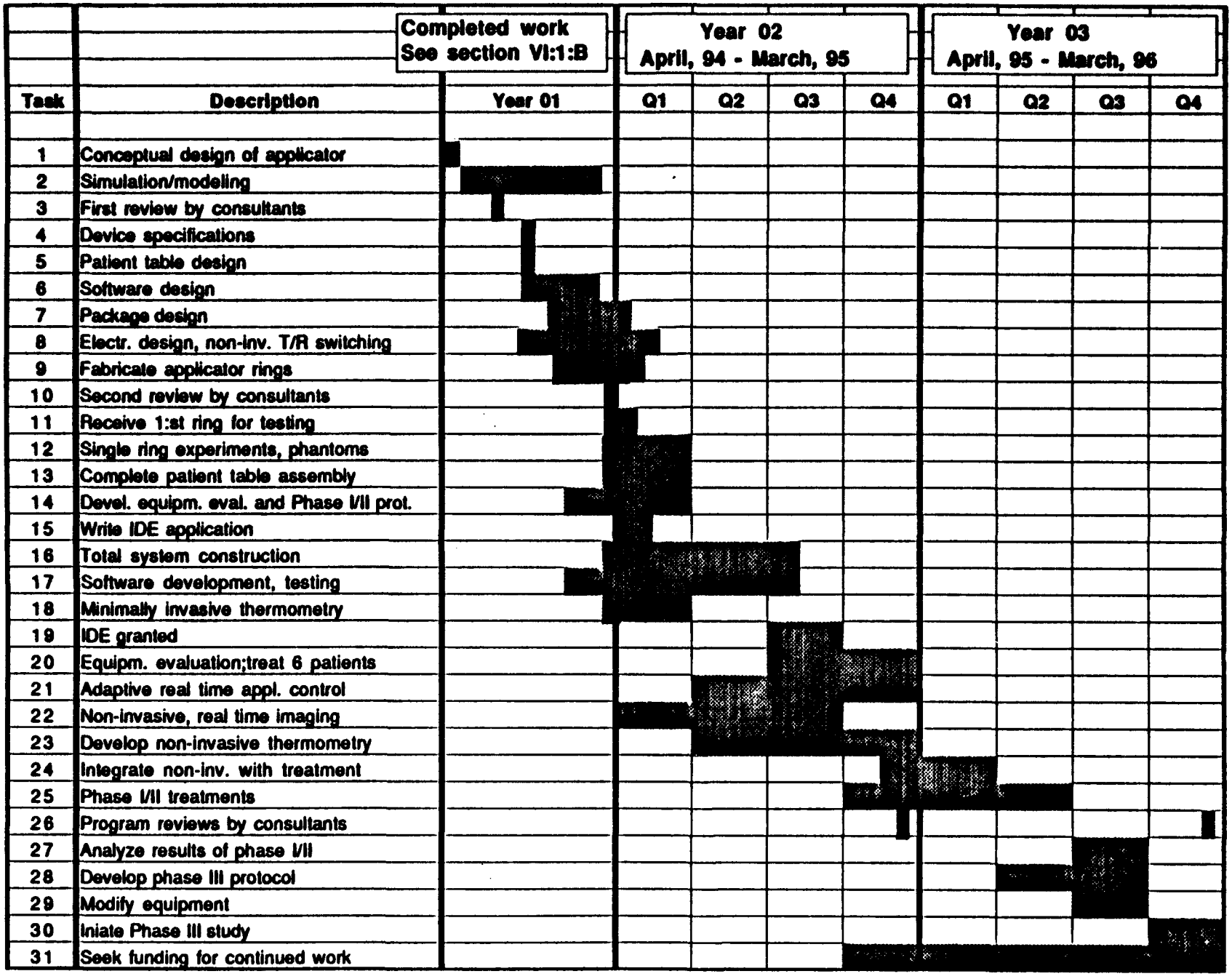

VII. References

1. Bornstein BA, Zouranjian PS, Hansen JL, Fraser SM, Gelwan LA, Teicher BA, Svensson GK. Local hyperthermia, radiation therapy, and chemotherapy in patients with local-regional recurrence of breast carcinoma. Int J Rad Oncol Biol Phys 1992, 25: 79-85.

2. Bornstein BA, Herman TS, Buswell L, Hansen JL, Zouranjian, PS, Fraser SM, Teicher BA, Svensson GK, Coleman CN.: Pilot study of local hyperthermia, radiation therapy, etanidazole, Meeting of the North American Hyperthermia Society, Nashville, Tennessee, 1994.

3. Bowman, H.F.: Heat Transfer and Thermal Dosimetry. J Microwave Power 16 (2), 121-133, 1981.

4. Bowman HF, Curley MG, Newman WH, Summit SC, Chang S, Hansen J, Herman TS and Svensson GK. Use of effective conductivity: Will it permit quantitative hyperthermia treatment planning? Proceedings of the Annual International Conference of the IEEE Engineering in Medicine and Biology Society, Vol 11, 1989, Kim Y and Spellman FA, Eds. Part I, pgs 1-8.

5. Bowman HF, Curley MG, Newman WH, Summit SC, Chang S, Hansen J, Herman TS and Svensson GK. Use of effective conductivity for hyperthermia treatment planning. Bioheat Transfer: Applications in Hyperthermia , Emerging Horizons in Instrumentation and Modeling. ASME HTD-V 126/BED-V12. p 23-28, 1989.

6. Bowman HF, Newman WH, Curley MG, Summit SC, Kumar S, Martin GT, Hansen J, Svensson GK. Tumor hyperthermia: dense thermometry, dosimetry, and effects of perfusion. In: Advances in Biological Heat and Mass Transfer, HTD-volume 189/BED, 18:23-31, ASME, 1991.

7. Chen MM: Microvascular Contributions in Tissue Heat Transfer, Annals of New York Academy of Sciences, Vol. 335: 137-150, 1980.

8. Duck FA: Physical Properties of Tissue - A Comprehensive Reference Book. Academic Press, Inc, 1990.

9. Eberhart RC, Shitzer A, Hernandez EJ: Thermal dilution methods; Estimation of tissue blood flow and metabolism", Annals N.Y. Acad. Sci. Vol 335:107-132, 1980.

10. Fenn AJ, Bornstein BA, Svensson GK, Bowman HF: Minimal invasive monopole phased arrays for hyperthermia treatment of breast carcinomas: design and phantom tests. In:

Proceedings of the IEEE Int'l Symposium on Electromagnetic Compatibility, Sendai, Japan, May 1994. In Press.

11. Foster, F.S., Hunt, J.W.: Transmission of ultrasound beams through human tissue - focusing and attenuation studies. Ultrasound in Med & Biol., Vol. 5, 257-268, 1979.

12. Kapp, D.S., Cox , R.S., Fessenden, P., Meyer, J.L., Prionas, S.D., Lee, E.R., Bagshaw, W.A.: Parameters predictive for complications of treatment with combined hyperthermia and radiation therapy. Int J Rad Oncol Biol Phys 22(5) 999-1008, 1992.

13. Kaye, G.W.C., Laby, T.H.: Tables of Physical and Chemical Constants. Longman, 1973, London.

14. Lu X-Q, Svensson GK, Hansen JL, Bornstein BA, Harris JR, Burdette EC, Slayton M, Barth P.: Design of an ultrasonic hyperthermia unit for breast cancer treatment. 14 th Annual Meeting of the North American Hyperthermia Society, Nashville, Tennessee, 1994.

15. Ocheltree, K.B. and Frizzell, L.A. Sound Field Calculations for Rectangular Sources. IEEE Transactions on Ultrasonics, Ferroelectrics, and Frequency Control.Vol. 36, No. 2, 242-247, March 1989.

16. Press WH, Flannery BP, Teukolsky SA, Vetterling WT: Numerical Recipes, The Art of Scientific Computing. Cambridge University Press, 1985.

17. Recht, A., Come, S.E., Gelman, R.S., Goldstein, M., Tishler, S., Gore, S.M., Abner, A.L., Vicini, F.A., Silver, B., Connolly, J.L., Schnitt, S.J., Coleman, C.N., Harris, J.R.:Integration of conservative surgery, radiotherapy, and chemotherapy for the treatment of early stage, node-positive breast cancer: sequencing, timing and outcome. J Clin Oncol 9(9):1662-1667, 1991.

18. Roemer, R.B.: Heat transfer in hyperthermia treatment: Basic principles and applications. American Association of Physicists in Medicine, Med Phys Monograph No. 16, 210-242, 1988.

19. Sarti DA: Diagnostic Ultrasound Text and Cases, Second Edition, Year Book Medical Publishers, Inc., 1987.

20. Sekins, K.M., Emery, A.F.:Thermal science for physical medicine.Chpt.3, pp 70-132 In: Therapeutic Heat and Cold, Lehmann,J.F. (Ed), 1982.

21. Svensson GK, Lu, X-Q, Hansen JL, Bornstein BA, Burdette EC.: Simulation of a multi-transducer, dual frequency ultrasound applicator for hyperthermia treatment of breast cancer.

Proceedings of the IEEE Int'l Symposium on Electromagnetic Compatibility, Sendai, Japan May 1994. In Press.

VIII. Appendices

Appendix 1. Paper submitted for presentation at the IEEE Meeting on Electromagnetic Compatibility, Sendai, Japan, May, 1994. Copies of this paper has been sent to USAMRDC as required by the contract.

Appendix 2. Review paper on the Technical Developments in Ultrasound-induced Hyperthermia. EC Burdette and SA Goss.

No. 14 1

APPENDIX I

SIMULATION OF A MULTI-TRANSDUCER, DUAL-FREQUENCY ULTRASOUND APPLICATOR FOR HYPERTHERMIA TREATMENT OF BREAST CANCER

G.K. Svensson, X-Q. Lu, J.L. Hansen, B.A. Bornstein
Joint Center for Radiation Therapy,
Department of Radiation Oncology, Harvard Medical School, Boston, MA 02115

E.C. Burdette,
Dornier Medical System Inc. Champaign, IL 61820

ABSTRACT

A site-specific ultrasound hyperthermia breast treatment unit will be designed and built. It is dedicated to optimize the synergistic effect between hyperthermia and radiation for the treatment of breast cancer. With the patient in prone position, the breast will be immersed in water and surrounded by a cylindrical transducer array operating with two frequency bands. This paper describes extensive simulations, to determine the design and the operating parameters for a variety of breast treatment conditions, including variations and uncertainties in tissue attenuation, tissue perfusion and size of target volumes.

INTRODUCTION

In order to treat breast cancer with hyperthermia we designed and built a site-specific ultrasound hyperthermia applicator for treatment of breast cancer.

Our goals were to:

1. Achieve 42°C but not more than 44°C in the whole breast or a quadrant of breast [1].

2. Have operational flexibility to accommodate a range of tissue characteristics ultrasound attenuation, perfusion rate, and the different geometry's and heating patterns.

3. Be easy to use in the clinic.

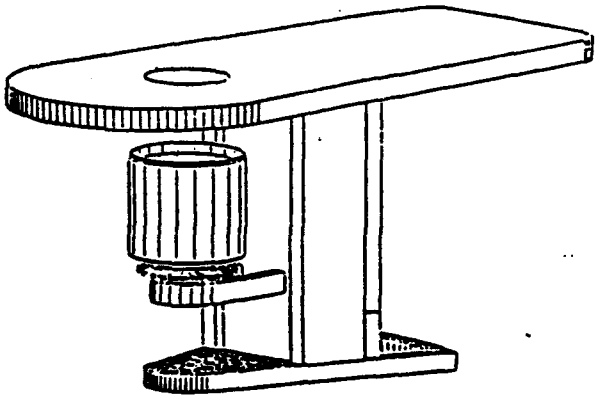

Figure 1. Hyperthermia treatment table with cylindrical ultrasound transducer array.

The cylindrical applicator consists of a stack of 8 - 10 rings, each being approximately 1.5 cm high. The ring located at the base of the breast contains 48 transducers. The number of transducers in each ring decreases toward the apex of the breast. The ring closest to the nipple contains 16 transducers. Each ring deposits power in a plane parallel to the chest wall and the heating effect of each ring is relatively independent of adjacent rings. This property facilitates control of heating.

The patient lies in a prone position with her breast submerged through a whole in the table into the water filled applicator. This position takes advantage of the convex shape of the breast. Water bath temperature is controlled from 30°C to 40°C. This arrangement provides an excellent coupling for ultrasound, and good control of the surface temperature, which not only spares the skin, but also provide well defined boundary conditions. Temperature and the thermal perfusion rate properties will be monitored by minimally invasive multisensor probes.

This paper reviews the computer simulations we performed to design the ultrasound breast treatment device.

METHOD OF SIMULATION

The objective of the simulation is to determine reasonable design and operating parameters for the breast treatment applicator. To guide this effort, a three-dimensional acoustic and thermal computer model has been derived. The simulation consists of two parts: the acoustic field simulation and the bio-heat transfer simulation.

For the acoustic field simulation the calculation for continuos wave (CW) rectangular sources is based on the piston model developed by Ocheltree and Frizzell [2]. This model is only for homogenous media. When two media, breast tissue surrounded with water, is simulated, the model is modified so that the speed of sound is the same in both breast tissue and the surrounding water.

The standard format the bio-heat transfer equation is used [3]. We used the finite difference method to solve the bio-heat transfer equation for the three-dimensional numerical calculation of the initial value problem. This approach gives us a great deal of flexibility in changing the equation format and boundary conditions. We can then study the detailed temperature evolution over time even under conditions of non-equilibrium temperature.

The model we used has limitations and uncertainties. Therefore, we have selected to use ranges of parameters in the model to assure that the proposed system has the ability to accommodate significant uncertainties in tissue composition, ultrasound attenuation and heat transfer parameters. The parameters used in the simulation are listed in Table 1. When data for breast tissue are not specifically reported (i.e. perfusion rate), we used data for resting muscle tissue. In this model the perfusion rate is increasing linearly with increasing temperature.

Table 1. Parameters used in the model.

Parameter [Ref.]	Default value	Range studied
Attenuation breast, [4]	0.086 ($f^{1.5}$ Np, cm^{-1})	0.052-0.12
Attenuation water, [5]	0.0002 (f^2 Np, cm^{-1})	0.0002
Conductivity [6]	0.5 (W, m^{-1}, K^{-1})	0.4 - 0.8
Perfusion, [7]	30 at 37°C 100 at 44°C (ml, Kg^{-1}, min^{-1})	30 -100 30 - 200
T_{water}, °C	37°C	30°C - 40°C
D, cm	15	10 - 15
H, cm	8	5 - 8
h, cm	0.9	0 - 1.2

Simulations are performed over the range of reported parameters. Figure 2 shows the theoretical breast model used in this work.

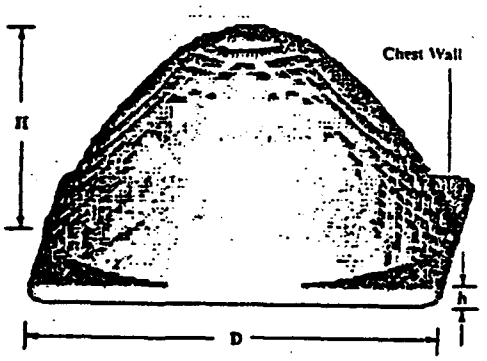

Figure 2. Theoretical breast model. *D* is the diameter at the base of the breast. *H* is the height of the breast. At a depth *h* into the chestwall we assume the temperature boundary to be 37°C.

Clinically relevant breast sizes were determined from direct measurements on patients positioned prone with the breast hanging freely in air. The measurements and detailed shape of the breast tissue was also studied using CT scans of women in the prone position. The boundary conditions have a profound impact on the temperature distribution inside the breast. On the breast surface temperature is a function of the temperature of the circulating water (30°C to 40°C).

RESULTS AND DISCUSSION

Our first goal is to achieve a minimum temperature of 42°C, but not more than 44°C. At temperature above 44°C we expect to see subcutaneous fibrosis and other potential tissue toxicity [1]. This narrow temperature range is a major technological challenge for the design of the breast ultrasound hyperthermia system and require control of the power output and ultrasound frequency to adjust for breast size, border temperature conditions, tissue attenuation, and perfusion dynamics.

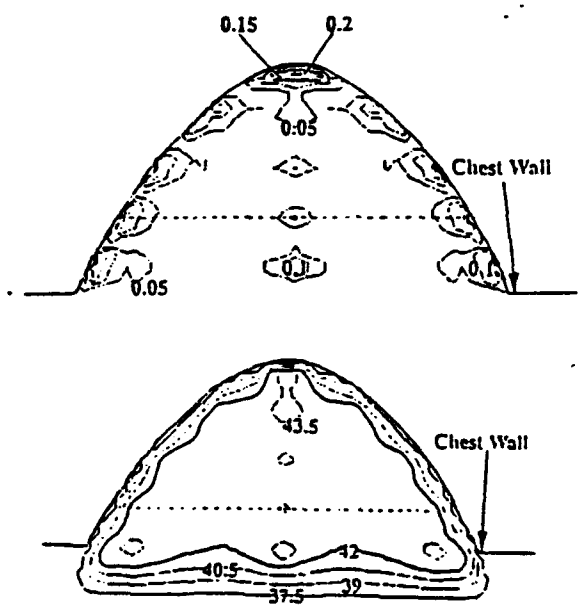

Figure 3. Top panel: SAR distribution (W/cm^3) required to maintain steady state temperature 42°C ≤ T ≤ 44°C. The calculation is for a large breast with *D* = 15 cm, *H* = 8 cm and *h* = 0.9 cm.
Bottom panel: The steady state temperature distribution. The calculation is optimized for perfusion rate of 30 ml, kg^{-1}, min^{-1} at 37°C increasing linearly with temperature to 100 ml, kg^{-1}, min^{-1} at 44°C. The maximum temperature is 43.7°C. Dotted line is the level of the cross-sectional view shown in figure 4.

The individual transducer rings are stacked to form a cylindrical applicator. Power deposition (SAR) to a given point within the breast tissue is delivered predominantly from the ring that defines the

plane in which the point is located. The equilibrium temperature at a point in the breast is determined by the three-dimensional heat transfer conditions. Therefore, the control problem is reduced to control of power deposition within each ring, as a first approximation.

As seen in figure 3, the power deposition occurs in five distinct cross-sectional planes, each plane defined by the individual transducer rings. At steady state temperature, most of the breast tissue is surrounded by the 42°C iso-temperature line and the maximum temperature is 43.7°C. Figure 4 shows the SAR and the equilibrium temperature distributions of figure 3 in the cross-sectional plane.

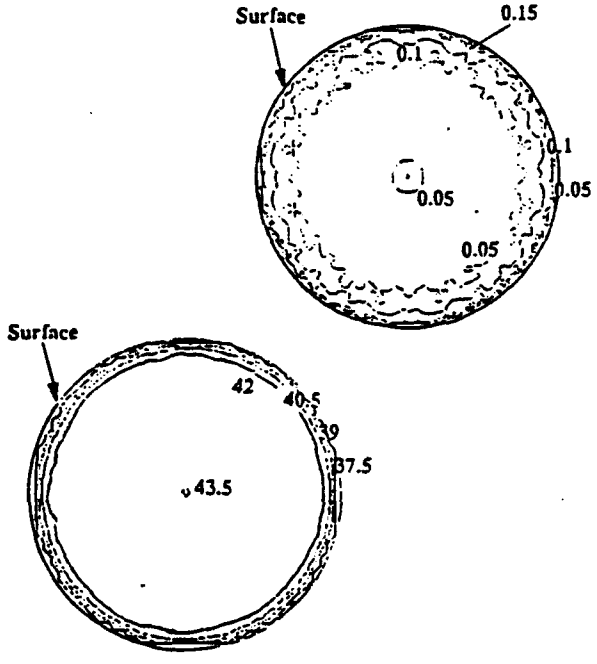

Figure 4. Top panel: SAR distribution (W/cm^3) required to maintain steady state temperature equilibrium 42°C ≤ T ≤ 44°C. The displayed cross-section is shown as a dotted line in figure 3. The diameter is 12 cm. Bottom panel: The steady state temperature distribution. Perfusion rate 30 ml,kg^{-1},min^{-1} at 37°C and 100 ml,kg^{-1},min^{-1} at 44°C. The maximum temperature is 43.7°C.

Breast tissue perfusion rate and its dependence on the temperature and other physiological factors determine the choice of ultrasound frequency and power. We have assumed that the perfusion rate in breast is similar or less than that of resting muscle, because we were unable to find that specific value in the literature. We feel this is a reasonable assumption because breast tissue has a high content of adipose tissue, which would tend to reduce the perfusion rate relative to muscle. However, it is desirable to test the effect of increased perfusion rate on the ability to control the equilibrium temperature distribution.

If we increase the perfusion rate to 100 ml,kg^{-1},min^{-1} at 37°C and 200 ml,kg^{-1},min^{-1} at 44°C, and if we maintain the same SAR distribution as shown in figure 4 (top panel), than the corresponding equilibrium temperature distribution is shown in figure 5. The temperature distribution is heterogeneous and not in compliance with the required 42°C ≤ T ≤ 44°C.

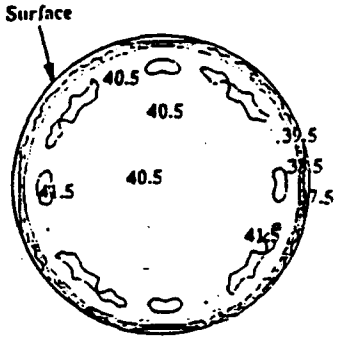

Figure 5. The steady state temperature distribution. Perfusion rate increased to 100 ml,kg^{-1},min^{-1} at 37°C and 200 ml,kg^{-1},min^{-1} at 44°C. SAR distribution as in top panel figure 4.

To achieve an acceptable equilibrium temperature distribution, under this high perfusion rate, we need to increase the SAR distribution. Figure 6 (top panel) shows the SAR distribution, which results in an acceptable equilibrium temperature distribution, 42°C ≤ T ≤ 44°C (bottom panel in figure 6).

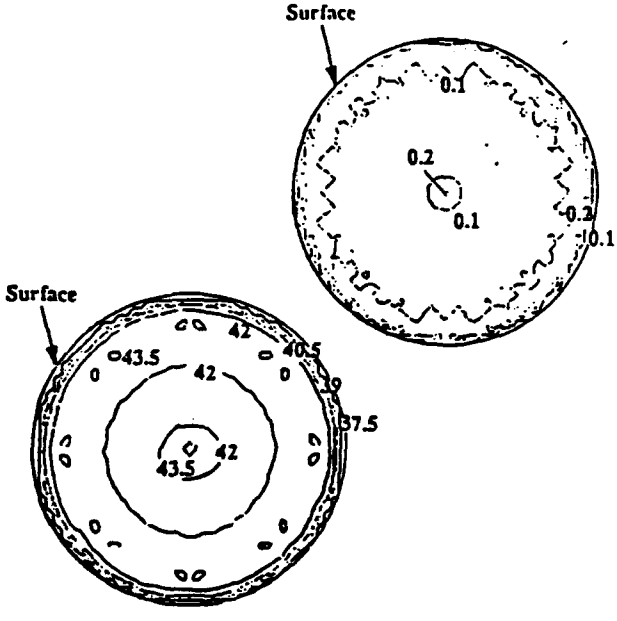

Figure 6. Top panel: SAR distribution (W/cm^3) to maintain steady state temperature equilibrium 42°C ≤ T ≤ 44°C. Perfusion rate increased to 100 ml,kg^{-1},min^{-1} at 37°C and 200 ml,kg^{-1},min^{-1} at 44°C.
Bottom panel: The resulting steady state temperature distribution.

Figure 7 illustrates the ability to heat a quadrant of the breast. It is achieved by depositing energy in the periphery of the target volume using a proper mix of high and low frequency ultrasound.

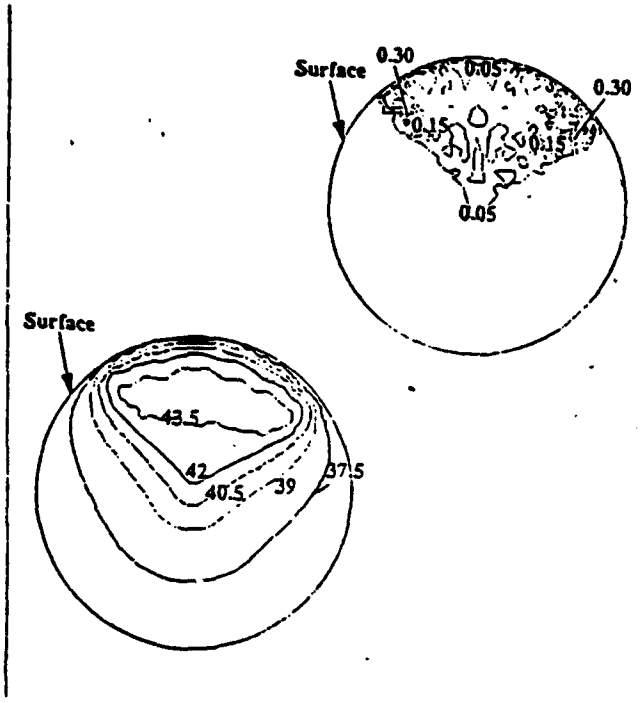

Figure 7. Top panel: SAR distribution (W/cm^3) required to maintain steady state temperature equilibrium 42°C ≤ T ≤ 44°C for treatment of a quadrant of the breast. Bottom panel: The resulting steady state temperature distribution. The maximum temperature is 43.7°C.

CONCLUSION

The three dimensional simulation has offered insight into the design and control capabilities of an ultrasound hyperthermia breast applicator. By varying the parameters that affect ultrasound absorption and heat transfer in tissue, we have determined the need for a dual frequency transducer array. A low frequency, in the range of 1.5 - 2.5 MHz, is needed to compensate for the heat removed by the blood flow and permits an initial quick temperature elevation at depth in the breast tissue. Due to considerable uncertainty in the breast tissue attenuation, a broad frequency band for the low frequency transducers is desired. A high frequency transducer, in the range of 4-4.5 MHz, is needed to maintain a steep temperature gradient near the surface of the target volume. These high and low frequency transducers are mounted alternatively in each ring.

Each ring offer power and frequency control sufficient to heat the whole breast or a quadrant of the breast to a minimum of 42°C but not exceeding 44°C.

REFERENCES

1. Kapp, D.S., Cox , R.S., Fessenden, P., Meyer, J.L., Prionas, S.D., Lee, E.R., Bagshaw, W.A.: Parameters predictive for complications of treatment with combined hyperthermia and radiation therapy. Int J Rad Oncol Biol Phys 22(5) 999-1008, 1992.

2. Ocheltree, K.B. and Frizzell, L.A. Sound Field Calculations for Rectangular Sources. IEEE Transactions on Ultrasonics, Ferroelectrics, and Frequency Control. Vol. 36, No. 2, 242-247, March 1989.

3. Roemer, R.B.: Heat transfer in hyperthermia treatment: Basic principles and applications. American Association of Physicists in Medicine, Med Phys Monograph No. 16, 210-242, 1988.

4. Foster, F.S., Hunt, J.W.: Transmission of ultrasound beams through human tissue - focusing and attenuation studies. Ultrasound in Med & Biol., Vol. 5, 257-268, 1979.

5. Kaye, G.W.C., Laby, T.H.: Tables of Physical and Chemical Constants. Longman, 1973, London.

6. Bowman, H.F.: Heat Transfer and Thermal Dosimetry. J Microwave Power 16 (2), 121-133, 1981.

7. Sekins, K.M., Emery, A.F.: Thermal science for physical medicine. Chpt. 3, pp 70-132 In: Therapeutic Heat and Cold, Lehmann, J.F. (Ed), 1982.

ACKNOWLEDGMENT

This work is supported by the US Army Medical Research and Development Command, under Contract #DAMD17-93-C-3098. The views, opinions and/or findings contained in this report are those of the authors and should not be construed as an official Department of the Army position, policy or decision unless so designated by other documentation.

Syllabus: A Categorical Course in **Radiation Therapy: Hyperthermia**

Editors: **Richard A. Steeves, M.D., Ph.D.**
Madison, Wisconsin

Bhudatt R. Paliwal, Ph.D.
Madison, Wisconsin

Presented at the 73rd Scientific Assembly and Annual Meeting
of the Radiological Society of North America

November 29–December 4, 1987

The Board of Directors of the Radiological Society of North America, and the society's Refresher Course Committee, acknowledge with warm appreciation the scientific contribution of Richard A. Steeves, M.D., Ph.D., and Bhudatt R. Paliwal, Ph.D., in their role as editors of this syllabus.

Robert E. Campbell, M.D., *Chairman*
Board of Directors

Michael A. Sullivan, M.D., *Chairman*
Refresher Course Committee

Melvin L. Griem, M.D., *Subchairman*
for Therapeutic Radiology,
Refresher Course Committee

Technical Developments in Ultrasound-induced Hyperthermia[1]

Everette C. Burdette, Ph.D.
Stephen A. Goss, Ph.D.

The design and testing of systems that will generate well-controlled local hyperthermia are extremely important. In fact, they are necessary for the proper evaluation of the clinical effectiveness of local hyperthermia. Because of its localization ability, ultrasound may be the modality of choice for many deep-seated tumors (1, 2). Ultrasound hyperthermia applicator systems have been developed in several laboratories, including (*a*) unfocused single transducers as used by Corry and his colleagues (3), (*b*) mechanically scanned focused transducers (1, 4), and (*c*) multiple unfocused transducers at Stanford University (Calif.) (5). A single unfocused transducer is limited largely to treating surface or near-surface tumors, whereas the other two systems can be employed for treating deep-seated tumors. However, the Stanford system requires mechanical adjustments of transducer alignment for individual tumors, and no adjustments to the relative position of each transducer can be made during a treatment. Good control of the scan path and intensity is provided, but the scan rate may be slower than desired and scanning involves a complex mechanical system.

An ultrasonic phased array applicator for hyperthermia provides the advantage of electronic steering of the sound beam rather than mechanical movement of the transducer assembly. This allows the focal region to be moved to follow an arbitrary scan path that can be used to heat the periphery of an irregularly shaped tumor or to heat cooler areas of the tumor adaptively when used in conjunction with temperature feedback (6–9).

Microwave and radio frequency (RF) approaches have historically been more widely used than ultrasound for heating applications. This type of equipment has thus been more readily available and more familiar to clinicians. Microwave and RF energies, however, cannot reach deep tumors because power is rapidly "lost," or attenuated, en route to deeper tumors. As the microwave frequency is increased, focusing ability improves; however, attenuation further increases, and thus microwaves are less able to heat tumors located deep in the body.

Ultrasound is more easily focused and, because of its attenuation characteristics at megahertz frequencies, is capable of heating at greater depths than is

[1]From Labthermics Technologies, Inc., Champaign, Ill.

microwave energy. It also offers the advantage of requiring no special treatment-room shielding (RF shielding is required for most electromagnetic frequencies). Ultrasound is inappropriate, however, for use in treating tumors involving bone or when it is necessary to pass through air-filled body cavities.

Ultrasound and microwave modalities are therefore useful in different treatment situations, and each will play an important role in clinical hyperthermia therapy.

Interstitial treatments send RF energy through probes located close to the tumor. Clinicians can achieve a fine degree of control with these techniques because the interstitial antennae are placed in close proximity to the tumor. With the exception of experimental devices, noninvasive systems are not yet sophisticated enough to focus as accurately as interstitial probes. While noninvasive methods are generally preferred by clinicians, invasive techniques are still appropriate for a variety of treatment situations. This is especially true when the therapy includes the use of interstitial seeds or brachytherapy.

During the last decade or so, there has been a revival in the application of therapeutic ultrasound. Reduction of mean tumor weight and size when treated with ultrasound alone were reported by Longo et al. (10). Increases in median survival were observed in Furth-Columbia rats with Wilms tumor, and these results were attributed to a thermal mechanism (10, 11). The threshold for growth control was reported to be approximately 1.5 W/cm^2. Marmor et al. at Stanford University have reported tumor regression and cures with ultrasound treatment of EMT-6 sarcoma and KHJJ and KHT carcinomas in mice (12). They indicated heat and immune recognition to be major factors in the antitumor effect observed. Additional work in spontaneous pet animal tumors yielded similar results (13). Reports of treatment of superficial neoplasms in humans by the same group concluded that ultrasound could effectively heat and appeared to have an antitumor effect on squamous cell carcinomas of the head and neck (14).

On the basis of their work with melanoma cells in culture, Armour et al. (15) reported that ultrasound causes preferential damage to melanin-containing cells. The degree of damage was dependent on the intracellular melanin concentration. Studies performed with high-intensity, short-duration ultrasound treatment of murine gliomas showed growth inhibition, whereas long-duration low-intensity treatments produced growth enhancement (16, 17).

Clinical studies by Corry et al. (3, 18) showed that heating obtained with ultrasound was more uniform and better controlled than that obtained with other modalities. A total of 1,297 treatment sessions were applied to 162 tumors in 159 patients. The tumors were in a wide variety of anatomic locations and of a wide variety of histologic types. Ultrasound systems in which transducers from 2.5 to 10 cm in diameter are used at frequencies from 0.5 to 2.2 MHz were evaluated for their ability to raise tumor temperature, the distribution of intratumoral temperatures they created, and their ability to maintain elevated tumor temperatures. By arbitrarily defined criteria, ultrasound was successful in tumor temperature elevation in 79% of the tumors studied. The greatest success rate (91%) was obtained in the breast, with good results in other, more superficial locations. As might be expected, the poorest performance was in the thorax and pelvic anatomic classifications. The effect of the extent of thermometry (number of intratumoral temperature points) was also examined. The apparent success rate was found to decrease sharply with increasing intratumoral temperature points. Of the toxicities and limiting factors, pain in the treatment field was the most prevalent single problem encountered. This pain was usually associated with tumor involvement in the periosteum or bone itself.

The induction of local hyperthermia selectively in tissues at depth has been discussed by Lele (19). In examining tradeoffs between ultrasound and electromagnetic hyperthermia induction, he concluded that "focused ultrasound currently is the only modality that can be used for producing controllable levels of hyperthermia localized to deep-seated tumors, noninvasively and safely."

Unfocused Therapeutic Ultrasound

Ultrasound has been widely used for therapeutic heating in physical medicine, and resultant temperature distributions have been quantitated in various tissues (20, 21). Heating patterns in fat-muscle-bone tissues and interfaces have been computed for plane-wave fields (22). Temperature rise and heating pattern have been found to be dependent on both the tissue acoustic properties and the incidence angle of the plane-wave field. It is well known that the intensity of the close-in near field is highly nonuniform and that this region extends in proportion to the aperture size of the transducer. For large therapy transducers operating in the one to several megahertz frequency range, the near field can extend to 20 cm or more.

Let us consider heat generation by plane-wave ultrasound for a uniform-intensity field within a homogeneous lossy medium. The intensity I decays exponentially with increasing depth as

$$I = I_o e^{-ux}$$

where I_o is the surface intensity, x is the distance into the medium, and u is the attenuation coefficient. For a medium with uniform thermal characteristics, the rate of heat generation will be proportional to the local intensity, decaying exponentially. Likewise, the temperature distribution pattern will decay exponentially with increasing depth. Cooling of the skin in vivo will not compensate for the overall temperature gradient, but it will lower the surface temperature and possibly increase subcutaneous

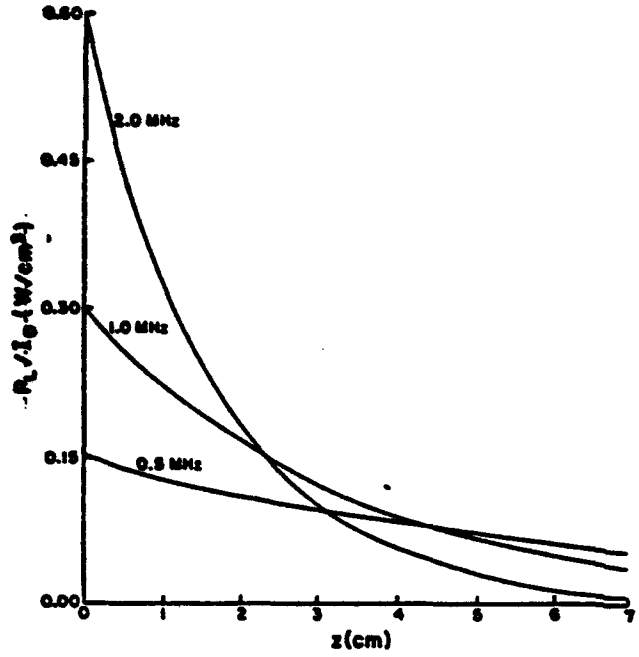

Figure 1. Ultrasound power deposition curves in muscle. Relative heating as a function of depth in tissue for unfocused plane-wave fields at three frequencies.

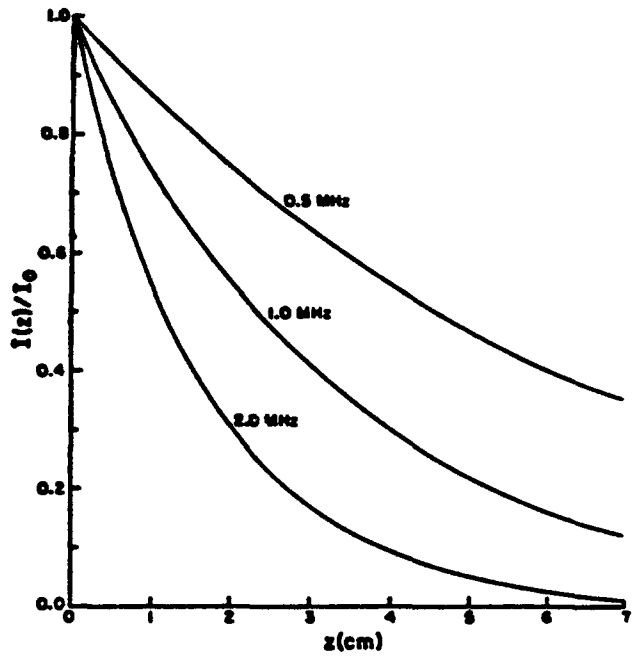

Figure 2. Attenuation of ultrasound in muscle. Relative heating as a function of frequency for three different depths, for determination of optimal heating frequency.

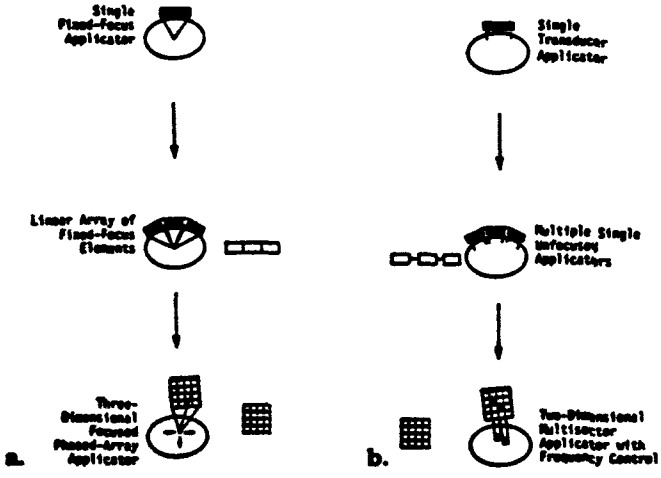

Figure 3. Ultrasound applicators used for hyperthermia induction. (a) Focused applicators, used for deep, localized tumors. (b) Unfocused applicators, used for superficial and mid-depth tumors.

temperatures. Since the absorption coefficient in most soft tissue increases linearly with frequency, greater heat penetration results when lower frequencies are used. However, more energy is required to produce the same degree of temperature elevation due to the dependence of the heating rate on the reduced absorption coefficient. Figure 1 illustrates the relationship between relative heating rate and depth for three different frequencies. Figure 2 displays the heating rate in terms of the optimal frequency for heating at a specified tissue depth. For optimal heating at 2 cm, frequencies from 2.5 to 3.5 MHz are well suited. However, at a depth of 10 cm, the optimal frequency is close to 0.5 MHz (9).

The evolution of unfocused, plane-wave devices for hyperthermia is depicted by Figure 3. Single transducers have been used for many years in therapeutic ultrasound applications in physical medicine (23) and for hyperthermia cancer treatment (3, 12). One of the ways in which higher intensities can be obtained at depth, compared with those at the surface, is by superposition of two or more beams entering the medium through different surface portals but superimposed at the target at depth (Fig. 3). Rotation of the source of energy in an arc or plane centered at the deep target, as is commonly done in radiation therapy, delivers a higher total dose to the target volume compared with that to the surrounding tissues, but not higher instantaneous intensities. Superposition of multiple beams of ultrasonic energy, however, poses problems with respect to phasing because the wavelengths are relatively large compared with those of x rays, potentially resulting in destructive interference in the treatment zone or undesired reinforcement in regions outside the treatment zone. If two beams are out of phase where they overlap, they would interfere destructively, and the local intensity (and the consequent heat production) may be lower in the overlap than in the individual beams. The phase at any point in the medium is governed by both the path length and the velocity in the medium. It also should be noted that the intensity in each beam will decay exponentially from the body surface inward.

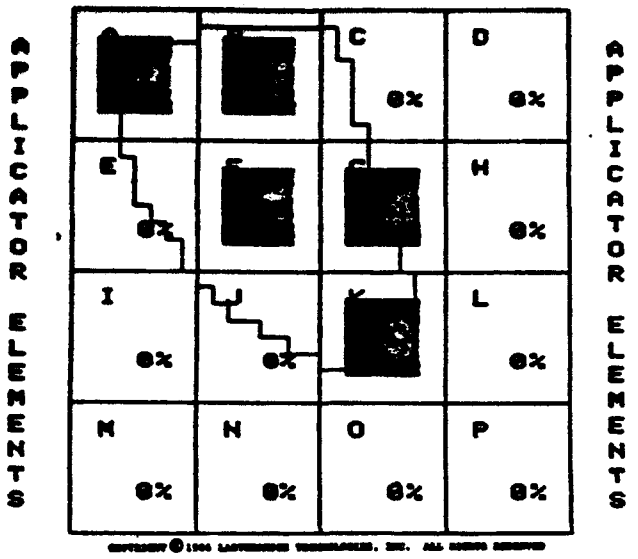

Figure 4. Activated elements within 4 × 4 16-element square array of unfocused transducers matched to tumor shape. Darkened regions denote activated elements.

In reality, tissues are not uniform in their attenuation or heat transfer characteristics. Further, ultrasound sources do not have truly uniform planewave field distribution. These facts further complicate matters with respect to heat generation. Even when modulated by blood perfusion, heat conduction, and the small variations in the ultrasound absorption properties of soft tissue, the resultant temperature distributions can be relatively nonuniform. With electromagnetic fields, differences in attenuation coefficients (dielectric properties) of fat, muscle, and skin are significant, but for ultrasound they are small (24–26). Bone presents a problem to both electromagnetic and ultrasound modalities.

Many of the nonuniform heating distribution problems can be overcome with the ability to control the power deposition spatially with a given tissue treatment region. One approach that accomplishes this is application of a two-dimensional array of unfocused transducers, each independently excited with variable-excitation amplitude and each bearing a specific spatial relationship to various portions of the treatment region (9). An example of such a two-dimensional array with excited transducers matched to the treatment region is illustrated in Figure 4.

Focused Ultrasound Fields

Focused ultrasound at high intensity levels has been used successfully in surgery for producing tracidess focal lesions at predetermined sites at various anatomic locations without causing damage to intervening tissues (27, 28). Focal lesions are produced, with the margins sharply demarcated from surrounding normal tissue; the lesion site is predictable and highly controllable.

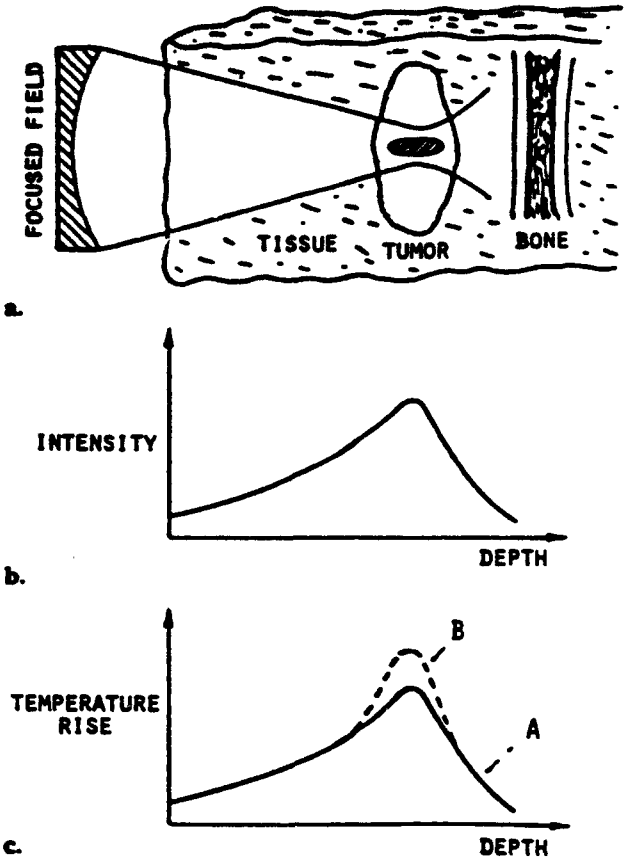

Figure 5. Intensity and temperature distribution patterns with a focused radiation field. In (c), the curve labeled *A* represents the pattern of temperature distribution, if the ultrasonic and thermophysical properties of the tumor are the same as those of the tissues. Curve *B* represents the pattern of temperature distribution, if the ultrasonic absorption coefficient in the tumor was higher than that of tissues or/and the heat diffusivity in the tumor was lower than that in tissues. (Reprinted, with permission, from reference 19.)

The use of focused ultrasound for heat generation is dependent on the intensity distribution within the ultrasonic focus in the tissue and on the tissue absorption and thermal properties, as previously discussed. Focused ultrasound can also be used for production of hyperthermia that is controlled in both degree and extent. Focusing can be accomplished by many methods, including single focused transducers, lenses combined with unfocused transducers, annular transducer arrays, and linear or rectangular phased arrays. The use of a single-transducer convergent beam alleviates the problems associated with field inhomogeneity and phasing. The path length from the transducer to the tissue is fixed, with minimal possibilities of destructive interference at the focus. The effect of field convergence at depth is illustrated in Figure 5. Higher intensities and correspondingly higher temperatures can be achieved at depth, as shown in Figures 5b and 5c. However, since tissue attenuation of the field increases with in-

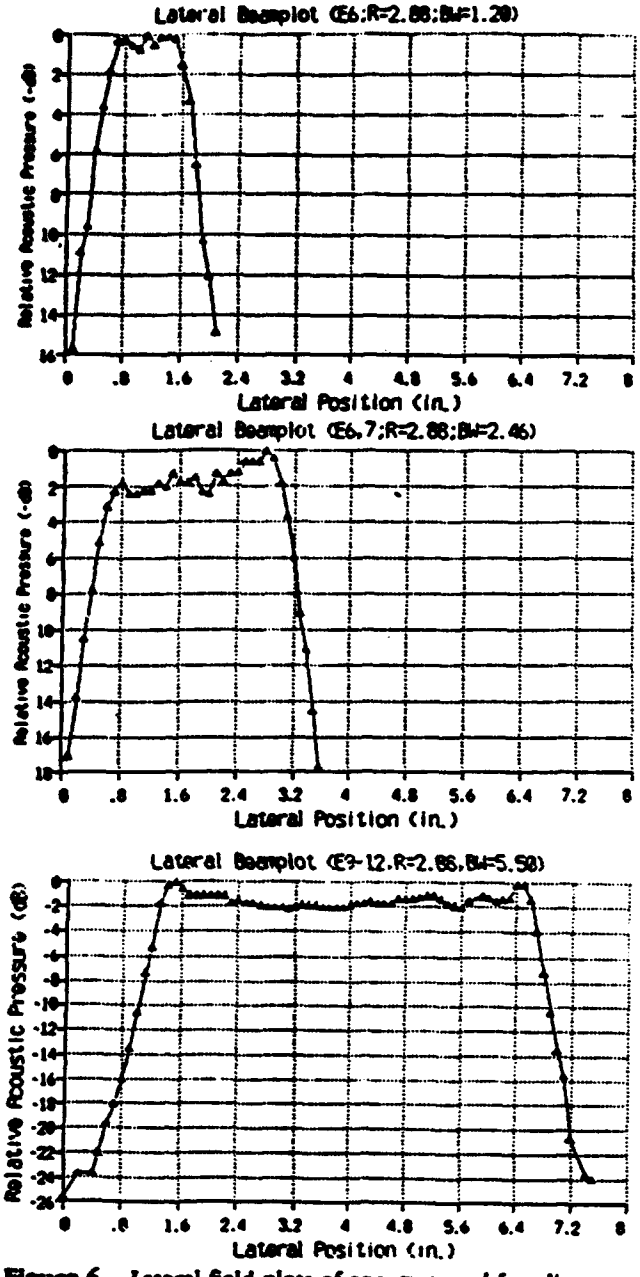

Figure 6. Lateral field plots of one, two, and four linear unfocused elements, each 1.5 inch (3.8 cm) wide. *E* = sector(s) activated, *R* = range from applicator (cm), *BW* = half-power beam width.

creasing path length, the intensity gain with increasing field convergence is ultimately limited. Attenuation by the tissue is also frequency dependent, with the wavelength determining the size and shape of the focus and thus the volume that can be heated. Lele (19) pointed out that focused systems with apical angles of 45°–60° have axially elongated focal regions, with the half-power beam length being four to six times the half-power beam width. The longest wavelength practically usable for heating a specific tissue volume is thus predominantly influenced by the axial dimension rather than the radial dimension.

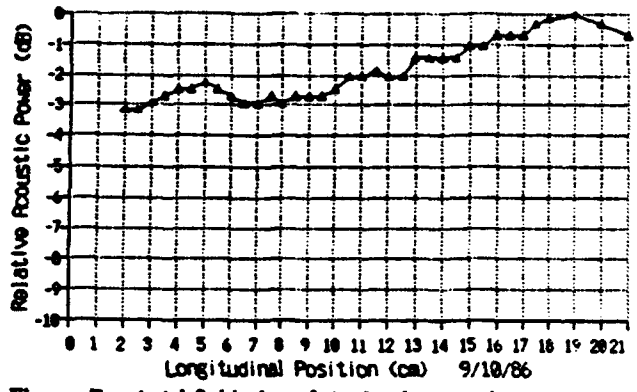

Figure 7. Axial field plot of single element, 3.8 cm wide.

For example, the axial focal length should not exceed the tumor thickness, even though multiple lateral positions may be required to contain the entire tumor volume radially.

Recent Developments—Unfocused Arrays

A major problem with current ultrasound hyperthermia systems is the inability to control accurately the deposition of the energy used to heat tumors in the body. Single unfocused ultrasonic transducers have been used to heat superficial tumors, but often these applicators are too small to heat the entire tumor volume without moving the applicator. A single-transducer applicator larger than the surface area of the tumor solves the problem of heating the entire tumor volume simultaneously, but it produces excess heating in normal tissues surrounding the tumor.

A better approach to heating superficial tumors would be to use an applicator that consists of many unfocused transducer elements whose acoustical power outputs can be independently controlled. The extent of this applicator's treatment field should be greater than the equivalent surface area of most surface tumors, so that movement of the applicator during treatment would not be required to heat the entire tumor volume. Superficial tumors can be heated, without excess heating of normal tissues, by controlling the acoustical power output of the individual elements of the applicator. The temperature in normal and tumor tissues would be monitored with thermocouples. Should the temperature of a particular region in the treatment field become excessive, the acoustical power of the element(s) supplying energy to that region would be reduced. This would make it possible to maintain the normal- and tumor-tissue temperatures in the treatment field at their desired levels.

Such a multielement applicator has been designed, constructed, and analyzed for the treatment of surface tumors of various dimensions (9, 24, 29, 30). The applicator employed in these studies consisted

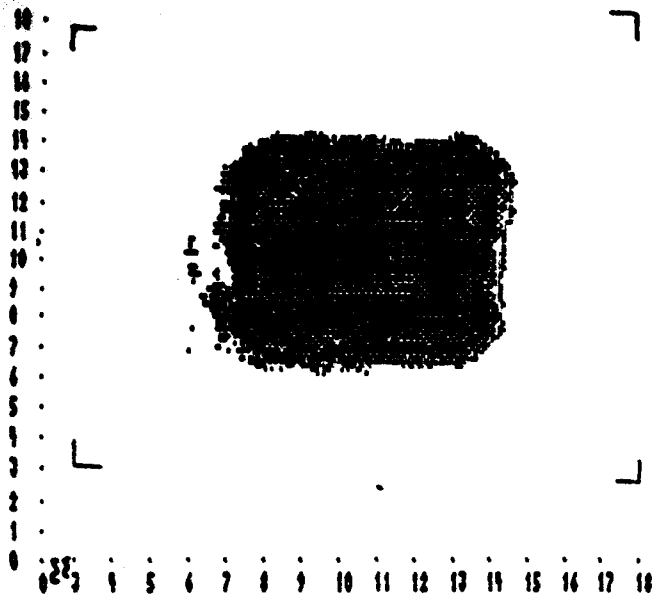

Figure 8. Sixteen-element ultrasound applicator. Center four elements are activated (z = 8 cm).

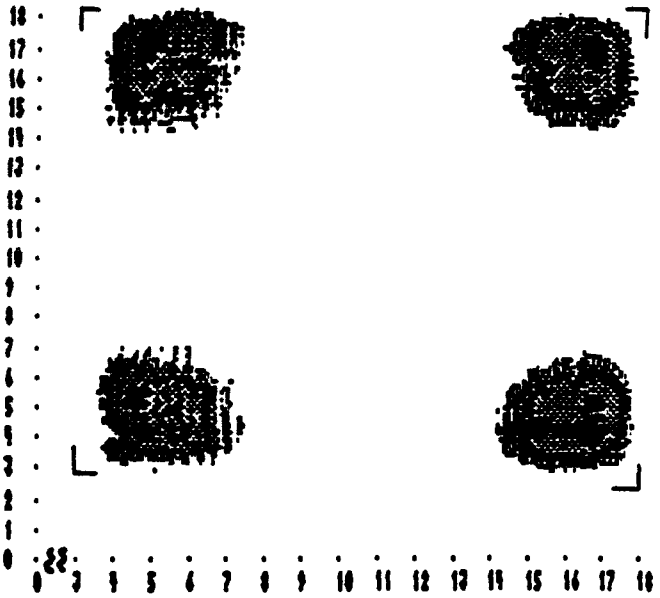

Figure 9. Sixteen-element ultrasound applicator. Corner elements are activated (z = 8 cm).

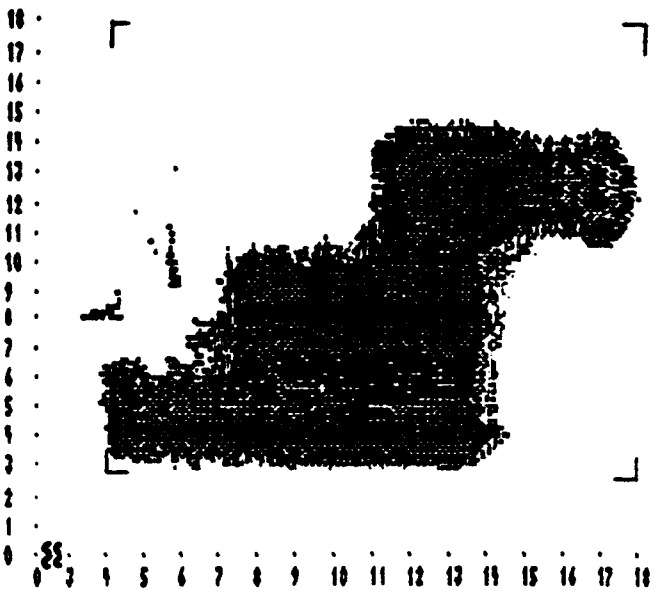

Figure 10. Sixteen-element ultrasound applicator. Elements are activated to match tumor geometry (z = 8 cm).

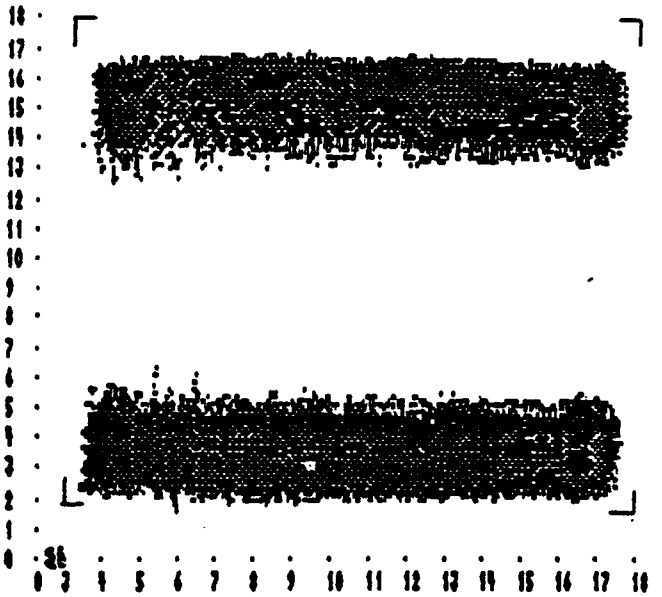

Figure 11. Sixteen-element ultrasound applicator. Two rows (four elements in each row) are activated (z = 8 cm).

of 16 3.8-cm-square elements with independently controlled acoustic power outputs. Field intensity profiles were measured with a scanned hydrophone probe in a tank filled with degassed water. Data were plotted as relative intensity versus position. Figure 6 is a lateral-field plot parallel to the face of the square array at an axial distance of 8 cm. In Figure 6a, one element of the array is excited. In Figures 6b and 6c, two and four elements of the array are excited. Note that the field intensity is relatively uniform over the excited element areas for each case. The axial field along the axis of one element is shown in Figure 7.

Figures 8–11 are surface gray-scale plots of the field intensity, with different elements excited, in a plane parallel to and 8.0 cm from the face of the applicator. These profiles show that the beam skirts from each of the elements are quite steep and well defined (Figure 7) and that the field intensity is quite uniform over the surface area of the excited elements. Two adjacent elements were excited and used as the source for the phantom studies. The field plotted in Figure 12 was for a plane at the surface of the phantom, a distance of 7.6 cm from the applicator.

Performance of the applicator was examined by heating a perfused pig kidney "phantom" (9). The kidney was heated with the applicator at several different perfusion rates, controlled by a roller pump,

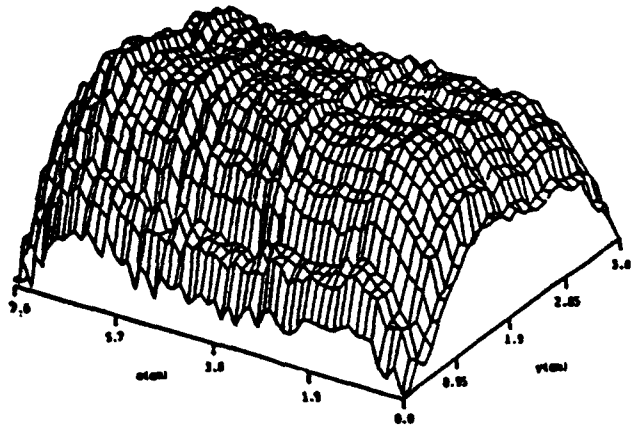

Figure 12. Surface plot of field intensity of two adjacent elements (z = 7.6 cm).

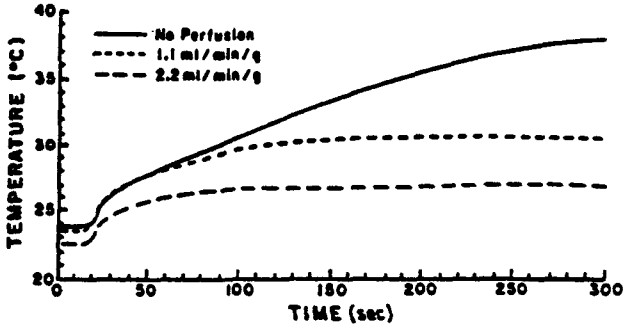

Figure 13. Plot of temperature versus time for several perfusion rates (depth of thermocouple in tissue = 11 mm, I_o = 5 W/cm²).

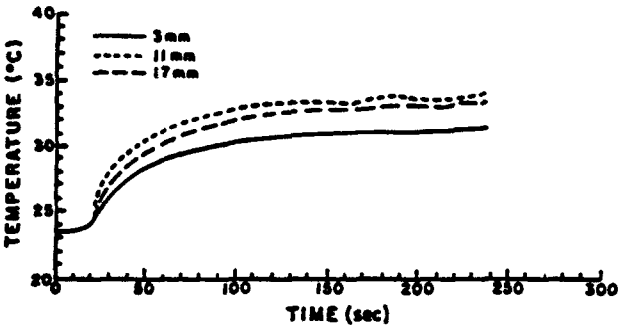

Figure 14. Plot of temperature versus time for three different depths (1.1 ml/min/g, I_o = 10 W/cm²).

and the temperatures within the kidney were monitored. The effect of perfusion rate on the temperature versus time response of the kidney is shown in Figure 13. As expected, an increase in perfusion results in a decrease in both the rate of temperature increase and the steady-state temperature within the phantom. Figure 14 is a comparison of the temperature versus time response at three different depths. The temperature at 3 mm was consistently lower than that at greater depths. This likely results from the combination of two factors: (*a*) greater heat loss by conduction to the nearby surface and (*b*) greater perfusion in the kidney cortex relative to the medulla. The temperature at the other two depths is consistent with the decrease in heating rate with depth.

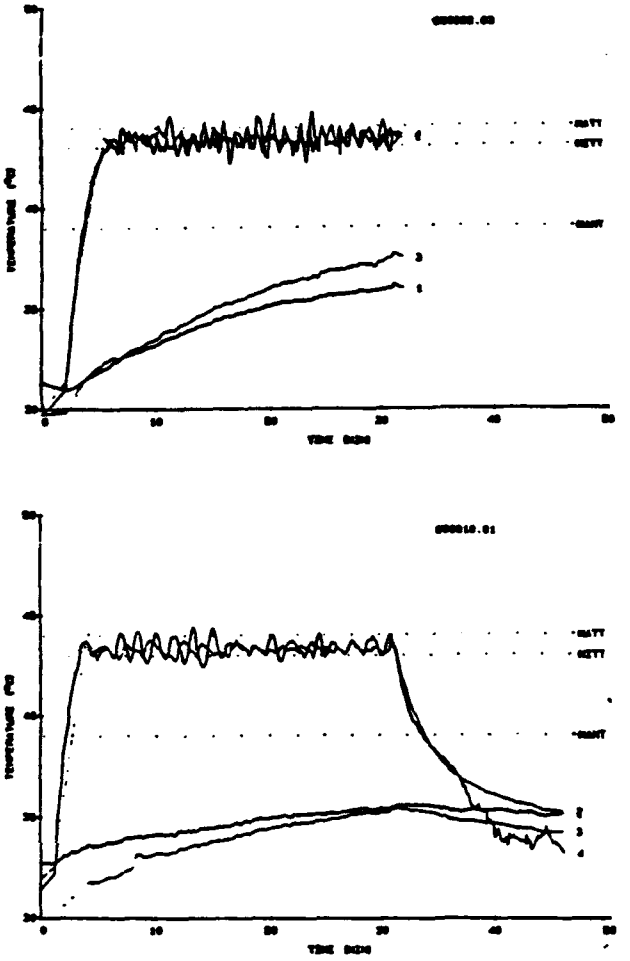

Figure 15. Results of in vivo heating in canine muscle tissue in two experiments. Prespecified therapeutic range (*MITT* to *MATT*) was 43°–44°C and normal-tissue (*MANT*) specification not to exceed 39°C.

In vivo animal testing of the multiple-element array was performed in 22 dogs (31). In each dog, five 18-gauge copper-constantan thermocouples 1 cm deep and 3.8 cm apart were implanted in a straight line from an area just above the coxofemoral joint toward the patellar ligament. Regions surrounding two of the implanted thermocouples were heated to a prespecified control level of 43°–44°C for 30 minutes with a 1-MHz, unfocused ultrasound applicator consisting of 16 independently controllable 3.75-cm² "sectors." The areas heated were directly over the proximal femur, and away from bone, 7.2 cm distal to the aforementioned region. Heating results are shown in Figure 15. Three groups of dogs (seven, eight, and seven animals each) were heated at weekly intervals for 1, 2, or 3 weeks, respectively, and the animals were subjected to necropsy 72 hours after their last treatment. Gross and histopathologic evaluations indicated that this system selectively delivered controlled ultrasonic heating to a well-defined region with minimal changes to surrounding bone-free tissues.

Recent Developments—Focused Systems

A number of focused systems have been developed for hyperthermia induction (4, 6, 8, 14, 19, 32–37). These systems have employed single focused transducers, scanned single focused transducers, multiple focused transducers, and electronically steered phased arrays. Two systems have been developed at Stanford: a plane-wave system for superficial lesions and a six-transducer isospherical focused system operating at 0.3 MHz for heating deep-seated lesions (5, 34). Lele has developed numerous devices for hyperthermia induction by ultrasound (19, 32).

Ultrasonic hyperthermia systems currently use fixed or mechanically scanned transducers for controlling the energy deposition in the tumor. Clinical testing of a simple unfocused ultrasound system led one group of investigators to conclude that the major drawback of their system was the lack of dynamic control of the field intensity distribution. Other systems provide for dynamic control by mechanically scanning one or more focused transducers (1, 4, 32). However, scanning of a transducer may involve a complex mechanical system that is often slow to respond and complicates the patient-applicator interface.

These disadvantages are largely eliminated through the use of phased arrays employing electronic scanning of the focus. Phased arrays can electronically generate and move a focal region of sound energy within the treatment field without the transducer assembly being moved. A planar two-dimensional phased array is illustrated in Figure 16. Appropriate choice of the phase of the signal applied to each element allows focusing of the energy and placement of the focus in three dimensions. Although such an approach would be ideal, such systems have not been developed for hyperthermia applications, primarily because the number of phase control and amplifier circuits (one for each source element) would be prohibitively large. In such an array, the elements must be spaced somewhat less than a wavelength apart (depending on how far off the two axes the focus will be moved) in order to eliminate grating lobes. An array as small as 10 × 10 cm operating at a frequency of 500 kHz would require more than 1,100 source elements, which would be extremely difficult to fabricate.

In an attempt to realize the advantages of electronic movement of the focus that is possible with phased arrays while limiting the number of elements and associated phase control and amplifier circuits, several alternatives to a true two-dimensional phased array have been examined. Two separate but similar approaches employ specially designed linear phased arrays: (*a*) a stack of linear phased arrays and (*b*) a tapered linear phased array (6–8). The focal region is steered in two dimensions by controlling the phases on each element, and in the third dimension

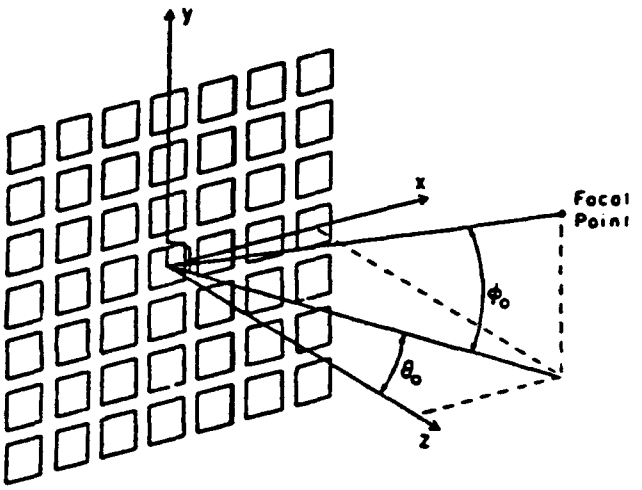

Figure 16. Two-dimensional planar phased array.

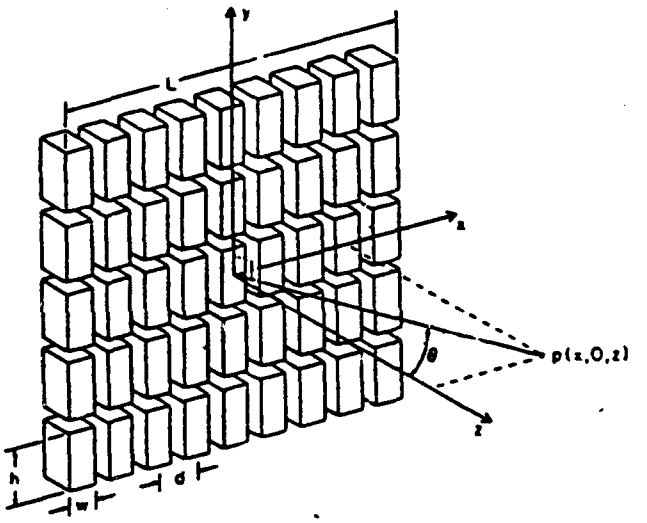

Figure 17. Stack of five linear planar phased arrays.

by (*a*) shifting from one group of linear arrays to another or (*b*) shifting frequency, respectively. A practical design of these arrays consists of approximately 64 elements with a center-to-center spacing between 0.5 and 0.8 wavelengths.

An ultrasonic stacked linear phased array (6, 7) uses a series of separate linear phased arrays stacked in the *y* direction, as shown in Figure 17. In this configuration, each linear array can be excited with phased signals to form a cylindrical focus, which can in turn be moved in the *y* dimension by changing the excitation from one group of linear arrays to another. It has been suggested previously that three adjacent linear arrays could be excited at any one time, with the same signals applied to each linear array, and that the tumor could be located at the distance from the source where the beam width in the *y* dimension was at a minimum. At this distance, corresponding approximately to the near-field–far-field transition distance for an unfocused source of dimensions equal to the height of the three adjacent arrays, the one-half power beam width is approximately

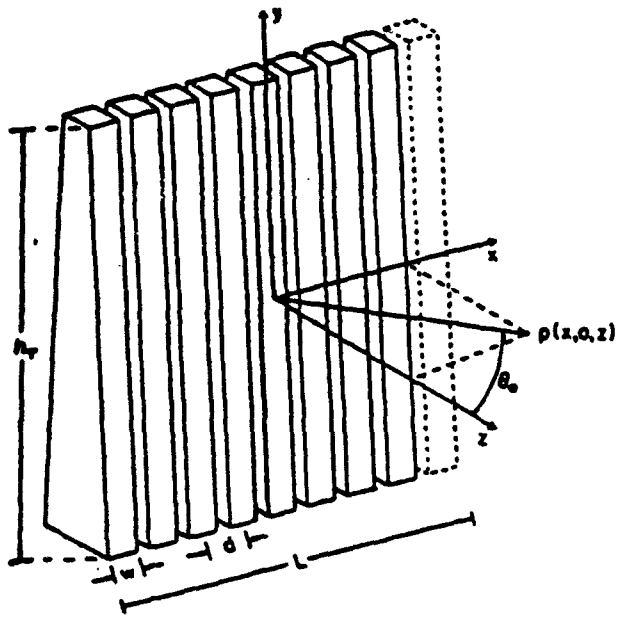

Figure 18. Tapered linear phased array.

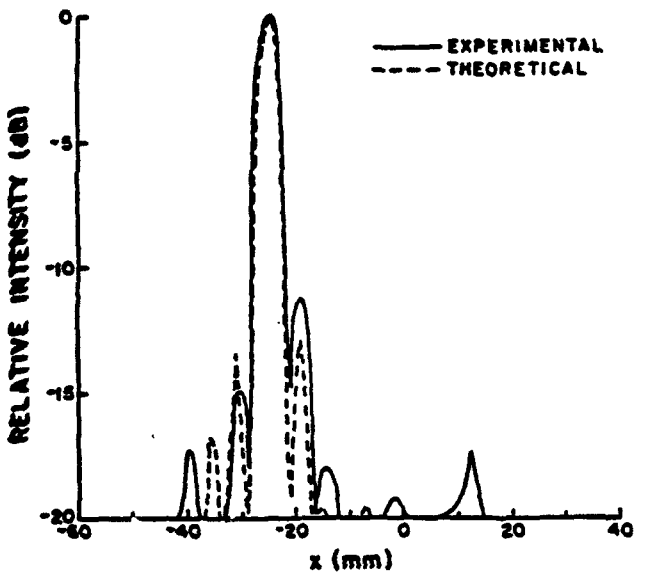

Figure 19. Comparison between the theoretical and experimental relative field intensity of the tapered array versus x position at 650 kHz (focus at $x = -2.5$ cm and $z = 10.0$ cm).

one-third of the y dimension of the group of three arrays. Thus, shifting by one linear array in the y direction provides fields that are overlapping at their half-power levels.

A stacked array has the advantage of requiring fewer phase-control and amplifier circuits than a two-dimensional phased array. This is not without sacrifice of gain in the ratio of focal intensity to intensity near the source. The necessary gain is achieved by using a longer array than might otherwise be required or by using two arrays combined in a single applicator.

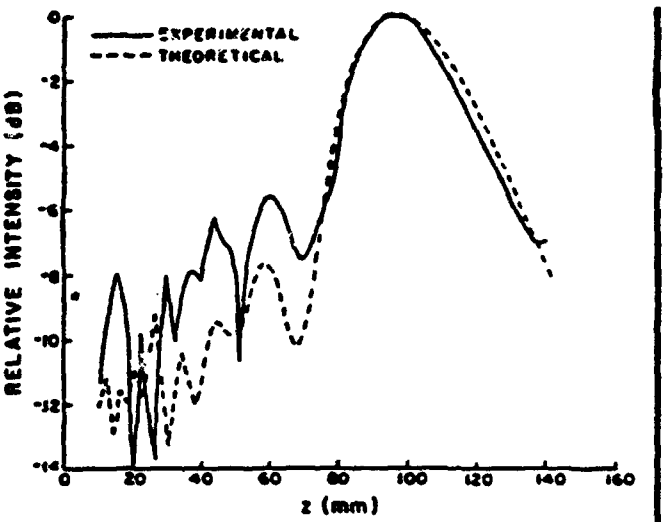

Figure 20. Comparison between the theoretical and experimental relative field intensity of the tapered array versus z position at 650 kHz (focus at $x = 0$ cm, $y = 5.0$ cm, and $z = 10.0$ cm).

An ultrasonic tapered linear phased array (8, 36, 37) uses tapered elements in a linear phased array and employs frequency shifting to move the region of excitation in the y direction from one segment of the array to another, as in Figure 18. The effect is similar to that for the stacked-array transducer except that the shifting of the region of excitation is accomplished simply by changing frequency as opposed to switching the high-voltage applied signal from one group of linear arrays to another. Elimination of the high-voltage switches and their control lines, required for the stacked array, results in considerable simplification and cost savings, since as many as 64 or more elements may be used for the linear arrays. A disadvantage to such an approach relates to the choice of array parameters appropriate for the entire frequency range of the array.

The resonant frequency range of the elements of the tapered phased array was measured by sweeping a hydrophone probe along the height of the element, close to its surface, to determine the location of the maximum acoustic pressure for a given frequency. Figure 19 shows a comparison of the experimental and theoretical field profiles in the x direction, at 650 kHz with the focus steered off axis by 2.5 cm. Figure 20 is a comparison of the experimental and theoretical profiles in the z direction with the focus on axis ($x = 0$). These two figures show that there is good agreement between the theoretically predicted fields and the experimental data for the focused lobe. The differences in the side lobe intensities are attributed to the variations in the output of the elements because of their impedance variations. Figure 21 is a comparison of the experimental and theoretical intensity profiles in the y direction at 580 kHz.

Additional field measurements have been made with the complete 64-channel system (37). Figure

22 shows that the beam profile along the x direction through the focus with 64 elements excited is narrower than with 32 elements excited (Fig. 19), as would be expected because of the larger aperture.

The elongated shape of the focal region cross section is illustrated in the two-dimensional gray-scale plot shown in Figure 23. The beam is very narrow in the x (focused) direction. The beam profile in the y direction with 64 elements excited is comparable with the profile with 32 elements excited, since there is no change of aperture in this direction. The field can be narrowed in the y direction by using elements with a greater rate of taper to decrease the width of the excited region of the ceramic. A gray-scale plot is provided in Figure 24 for the x z-plane through the focus. Note that the focus is larger in the z direction than in the x direction, as expected.

A gray-scale field plot resulting from a scan path with three diagonal locations is illustrated in Figure 25. These plots demonstrate that the focal region of the phased array can be scanned to control the power deposition pattern as has been predicted theoretically. ■

Acknowledgments: The authors gratefully acknowledge the significant contributions to this work made by L. A. Frizzell, Ph.D.; R.L. Magin, Ph.D.; P. J. Benkeser, Ph.D.; C. A. Cain, Ph.D.; H. R. Underwood, M.S.; and K. B. Ocheltree, Ph.D.

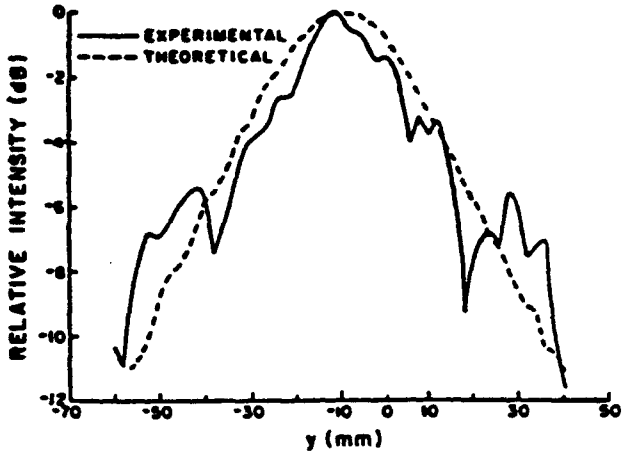

Figure 21. Comparison between the theoretical and experimental relative field intensity of the tapered array versus y position at 580 kHz (focus at $x = 0$ cm, $y = -1.0$ cm, and $z = 10.0$ cm).

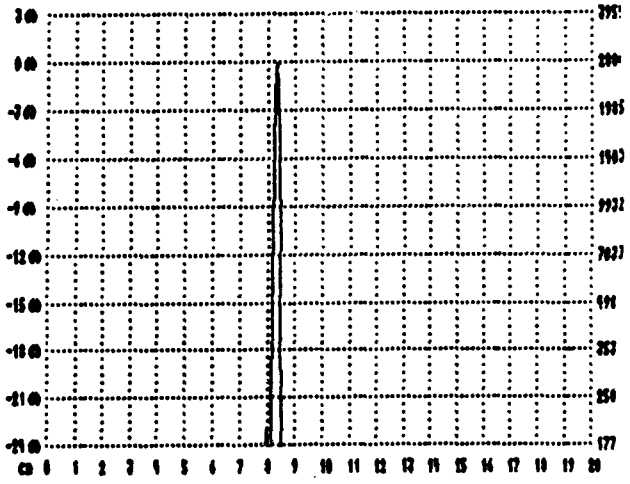

Figure 22. Measured relative field intensity with 64 elements excited, versus x position (focus at $x = 0$ cm, frequency = 600 kHz, and $z = 10.0$ cm).

References

1. Lele PP. Physical aspects and clinical studies with ultrasonic hyperthermia. In: Storm FK, ed. Hyperthermia in cancer therapy. Boston: Hall, 1983; 333–367.
2. Frizzell LA, Goss SA, guest eds. Special issue on ultrasound hyperthermia. IEEE Trans Sonics Ultrasound 1984; SU-31:443–531.
3. Corry PM, Jabboury K, Armour EP, Kong JS. Human cancer treatment with ultrasound. IEEE Trans Sonics Ultrasonics 1984; SU-31:444–456.
4. Hynynen K, Roemer R, Moros E, Johnson C, Anhalt D. The effect of scanning speed on temperature and equivalent thermal exposure distributions during ultrasound hyperthermia in vivo. IEEE Trans Microwave Theory Tech 1986; MTT-34:552–559.
5. Fessenden P, Lee ER, Anderson TL, et al. Experience with a multitransducer ultrasound system for localized hyperthermia of deep tissues. IEEE Trans Biomed Eng 1984; BME-31:126–135.
6. Ocheltree KB, Benkeser PJ, Frizzell LA, Cain CA. A stacked linear phased array applicator for ultrasonic hyperthermia. IEEE Trans Sonics Ultrasonics 1984; SU-31:526–532.
7. Ocheltree KB, Benkeser PJ, Frizzell LA, Cain CA. A stacked linear phased array applicator for ultrasonic hyperthermia. Proceedings of the IEEE Ultrasonics Symposium 1984b. New York: IEEE, 1984; 689–692.
8. Frizzell LA, Benkeser PJ, Ocheltree KB, Cain CA. Ultrasound phased arrays for hyperthermia treatment. Proceedings of the IEEE Ultrasonics Symposium 1985. New York: IEEE, 1985; 930–935.
9. Benkeser PJ, Frizzell LA, Holmes KR, Ryan W, Cain CA, Goss SA. Heating of a perfused tissue phantom using a multielement ultrasonic hyperthermia applicator. Proceedings of the IEEE Ultrasonics Symposium 1984; 685–688.
10. Longo FW, Tomashefsky P, Rivin BD, et al. The direct effect of ultrasound upon Wilms' tumor in the rat. Invest Urol 1977; 15:87.
11. Tomashefsky P, Longo FW, Rivin BD, et al. The reaction of a transplantable rat Wilms' tumor to ultrasound. In: White D, Brown RE, eds. Ultrasound in medicine. Vol 3B. New York: Plenum, 1977; 2051.
12. Marmor JF, Nagar C, Hahn GM. Tumor regression and immune recognition after localized ultrasound heating. Radiat Res 1977; 70:633–634.
13. Marmor JB, Pounds D, Hahn N, et al. Treating of spontaneous tumors in dogs and cats by ultrasound-induced hyperthermia. Int J Radiat Oncol Biol Phys 1978; 4:967–973.
14. Marmor JB, Pounds D, Postic TB, Hahn GM. Treatment of superficial human neoplasms by local hyperthermia induced by ultrasound. Cancer 1979; 32:188–197.
15. Armour EP, Corry PM, McGinness J. Preferential cytotoxicity of cultured melanoma cells by ultrasound and melanin binding drugs. Radiat Res 1977; 70:690–704.
16. Kishi M, Mishima T, Itakura T, et al. Experimental studies of effects of intense ultrasound implantable murine glioma. In: Kazner E, et al. eds. Proceedings of the 2d European Congress on Ultrasonics in Medicine. Amsterdam: Excerpta Medica, 1975; 28.
17. Mishima T. Effects of intense focused ultrasound on the implantable gliomas of mice. J Wakayama Med Assoc 1975; 26:149–166.
18. Corry PM, Jabboury K, Armour EP. Clinical ultrasound. In: Physical aspects of hyperthermia, American Association of

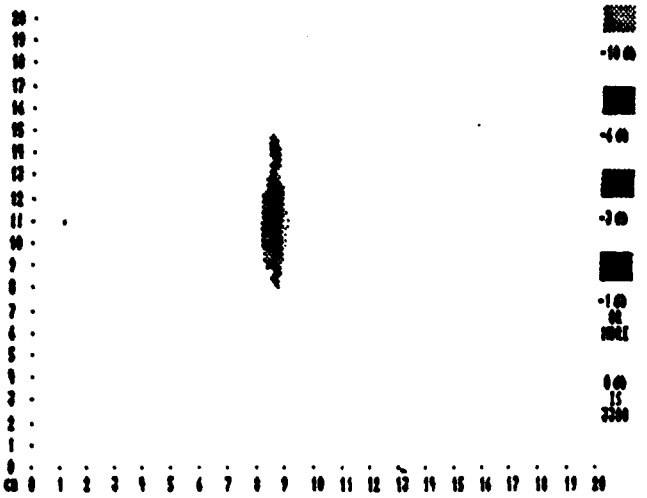

Figure 23. Gray-scale plot of intensity versus x and y positions with 64 elements excited (focus at x = 0 cm, frequency = 600 kHz, and z = 10.0 cm).

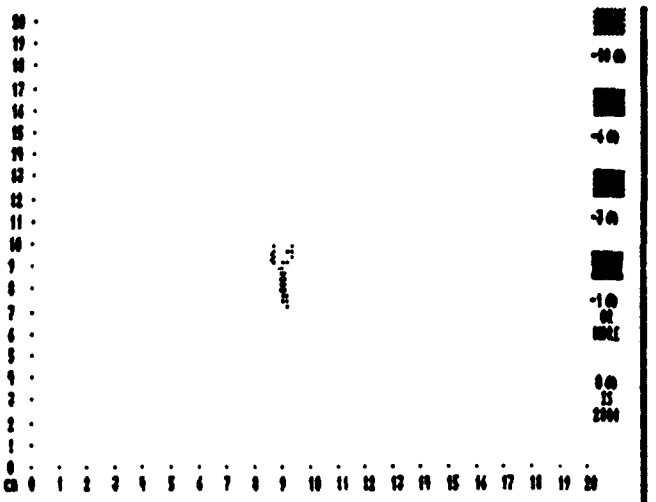

Figure 24. Gray-scale plot of intensity versus x and z positions with [illegible] excited (focus at x = 0 cm, frequency = 6[illegible] z = 10.0 cm).

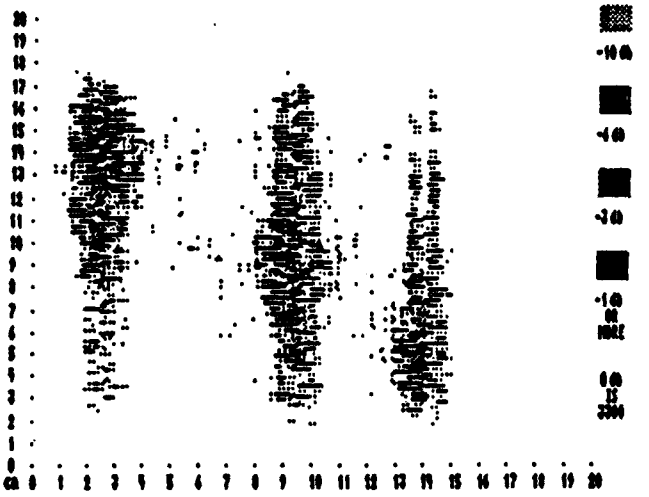

Figure 25. Gray-scale plot of intensity versus x and y positions with 64 elements excited (focus scanned through three locations in the z = 10.0 cm plane: x = −5.7 cm and frequency = 570 kHz, x = −0.8 cm and frequency = 600 kHz, x = 6.4 cm and frequency = 640 kHz).

Physicists in Medicine School, Duke University, Durham, N.C., April 27–May 1, 1987.

19. Lele PP. Induction of deep, local hyperthermia by ultrasound and electromagnetic fields. Radiat Environ Biophys 1980; 17:205–217.
20. Lehmann JF, Guy AW. Ultrasound therapy. In: Reid JM, Sikov MR, eds. Interaction of ultrasound and biological tissue. U.S. Dept of Health, Education, and Welfare publication No. (FDA) 73-8008. Washington D.C.: Government Printing Office, 1972.
21. Guy AW, Leyman JF, Stonebridge JB. Therapeutic applications of electromagnetic power. Proc IEEE 1974; 62:55–75.
22. Chan AK, Siegelman RA, Guy AW. Calculations of therapeutic heat generated in fat-muscle-bone layers. IEEE Trans Biomed Eng 1974; BME-21:280–294.
23. Lehmann JF, ed. Therapeutic hot and cold. 3d ed. Baltimore: Williams & Wilkins, 1982.
24. Goss SA, Burdette EC, Cain CA, et al. System for controlled delivery of clinical ultrasound hyperthermia. J Ultrasound Med 1984; 3:27.
25. Goss SA, Johnston RL, Dunn F. Comprehensive compilation of empirical ultrasonic properties and mammalian tissue. J Acoust Soc Am 1978; 64(2):423–457 and 1980; 68(1):93–108.
26. Burdette EC. Electromagnetic and acoustic properties of tissues. In: Nussbaum GG, ed. Physical aspects of hyperthermia. New York: Am Inst Phys AAPM, Medical Physics Monograph No. 8, 1982.
27. Lele PP. Production of deep focal lesions by focused ultrasound: current status. Ultrasonics 1967; 5:105–112.
28. Fry FJ. Intense focused ultrasound: its production, effects, and utilization. In: Fry FJ, ed. Methods and Phenomena: their applications in science and technology. Vol. 3, Ultrasound: its applications in medicine and biology. New York: Elsevier Scientific, 1978; 687–736.
29. Burdette EC, Goss SA, Cain CA, et al. Integrative systems concept for clinical ultrasound hyperthermia. Presented at the 32d annual meeting of the Radiation Research Society, Orlando, Fla., March 25–29, 1984.
30. Underwood HR, Burdette EC, Goss SA, Magin RL. Field characteristics of a multielement ultrasonic transducer applicator for hyperthermia therapy. Presented at the 34th annual meeting of the Radiation Research Society/North American Hyperthermia Group Conference, Las Vegas, April 12–17, 1986.
31. Ogilvie GK, Goss SA, Badger CW, Burdette EC. Performance of a multi-sector ultrasound hyperthermia applicator and control system: results of animal studies in vivo. Presented at the 34th annual meeting of the Radiation Research Society, Las Vegas, April 12–17, 1986.
32. Lele PP. Hyperthermia by ultrasound. In: Proceedings of the International Symposium on Cancer Therapy by Hyperthermia and Radiation. Washington D.C.: American College of Radiology, 1975; 168–178.
33. Higgins PD, Zeng XW, Zagzebski JA, Paliwal BR, Steeves RA. Versatility of distributed focus ultrasound in treatment of superficial lesions. Int J Radiat Oncol Biol Phys 1984; 10:1923–1931.
34. Fessenden P. Ultrasound methods for inducing hyperthermia. Front Radiat Ther Oncol 1984; 18:62–69.
35. Hahn GM. Hyperthermia and cancer. New York: Plenum Press, 1982.
36. Benkeser PJ, Frizzell LA, Ocheltree KB, Cain CA. A tapered phased array ultrasound transducer for hyperthermia treatment. IEEE Trans Ultrasonics Ferroelectrics Frequency Control (in press).
37. Frizzell LA, Goss SA. A 64-element ultrasonic tapered phased array for hyperthermia. IEEE Trans Biomed Eng (in press).